

A DIMENSIONAL ANALYSIS OF
THE BENZYLIC HYDROXYLASE
ACTIVE SITE IN
MORTIERELLA ISABELLINA

BY

Michael J. Chernishenko

A Thesis
Submitted to the Department of Chemistry
in Partial Fulfilment of the Requirements
of the Degree of
Master of Science

August 1994
Brock University
St. Catharines, Ontario

© Michael J. Chernishenko, 1994

ABSTRACT

The spatial limits of the active site in the benzylic hydroxylase enzyme of the fungus *Mortierella isabellina* were investigated. Several molecular probes were used in incubation experiments to determine the acceptability of each compound by this enzyme. The yields of benzylic alcohols provided information on the acceptability of the particular compound into the active site, and the enantiomeric excess values provided information on the "fit" of acceptable substrates.

Measurements of the molecular models were made using Cambridge Scientific Computing Inc. CSC Chem 3D Plus modeling program.

The dimensional limits of the aromatic binding pocket of the benzylic hydroxylase were tested using suitably substituted ethyl benzenes. Both the depth (para substituted substrates) and width (ortho and meta substituted substrates) of this region were investigated, with results demonstrating absolute spatial limits in both directions in the plane of the aromatic ring of 7.3 Angstroms for the depth and 7.1 Angstroms for the width. A minimum requirement for the height of this region has also been established at 6.2 Angstroms.

The region containing the active oxygen species was also investigated, using a series of alkylphenylmethanes and fused ring systems in indan, 1,2,3,4-tetrahydronaphthalene and benzocycloheptene substrates. A maximum distance of 6.9 Angstroms (including the 1.5 Angstroms from the phenyl substituent to the active center of the heme prosthetic group of the enzyme) has been established extending directly in

front of the aromatic binding pocket. The other dimensions in this region of the benzylic hydroxylase active site will require further investigation to establish maximum allowable values.

An explanation of the stereochemical distributions in the obtained products has also been put forth that correlates well with the experimental observations.

ACKNOWLEDGEMENTS

I would like to express my most sincere appreciation to Dr. H. L. Holland for his encouragement and enthusiasm throughout the course of this work, and for passing on some valuable experience in the area of my research.

I would also like to extend my appreciation to Dr. J. S. Hartman and Dr. J. K. Atkinson for finding the time to participate on my supervisory committee, and for valuable discussions throughout the course of this work.

I would also like to thank Dr. M. F. Richardson for assisting me with the modeling program that was used to obtain the molecular dimensions.

A sincere thanks is also extended to Mr. T. R. B. Jones for his expertise in obtaining the spectra required to make the determination of my results possible, and to F. M. Brown for her experience and assistance with the fungal cultures.

And last, but not least, thanks are extended to the faculty and staff of the chemistry department and to my peers who all helped to make this work both exciting and enjoyable.

**To My Family, Marianne
Michael and Matthew
And My Parents
For Their Encouragement
And Support.**

TABLE OF CONTENTS

<u>INTRODUCTION</u>	1
I General	2
I-1 The Catalytic Cycle	5
I-2 Membrane Topology	10
II Cytochrome P-450 Active site	13
II-1 Cytochrome P-450cam	15
III Modeling the Active Site	22
III-1 <i>Mortierella isabellina</i>	33
IV Current Research	37
 <u>RESULTS AND DISCUSSION</u>	 39
I Preparation of Substrates	40
I-1 Ortho- and Meta-Fluoroethylbenzene	40
I-2 Reduction of Ketone Starting Materials	44
I-3 Rigid Front End Probes	46
I-4 Preparation of Spiro Compounds	48
II Incubation of Substrates	50
II-1 Aromatic Binding Site Probes	51
II-2 Front End Probes	58
II-3 Front End Rigid Probes	65

III-	Stereochemical Considerations	75
IV	Model for the Benzylic Hydroxylase	78
V	Conclusions	82
	<u>EXPERIMENTAL</u>	84
I-1	Apparatus, Materials and Methods	85
I-2	Incubations with <i>Mortierella isabellina</i>	85
II	Preparation of Substrates	87
	2-Fluoro-ethylbenzene (2)	87
	2-Fluoro-ethylbenzene (3)	88
	4- <i>tert</i> - Butyl-ethylbenzene (5)	89
	Cyclobutylphenylmethane (10)	90
	Cyclohexylphenylmethane (12)	90
	Benzocycloheptene (19)	91
	1-Methylindan (14)	91
	1-Ethylindan (15)	92
	1-(1-Methylethyl)indan (16)	93
	1-Ethyl-1,2,3,4-tetrahydronaphthalene (17)	94
	1-(1-Methylethyl)-1,2,3,4-tetrahydronaphthalene(18)	95
	(9,10-Benzo)spiro[4.5]decane (20)	96
	(10,11-Benzo)spiro[5.5]undecane (21)	97
III	Incubation of Substrates	99
	3-Ethyltoluene (1)	99

2-Fluoro-ethylbenzene (2)	99
3-Fluoro-ethylbenzene (3)	100
4-Ethylbiphenyl (4)	100
4- <i>tert</i> - Butyl-ethylbenzene (5)	101
1,2,3-Trimethylbenzene (6)	102
1,3,5-Trimethylbenzene (7)	102
2-Methyl-1-phenylpropane (8)	102
2,2-Dimethylphenylpropane (9)	103
Cyclobutylphenylmethane (10)	104
Cyclopentylphenylmethane (11)	105
Cyclohexylphenylmethane (12)	106
Diphenylmethane (13)	107
1-Methylindan (14)	108
1-Ethylindan (15)	109
1-(1-Methylethyl)indan (16)	110
1-Ethyl-1,2,3,4-tetrahydronaphthalene(17)	111
1-(1-Methylethyl)-1,2,3,4-tetrahydronaphthalene(18)	111
Benzocycloheptene (19)	112
(9,10-Benzo)spiro[4.5]decane (20)	114
(10,11-Benzo)spiro[5.5]undecane (21)	114
1,4-Epoxy-1,2,3,4-tetrahydronaphthalene (22)	114
9,10-Dihydroanthracene (23)	114

<u>REFERENCES</u>	116
-------------------	-----

<u>APPENDIX</u>	122
Appendix 1 (Numbering schemes of compounds related to this work).	123
Appendix 2 (Readily available starting materials)	125
Appendix 3 (The amino acids)	126

LIST OF FIGURES

1.	Protoporphyrin IX, P-450 prosthetic group.	4
2.	The catalytic cycle of cytochrome P-450 dependent monooxygenases.	6
3.	The oxidized and reduced forms of the flavin prosthetic groups, (a) FMN and (b) FAD.	7
4.	Reduction sequences for cytochrome P-450.	8
5.	Proposed route for benzylic hydroxylation of ethylbenzene by <i>M. isabellina</i> .	11
6.	Early predictions of cytochrome P-450 membrane interaction.	12
7.	Proposed cytochrome P-450 membrane interactions.	14
8.	A representation of P-450 _{cam} .	17
9.	Interaction of the heme propionate groups with surrounding hydrogen bond donors.	18
10.	The active site of P-450 _{cam} showing the interaction between Tyr 96 and the camphor carbonyl.	19
11.	Space filled representation of P-450 _{cam} showing the proposed substrate access channel.	21
12.	Geometric and schematic representations of the relative positions of binding sites and hydroxylation in <i>Calonectria decora</i> .	23
13.	Possible orientations of the steroid nucleus in the active site accounting for the observed products	25
14.	A model for the hydroxylating enzyme of <i>Bacillus cereus</i> .	26

15.	The positions of hydroxylation of aphidicolan-16 β ol by <i>Cephalosporium aphidicola</i> .	28
16.	The hydroxylation of liguloxide by <i>Streptomyces purpurescens</i> .	29
17.	Original model developed to account for the hydroxylation of cyclic amide substrates by <i>Beauveria sulfurescens</i> .	30
18.	Second generation model for hydroxylation of cyclic amides by <i>Beauveria sulfurescens</i> .	31
19.	Second representation of the refined model of the active site of <i>Beauveria sulfurescens</i> .	32
20.	Oxidation of 2-Phenyloxathiolanes by <i>Mortierella isabellina</i> .	34
21.	Active site model developed for the oxidative reactions performed by <i>Mortierella isabellina</i> .	36
22.	Dimensional analysis of compounds 4 and 5, 2-ethylnaphthalene and 2-ethylanthracene.	54
23a.	Dimensional analysis of compounds 1,2,3 and 2-ethyltoluene.	56
23b.	Dimensional analysis of compounds 6,7, 1,2-diethylbenzene and 1,3-diethylbenzene.	57
24.	Perturbed orientation of 3-ethyltoluene 1 and normal orientation of ethylbenzene.	59
25.	Specific hydroxylation of 5,6,7,8-tetrahydro quinoline.	60
26.	Dimensional analysis of compounds 8 through 13.	63

27. The folding of cyclopentylphenylmethane, restricting access of the phenyl ring into the binding pocket. 66
28. A dimensional analysis of compounds 14 through 18. 69
29. A dimensional analysis of compounds 19,20, and 21. 73
30. Two views showing the relative location of the oxidation center in the benzylic hydroxylase of *Mortierella isabellina*. 76
31. Two possible ways in which the oxidation center could have access to the bottom face, accounting for the observed enantiomeric ratios. 77
32. A schematic representation of the active site of the benzylic hydroxylase of *Mortierella isabellina*. 79
33. The experimentally determined dimensions of the benzylic hydroxylase of *Mortierella isabellina*. 83

LIST OF SCHEMES

1.	Synthetic route to ortho- and meta-fluoroethylbenzene	41
2.	The formation of the aryl diazonium cation.	42
3.	General route for the production of saturated compounds from the corresponding ketones.	45
4.	Synthesis of 1-alkylindans and 1-alkyl-1,2,3,4-tetrahydronaphthalenes.	47
5.	Synthetic route for the preparation of spiro compounds.	49
6.	Mechanism of side chain cleavage in steroids	72

LIST OF TABLES

1.	Products of biotransformation of compounds 1 through 7 by <i>M. isabellina</i> .	52
2.	Products of biotransformation of compounds 8 through 13 by <i>M. isabellina</i> .	61
3.	Products of biotransformation of compounds 14 through 18 by <i>M. isabellina</i> .	67
4.	Products of biotransformation of compounds 22 through 24 by <i>M. isabellina</i> .	74

INTRODUCTION

Introduction

I General

The use of enzymes as synthetic reagents has increased the capacity of the organic chemist in the synthesis of complex target molecules. Nearly all oxidative, reductive, or hydrolytic reactions have an enzymic counterpart.

The ability of the oxygenase enzymes to effect the oxidation of otherwise unactivated C-H bonds is unique in that the chemical oxidation of such carbons is difficult, if not impossible to achieve.

The oxygenases may be subdivided into the dioxygenases in which both atoms of molecular oxygen are incorporated into the substrate molecule, as in the oxidation of catechol by pyrocatechase (1); the monooxygenases which, introduce one atom of molecular oxygen into the substrate, the other ultimately being reduced to water (eq. 1).



The reducing equivalents are derived from NADPH or NADH, and are transferred to the cofactor in several ways, depending on the source of the enzyme.

The most versatile monooxygenase system, cytochrome P-450, is one of the most widespread enzymes in nature. It is presumed to be responsible for most biological hydroxylations, epoxidations, and heteroatom dealkylations, although involvement in only a small number of cases have actually been proved. Cytochrome P-450 has been the

object of intensive study due to the fact that it oxidizes xenobiotic compounds. The oxidations result in transformation of hydrophobic compounds, such as environmental pollutants and drugs, allowing the organism to eliminate these substances, activation of prodrugs, as well as its involvement in the metabolic activation of polyaromatic hydrocarbons creating true or proximate carcinogens.

Most of the mechanistic background on this class of enzyme is derived from studies of mammalian cytochrome P-450's (2) and a unique soluble form of the enzyme (P-450 cam), isolated from the bacteria *Pseudomonas putida* grown on camphor as the sole carbon source.(3) The evidence suggests that all cytochrome P-450 dependent monooxygenases function in a similar manner.(4) In most instances, microbial systems yield metabolites similar to those reported in studies of P-450's from hepatic microsomes and/or in vivo mammalian systems.(5) The potential for the use of microbial systems in the preparation of mammalian metabolites of xenobiotic substances has far-reaching possibilities.

Cytochrome P-450 consists of a heme iron in the form of protoporphyrin IX (figure 1). Four of the iron ligands come from the nitrogens of the porphyrin ring. The fifth is a thiolate anion from a cysteine residue of the apoenzyme.(6) The sixth ligand in the camphor free, low-spin state of P-450 cam. is a water molecule or hydroxide ion trans to the thiolate ligand.(7)

The heme prosthetic group is responsible for the activation and delivery of oxygen to the substrate. The protein apoenzyme binds the substrate and is responsible for the regio- and stereochemistry of the product.

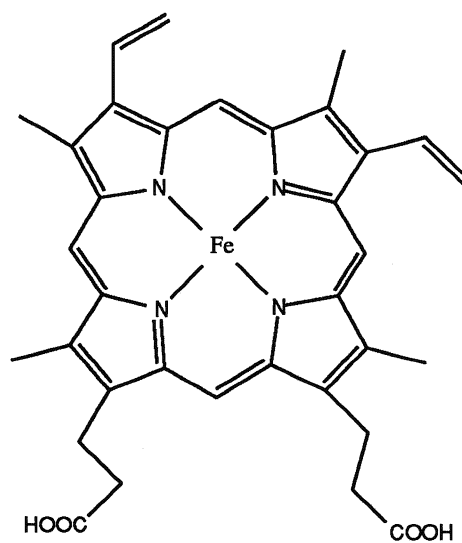


Figure 1. Protoporphyrin IX, P-450 prosthetic group.

I-1 The Catalytic Cycle

The reaction sequence (Figure 2) proposed for the action of cytochrome P-450 involves the following steps ; (a) binding the substrate by the enzyme, with iron in the ferric Fe^{3+} resting state. (b) introduction of one electron via cytochrome P-450 reductase, reducing iron to the ferrous Fe^{2+} state. (c) binding of dioxygen, giving the substrate bound ferrous dioxygen complex. (d) introduction of a second electron from the reductase or cytochrome b₅. (e) dioxygen cleavage, eliminating one atom of oxygen as water. (f) introduction of the second atom of oxygen into the substrate. (g) product release, returning iron to the ferric resting state.

The first step in the catalytic cycle is the binding of the substrate by the enzyme; the binding energy is largely derived from the hydrophobic interaction between the protein and the substrate.(8) The process of binding the substrate in the active site of the enzyme obstructs the coordination site of the sixth ligand, water. With the release of this ligand, the iron atom moves out of the plane of the porphyrin ring, changing the coordination sphere from octahedral hexacoordinate to a square pyramidal pentacoordinate geometry. This change in geometry causes the iron to change from a low spin ($S=1/2$) to a high spin ($S=5/2$) resulting in an increased ionic radius and a lowering of the reduction potential.(9)

The oxidation of a substrate by cytochrome P-450 requires the input of two electrons. The electrons are ultimately derived from NADPH (or NADH in *P. putida*). The electron transfer chain consists of a flavoprotein containing both FAD and FMN as prosthetic groups (10) (figure 3). FAD acts as the initial electron acceptor and FMN passes the electrons one at a time to the P-450 (11) (figure 4). In the soluble P-450_{cam} the

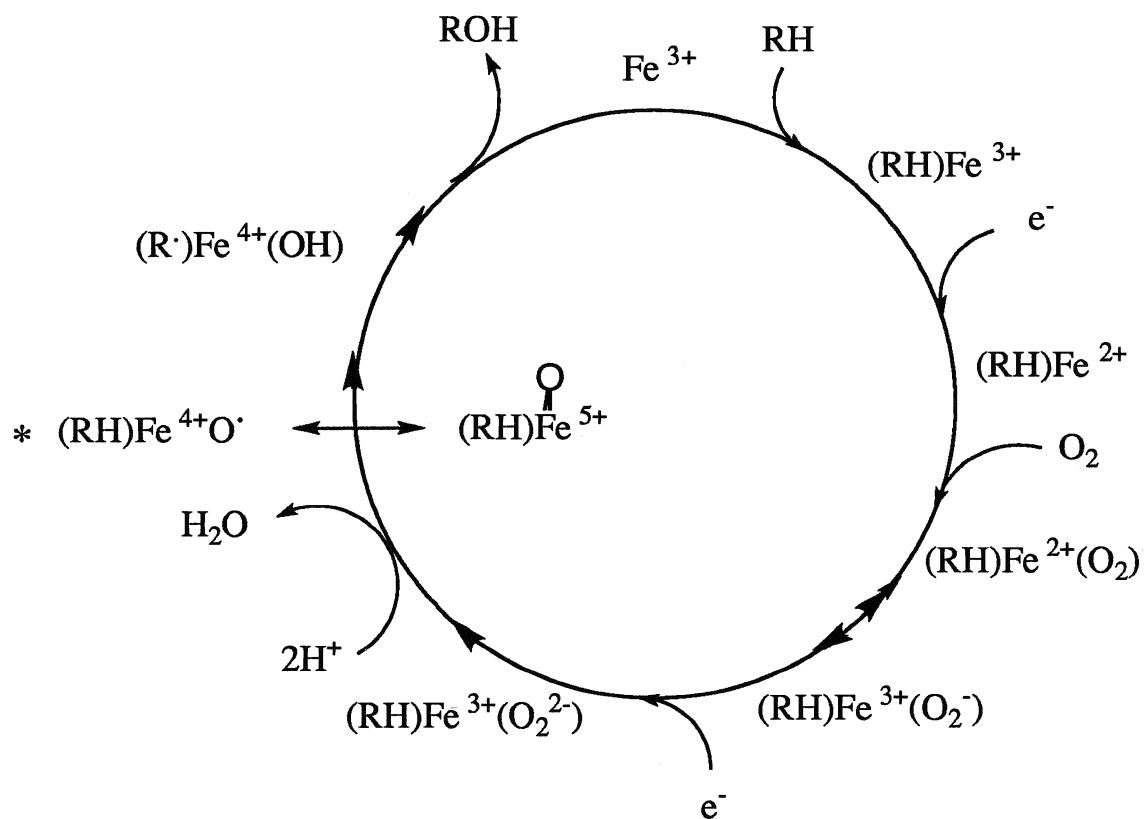


Figure 2. The catalytic cycle of cytochrome P-450 dependent monooxygenases.

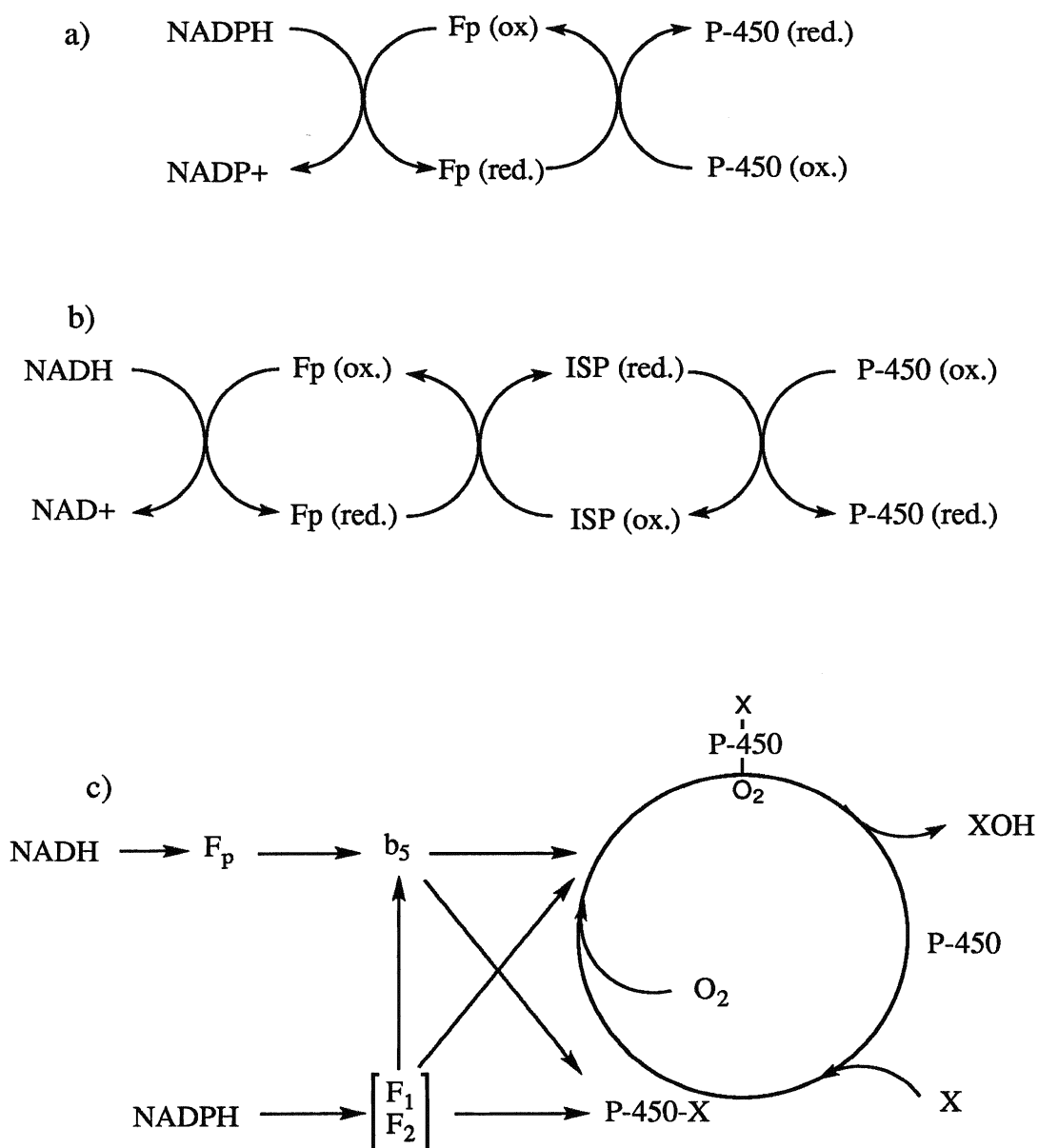


Figure 4. Reduction sequences for cytochrome P-450 (a) mammalian and microbial P-450's (b) bacterial P-450's (c) possible role of cytochrome b₅ in the reductive process.

flavoprotein passes the electrons to an iron sulfur protein which is the one electron donor. Although cytochrome P-450 requires two electrons to complete the catalytic cycle, the electrons are clearly introduced in a sequential manner.(9, 11) Introduction of the first electron yields the substrate iron complex in the ferrous state, setting the stage for oxygen binding and activation.

Subsequent to transfer of the first electron, the heme is able to bind dioxygen, which apparently coordinates trans to the thiolate ligand.(13) The binding of oxygen yields a ferrous dioxygen complex which is the first step in the activation of the catalytic species.

Introduction of the second reducing equivalent to the ferrous dioxygen complex by P-450 reductase or cytochrome b₅ is required for normal catalytic turnover. It is the introduction of this second electron that is responsible for the events leading to the cleavage of the dioxygen bond and the production of the actual catalytic species. This portion of the catalytic cycle is the least understood, because turnover of the enzyme and product release occur too rapidly for any intermediates to be observed. The oxidizing species has been formulated as $\text{Fe}^{4+}\text{-O}\cdot$ (figure 2).(14) The electrophilic nature of this species is apparent from reactions performed, such as benzylic hydroxylation, sulfur oxidation, hydroxylation of aromatic substrates, as well as epoxidation of dehydro substrates related to their normal saturated counterparts.(15)

Introduction of the oxygen into the substrate completes the process, releasing the oxidized substrate, and regenerating the enzyme in its ferric resting state.

The fungus *Mortierella isabellina* ATCC 42613 used in this study carries out the benzylic hydroxylation of simple aromatic hydrocarbons

(16,17,18,19) as well as more complex analogs.(20) The mechanistic details of the benzylic hydroxylase of this fungus have been studied (17,19) and the method for introduction of oxygen into the substrate has been proposed (figure 5).(21) The salient feature of this mechanism is the stepwise nature of events, removal of one electron, hydrogen loss (pro-R in the case of ethylbenzene) (19,22) and product formation, yielding the R-alcohol with enantiomeric excesses between 25% and 35%.(16)

I-2 Membrane Topology

Prior to obtaining the crystal structure of cytochrome P-450_{cam}, the structure of this family of enzymes had to be deduced based on the determination of the amino acid sequences. Ozols et al. (23) suggested that, based on the distribution of amino acid residues in the NH₂ terminus into non-polar segments of 18 - 23 residues, separated by shorter polar regions, multiple segments are embedded in the membrane. The membrane model (figure 6) was constructed based on a minimum number of charged residues contacting the hydrophobic portion of the bilayer.

Significant progress in the understanding of membrane topological features has been made with mammalian cytochrome P-450. The availability of several primary structures for comparison, and the crystal structure of P-450_{cam} has shed some new light on the subject of P-450 structure. The present understanding of protein structure dictates that a transmembrane segment must assume a secondary structure for thermodynamic reasons. A study beginning with the alignment of 34 P-

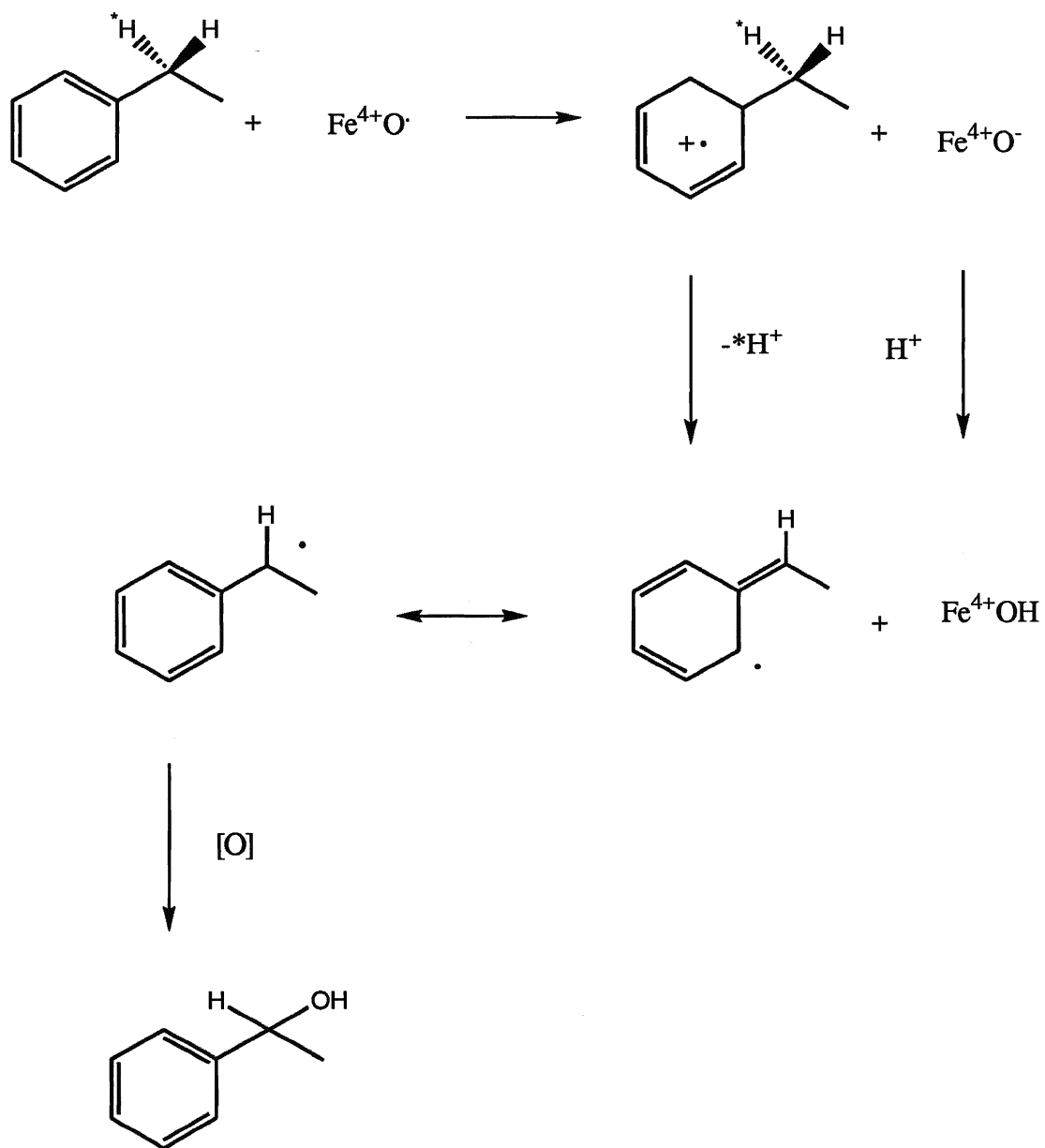


Figure 5. Proposed route for benzylic hydroxylation of ethylbenzene by *M. isabellina*.

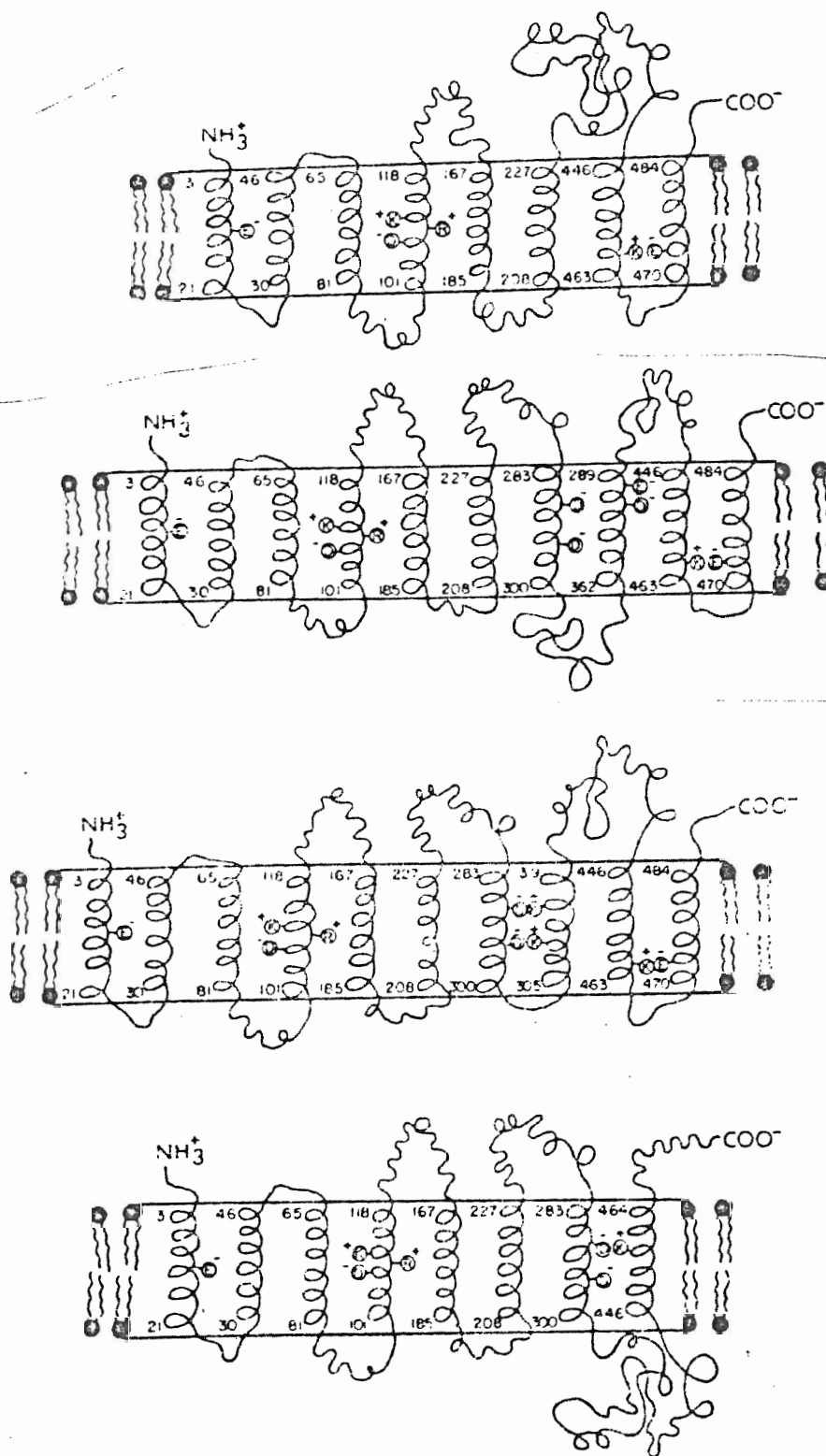


Figure 6 The early predictions of cytochrome P-450 membrane interaction. (23)

450 sequences from different protein families found 11 regions of common hydrophobic character. These regions were considered as potential transmembrane segments. The segments were then investigated, using techniques such as EPR, X-ray crystallography, chemical modifications, fusion protein experiments and secondary structure prediction, eliminating all but two of the sequences from the original group.

The NH₂- terminal segment (termed S1 in the study) in the 34 proteins studied is clearly the most hydrophobic segment in the sequence, and is thought to be the most likely candidate for a membrane spanning segment.(24) The enzyme is currently thought to be anchored to the membrane by one or two transmembrane sequences (figure 7).(25)

II Cytochrome P-450 Active Site

Processing of the multitude of substrates acted upon by microsomal P-450, is carried out by separate isozymes that exhibit broad and overlapping substrate specificity.(26,27) Many distinct forms of this enzyme have been isolated and characterized, and evidence exists that these cytochromes are distinct gene products. Variation of the multiple forms arises from slight variation in the protein sequences (or primary structure) although some structural homology has been observed in all forms examined to date.(25)

The bacterial P-450_{cam}, and two rabbit microsomal isozymes were the first purified forms submitted for amino acid analysis.(28,29) The results indicate that the compositions are very similar; the content of non-polar residues, particularly leucine is very high. Cysteine is also present in at least four equivalents per polypeptide. Only one of the cysteine

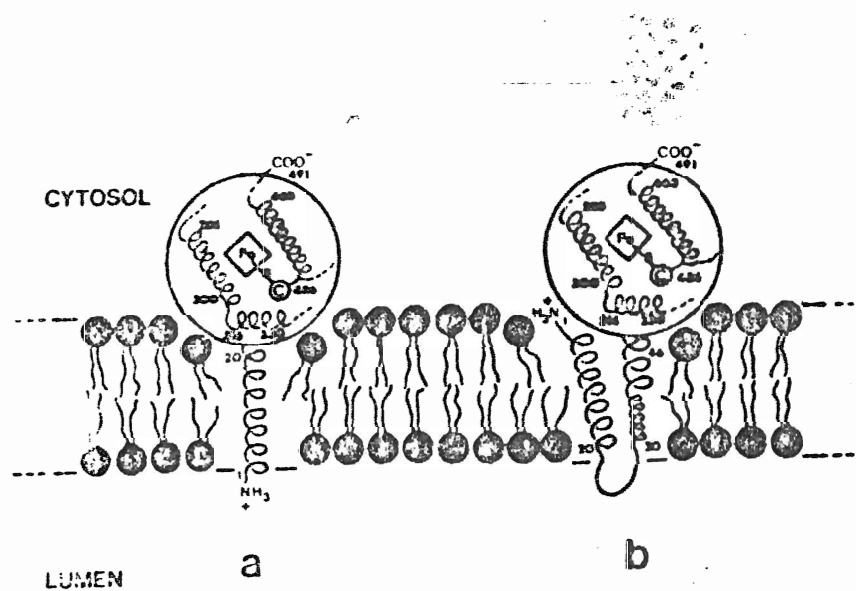


Figure 7. Proposed Cytochrome P-450 membrane interactions. (25)

residues, Cys 436 (rabbit isozyme 2) and the region surrounding it are conserved in all known primary structures. This suggests that this residue or its equivalent in other forms of P-450 may provide the fifth or proximal ligand to the heme.(30) This hypothesis has now been established by X-ray crystallographic studies performed with crystalline P-450_{cam}.(31)

The catalytic activity of the P-450 enzyme system begins with the binding of the substrate by the enzyme in close proximity to the heme prosthetic group. The regio and stereoselective nature of the oxidation process suggests that constraints exist for the orientation of the substrate in the active site.

In LM2, a P-450 isozyme obtained from phenobarbital induced rabbit liver, White et al. (32) demonstrated a correlation between the substrate induced spectral binding properties and the hydrophobicity of a series of small phenyl alkane molecules. A deviation occurred in the binding of 1-phenyloctane from that predicted based on its hydrophobicity. The study suggested a large active site, but not so large as to permit indiscriminate binding, with random orientation of all molecules.

II-1 Cytochrome P-450_{cam}

Currently, the best method for elucidating the 3-dimensional architecture of the active site of an enzyme is through high resolution X-ray crystallography. The problem with most P-450 systems is that crystals suitable for such a technique are not readily obtainable. Isolation

and purification of these enzymes has proved to be a very difficult task at best and this difficulty may be due to the interaction with the lipid bilayer.

The P-450 system of *P. putida* on the other hand, is not a membrane bound enzyme, and has been successfully obtained in a crystalline form suitable for structural analysis. The structure of P-450 cam was obtained by Poulos et al (31) (Figure 8) and provides a wealth of information about this system.

The heme group in this system is located between proximal helix L and distal helix I (Figure 8), the thiolate (fifth iron ligand) extending from the N-terminal end of the proximal helix. The cysteine residue forming the proximal heme ligand, as compared to several other sequences of P-450, is located in the most highly conserved region of the peptide chain. It is situated in a pocket formed by Phe, Leu, and Gln residues. Examination of other P-450 forms indicated similar if not identical arrangement of the residues on the proximal heme surface. Consequently, the heme is situated in this hydrophobic pocket except for contact of the protoporphyrin propionates with Arg, His, Gln and Asp residues (figure 9).(31) It is interesting to note that the prosthetic group is completely buried inside the polypeptide, with no portion of the heme exposed to the enzyme surface. The heme cannot accept reducing equivalents by direct contact between prosthetic groups, and must therefore receive electrons via a protein conduit.(33,34,35,36,37)

The arrangement of camphor in the active site is depicted in figure 10.(31) The substrate sits approximately 4 angstroms above pyrole ring A. The carbonyl group of camphor is hydrogen bonded to Tyr 96 and is directed away from the heme center, thereby controlling the

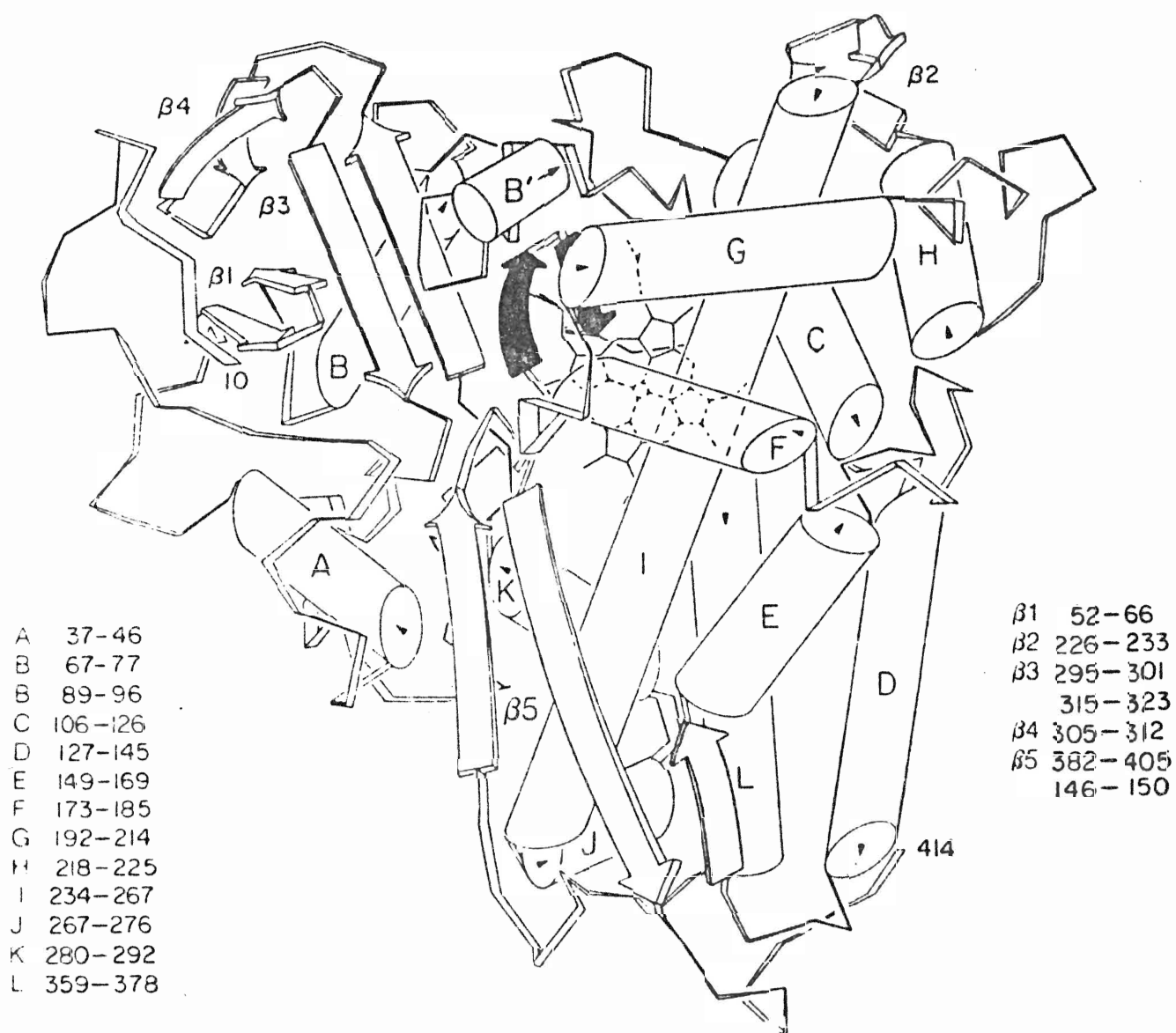


Figure 8. A representation of P-450_{cam}. Helices are indicated as cylinders, and β structure by arrows. (31)

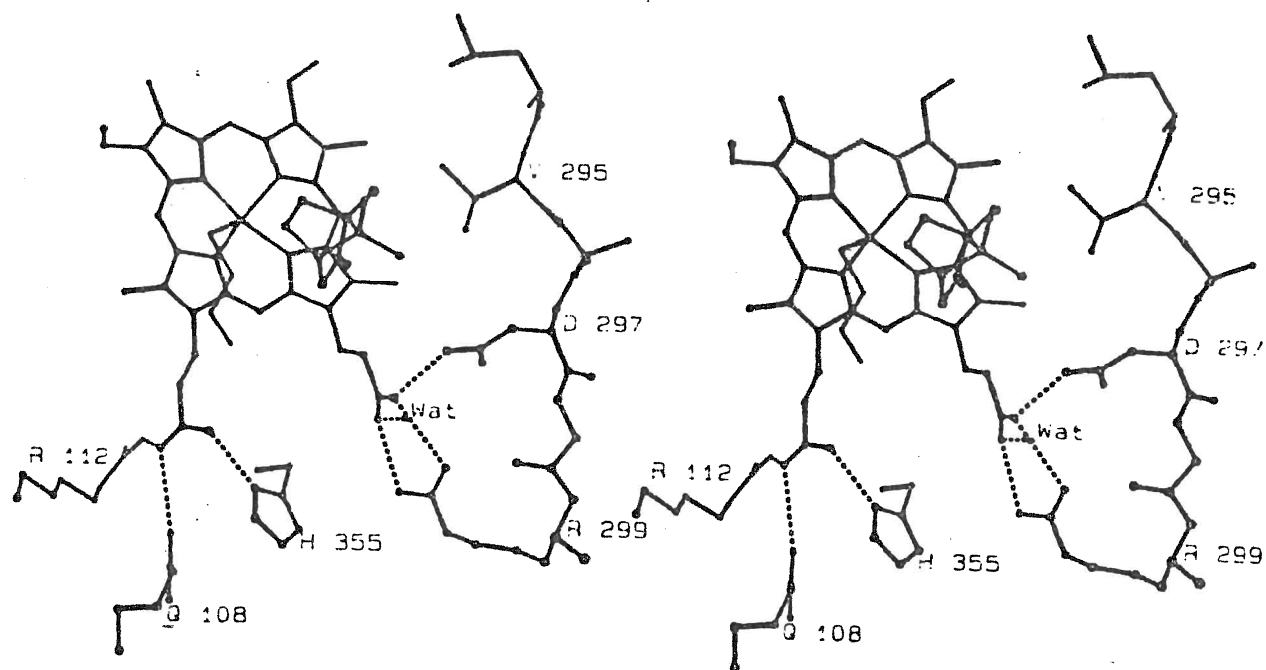


Figure 9. Interaction of the heme propionate groups with surrounding hydrogen-bond donors. (31)

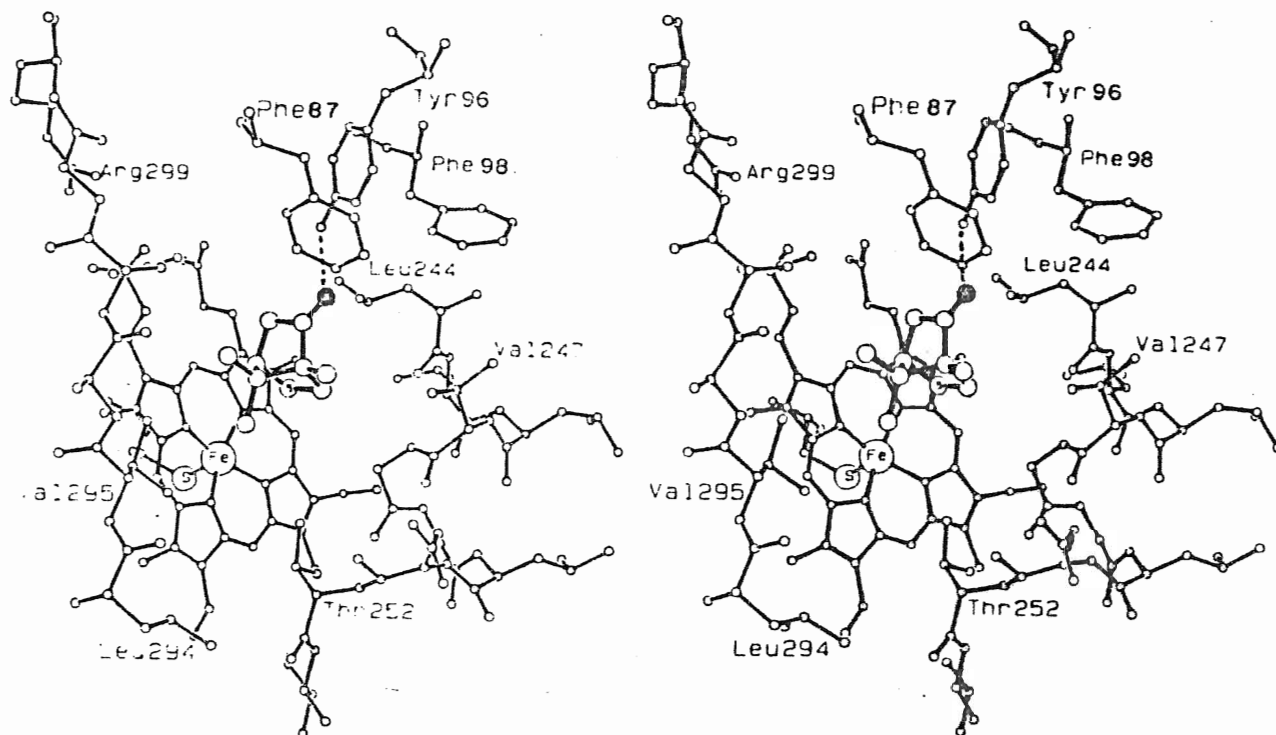


Figure 10. The active site of P-450_{cam} with camphor, showing the interaction between Tyr 96 and the camphor carbonyl (black atom). (31)

regiochemistry by positioning C5 of camphor towards the active center. Several hydrophobic interactions with neighboring residues assist in positioning the substrate and account for the stereochemistry of the hydroxylated product.

The substrate itself is buried deep within the tertiary structure of the enzyme, with no visible means of arriving there. A distinct depression and small opening exist above the camphor molecule, but do not appear large enough to accommodate the migration of the camphor molecule into the active site (Figure 11). Because the site is known to process larger molecules (38) it is assumed that this portion of the enzyme is flexible enough to allow access.

The portion of the distal helix above the heme consists of a hydrophobic segment, which also seems to be the case in several other P-450 systems.(39,40,41,42,43,44) The normal helical hydrogen bonding pattern is modified in this region above the heme suggesting a local deformation in this area. Although the hydrophobic nature of the segment is conserved, the specific residues are not, suggesting a correlation between the amino acid sequence in this region and the substrate specificity of the particular isozyme.

The left half of the enzyme (Figure 8) or helical-poor domain has been postulated as the location of the primary variable sites controlling substrate specificity. The helical rich domain consists of a more rigid tertiary structure which would be relatively inflexible, whereas the helical poor domain would be more susceptible to variation in the topography due to poor helical content and lack of secondary structure.

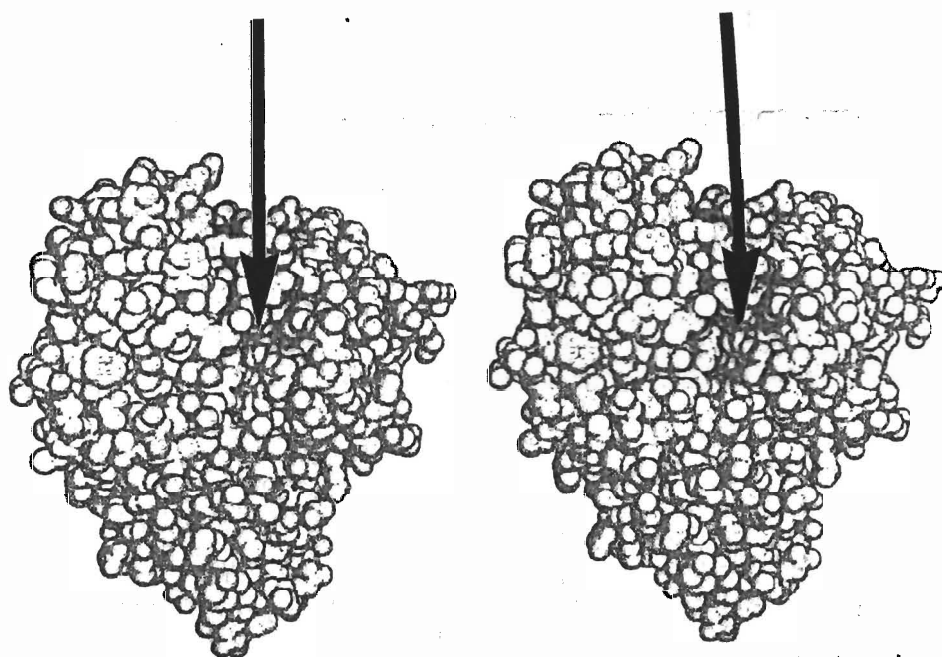


Figure 11. Space filled stereoscopic representation of P-450_{cam} showing the proposed substrate access channel. (31)

III Modeling the Active Site

The convenience of cytochrome P-450_{cam} (i.e. crystallizable) is not shared by any of the other P-450 systems examined to this point. Mapping of the active site topography in the latter cases must be obtained by indirect methods, and careful extrapolation of information obtained from the P-450_{cam} enzyme.

Several models specific to individual organisms and substrate groups have nevertheless evolved in order to form a picture to better understand a particular system. The importance of these models lies in predicting the regio and stereochemistry of oxidation of new substrates by microorganisms whose reactions for a series of compounds is known.

The most thoroughly studied group of substrates in oxidative biotransformation is the steroids. The vast majority of hydroxylations occur at sites which are remote from the existing functionality in the steroid nucleus. The products however show a definite spatial relationship to these functionalities in most cases.

One such model was developed by the Oxford research group of Sir Ewart R. H. Jones for the fungus *Calonectria decora* .(45) The data for this model were obtained by utilizing steroid substrates with hydroxy and/or carbonyl functionalities in defined locations, and systematically varying these locations. A series of ketosteroids, diketosteroids, and steroid alcohols was employed and the pattern of hydroxylation was established. (46,47) A geometrical relationship was established (figure 12) which was then extended to other steroid nuclei, and shown to correlate well. This model was also extended to hydroxylation of steroids by different microorganisms, such as *Rhizopus nigricans* (48,49), *Rhizopus arrhizus*

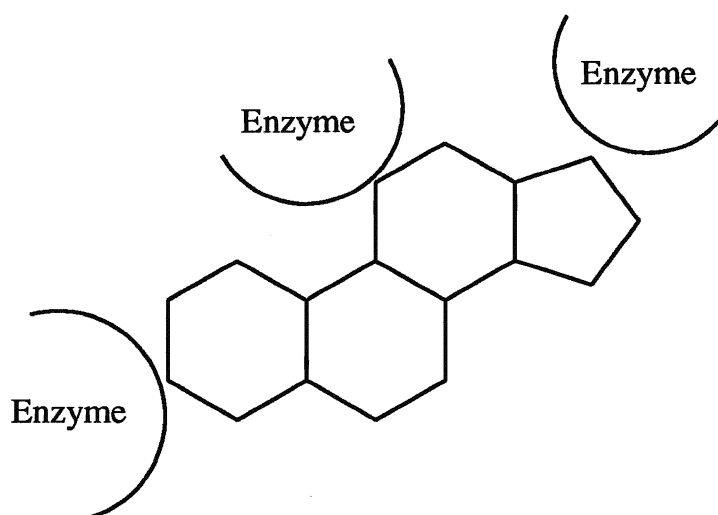
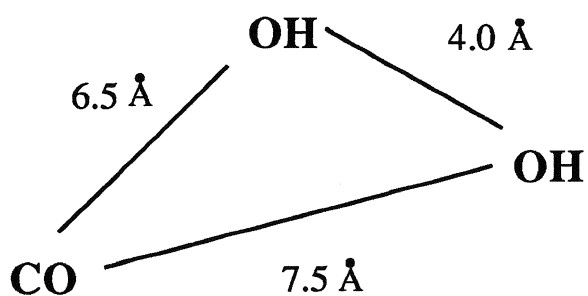


Figure 12. Geometric and schematic representations of the relative positions of binding sites and hydroxylation in *Calonectria decora*.

(50), *Wojnowicia graminis* (51), *Ophiobolus herpotrichus* (51), *Deadalea rufescens* (52), and *Leptoporus fissilis* (53) and again results correlated well with the proposed model. Although in the case of *R. nigricans* the dimensions differ from those of the original study with *C. decora*, the triangular relationship on the enzyme surface of three sites (corresponding to C-3, 11, and 16 or C-3, 7 and 16 in *R. nigricans*) with both binding and hydroxylating capabilities was observed. The keto group of the steroid being bound by one of the sites, the other sites hydroxylate the position of the nucleus which is in its vicinity. The tendency of most ketosteroids to give dihydroxyketones parallels the behavior of *C. decora*. Addition of a second oxygen functional group, causes the dioxygenated substrate to become bound so as to maximize the hydrophilic interactions between the two functional groups and two of the three binding sites, the third hydroxylating the closest carbon. Extension of the triangular model to difunctional compounds was complicated by the fact that the difunctional substrates are bound at two points and hydroxylated at a third. The two point binding gives rise to the possibility of four different orientations of the substrate in the active site (Figure 13) allowing for the possibility of four products. The regio and stereochemistry are defined by other interactions within the active site.

A similar rationale has been used to explain the hydroxylation of 1,4-cineole by *Bacillus cereus* (54). The methyl and isopropyl groups limit the ways in which the substrate can become oriented in the active site. The model produced to explain the observed results is shown in figure 14. Polar interactions do not play an important role in this case as there is no preferred orientation for the oxygen bridge, implicating a strictly

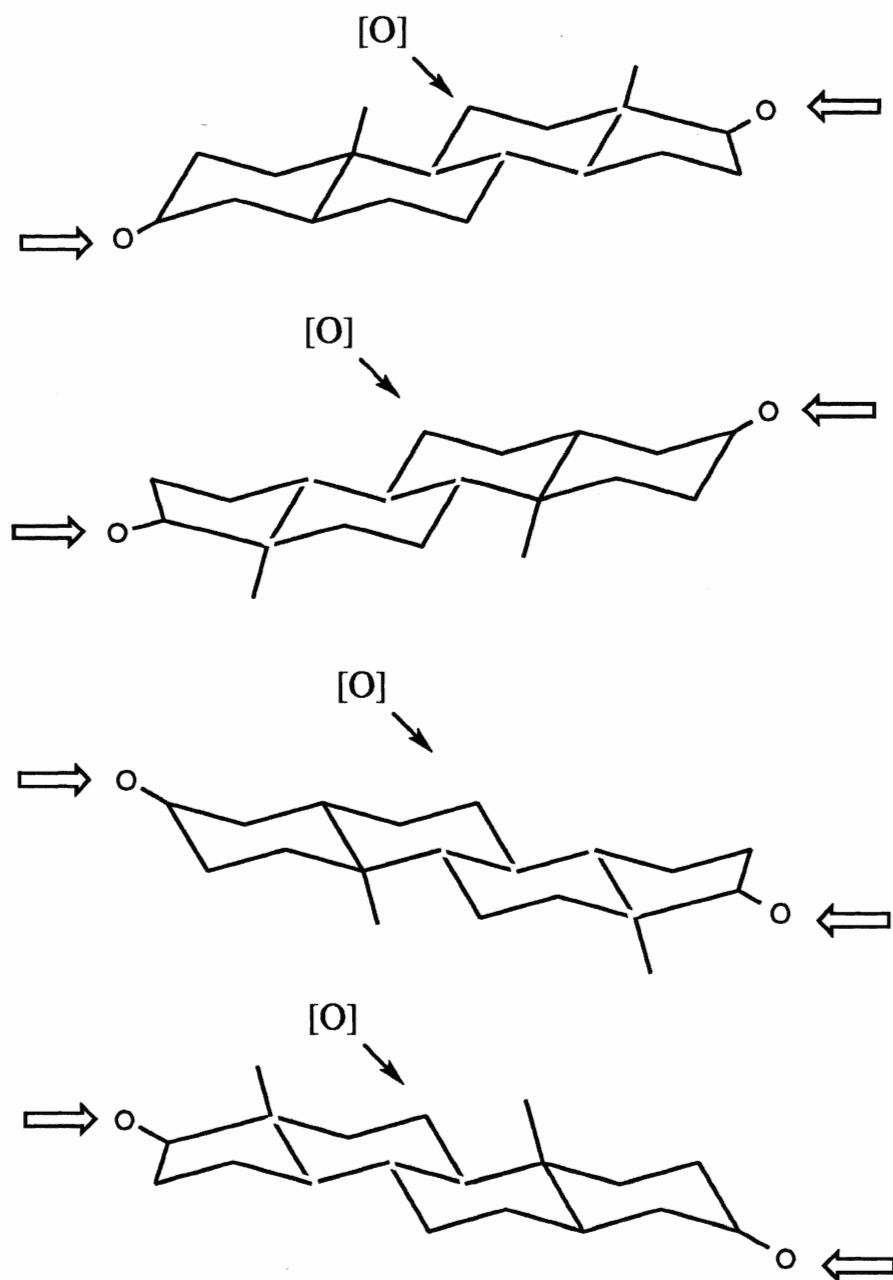


Figure 13. Possible orientations of the steroid nucleus in the active site accounting for the observed products.

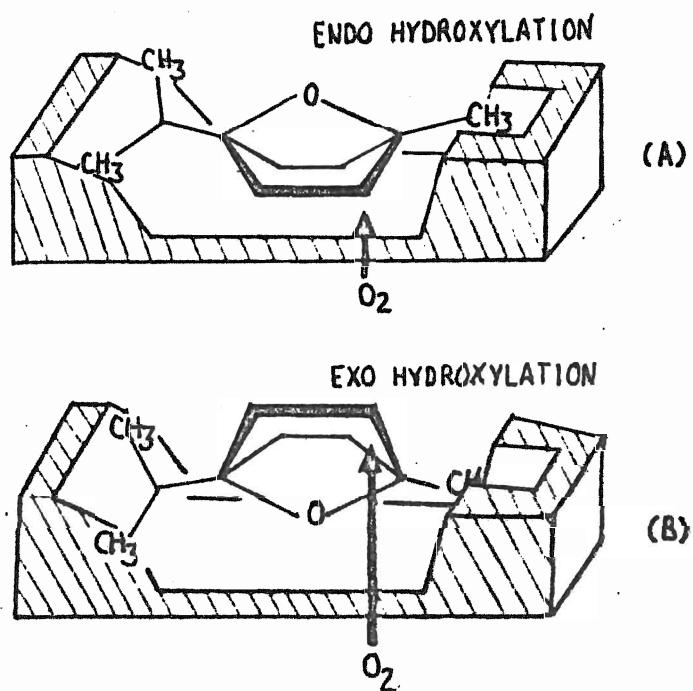


Figure 14. A model for the hydroxylating enzyme of *Bacillus cereus*. (54)

hydrophobic interaction between enzyme and substrate. This non-polar binding mode is also exhibited by *Cephalosporium aphidicola* (55) in the hydroxylation of aphidicolan-16 β -ol (figure 15) allowing two orientations of the substrate with no preferential positioning (i.e. polar interactions) of the hydroxy function, and the hydroxylation of liguloxide (figure 16) by *Streptomyces purpurescens* (56)

The earliest indication that the regiochemistry of biocatalytic reactions could be influenced by the position of functionality in the molecule, was shown by Fonken et al. (57,58,59,60,61,62,) and later refined by Furstoss et al. (63,64,65,66)

A series of cyclic amides was incubated with *Beauveria sulfurescens*. From the data obtained the existence of an enzyme-substrate complex was postulated in which the hydroxylation occurs at a position approximately 5.5 angstroms away from an electron rich center in the substrate. Figure 17 shows the first generation model proposed to account for the position of hydroxylation of the selected substrates. This model has subsequently been refined to account for the formation of multiple products, and for the observed chirality in the products, but the overall features remain the same. Two representations of this model are depicted in figures 18 and 19. The models for this substrate-enzyme interaction propose a three point contact between the enzyme and the substrate: a polar coordination of the amide function, hydrophobic interactions between the aromatic portion of the molecule and non-polar residues in the active site and spatial and hydrophobic requirements of the cyclic portion of the substrate.

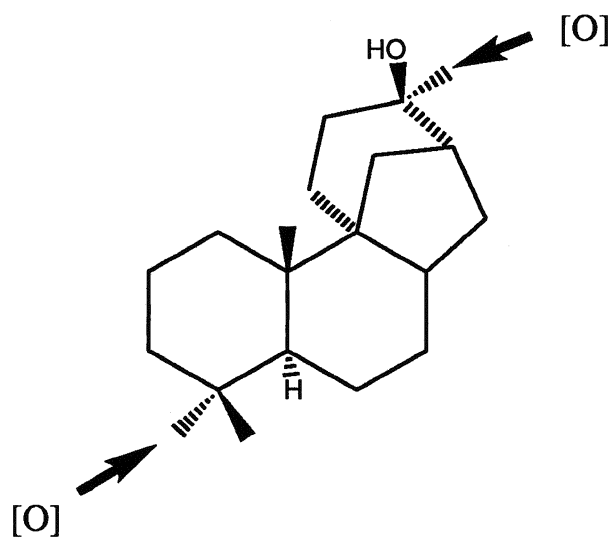


Figure 15. The positions of hydroxylation of aphidicolan-16 β -ol by *Cephalosporium aphidicola*. The lack of a preferential orientation demonstrates a non-polar binding mode between enzyme and substrate.

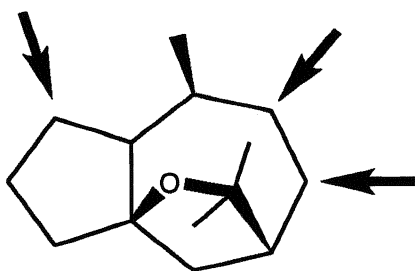
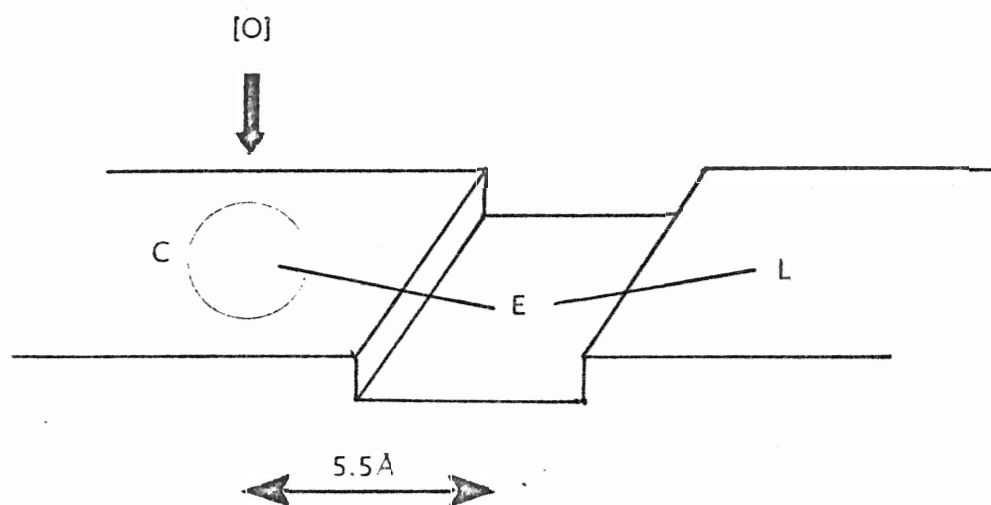


Figure 16. The hydroxylation of liguloxide by *Streptomyces purpurescens* shows a lack of preferred regiochemistry demonstrating a purely hydrophobic binding interaction.



C = cyclic system; E = electron rich group; L = lipophilic group which can incorporate C
[O] = site of hydroxylation

Figure 17. Original model developed to account for the hydroxylation of cyclic amide substrates by *Beauveria sulfurens*.

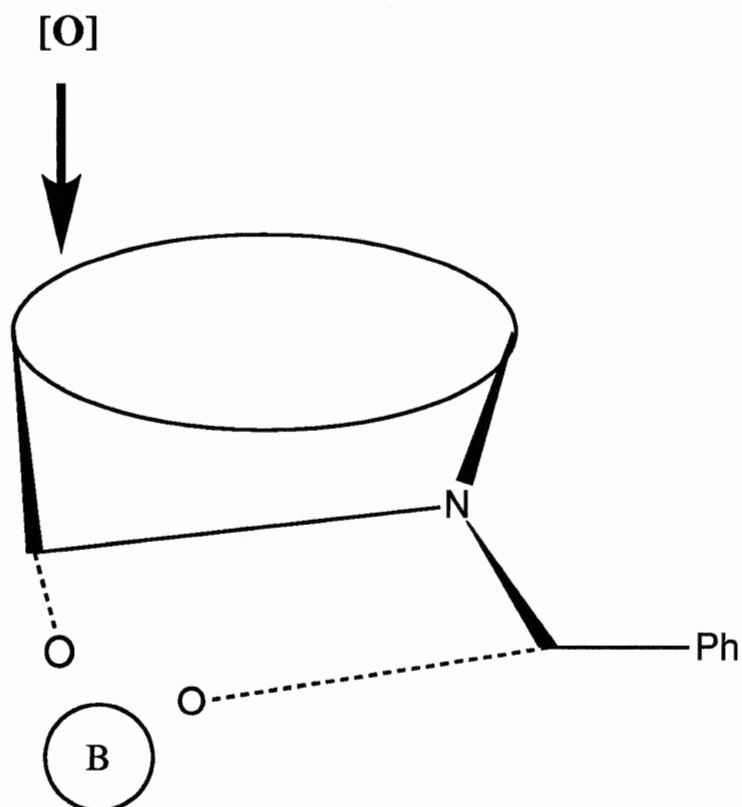


Figure 18. Second generation model for hydroxylation of cyclic amides by *Beauveria sulfurescens*, refined with more flexible dimensional limits and the introduction of absolute stereochemistry.

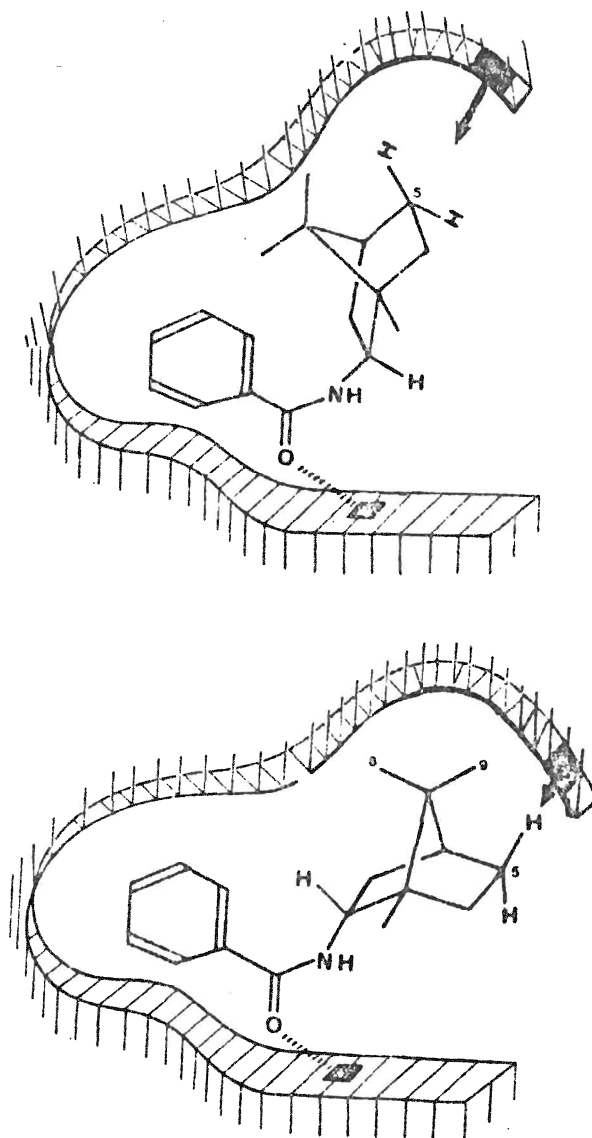


Figure 19. Second representation of the refined model of the active site of *Beauveria sulfurescens*.

The predictive value of this model has been demonstrated for the microbial hydroxylations of a series of adamantanes containing amide functional groups (67) and other cyclic amides.(68,69) The key elements of this particular model are that there is definitely an interaction between an electron rich center in the substrate and an electrophilic center in the enzyme, providing orientation to the substrate that is responsible for the observed regiochemistry of the products; and secondly, the hydrophobic and spatial interactions provide the second degree of positioning of the substrate, which is implicated in providing stereoselectivity to the products obtained. This situation can be compared to the interactions between P-450_{cam} and the camphor molecule in its respective active site.

III-1 Mortierella isabellina

Studies involving the fungus *Mortierella isabellina* NRRL 1757 have been ongoing in our lab for several years in view of its ability to perform the oxidation of aryl and benzyl sulfides (20,70,71), benzylic hydroxylation of ethyl benzenes, and related compounds (16,17,18,19), as well as more complex substituted aromatic compounds.(20,72,73,74) Useful models have been developed for both sulfide oxidation and benzylic hydroxylation.

It has been shown in the oxidations of aryl and benzyl sulfides that the aromatic ring plays an important role in the orientation of the substrate in the active site. This can be exemplified by the results obtained from the biocatalytic turnover of 2-phenyl-1,3-oxathiolanes (figure 20) to produce the corresponding sulfoxides.(75)

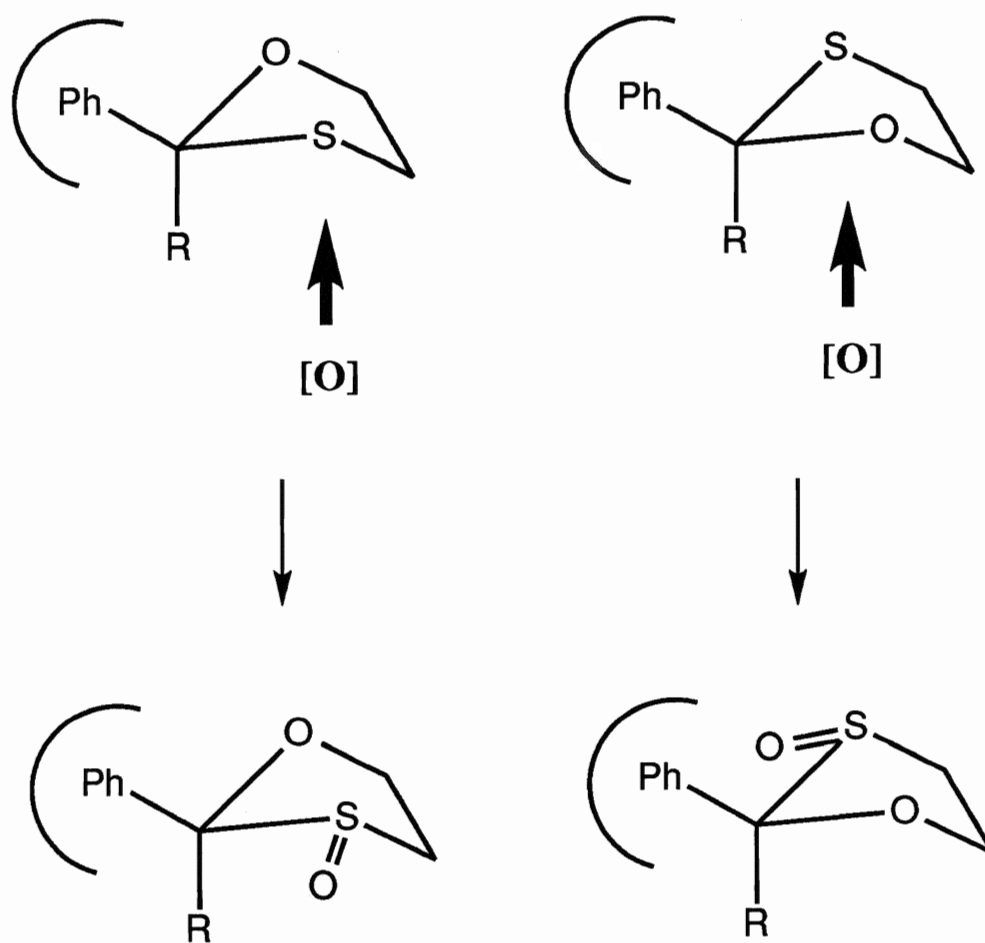
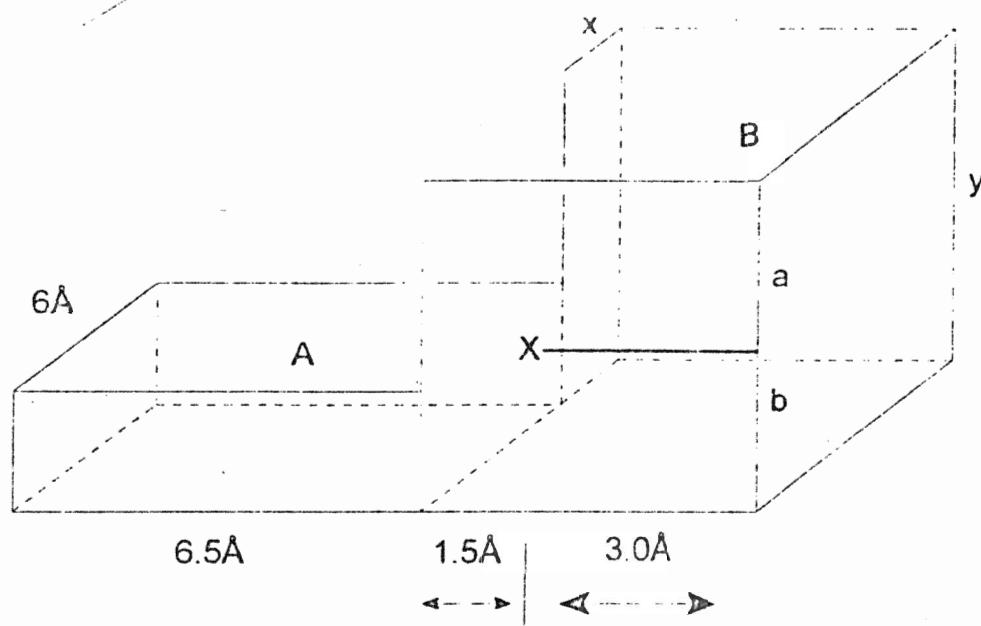


Figure 20. Oxidation of 2-Phenyloxathiolanes by *Mortierella isabellina*.

Similar results are obtained in the benzylic hydroxylation of acceptable substrates by *M. isabellina*, and a model for these oxidations has been proposed (figure 21).(21) A large number of aromatic substrates was examined, generating data useful in defining the substrate specificity of the benzylic hydroxylase of this enzyme. The features that lead to the development of the model are: the inability of the enzyme to process 1-ethylnaphthalene or 2-ethylanthracene while 2-ethylnaphthalene is a good substrate; a limit of a four carbon ring in the phenyl cycloalkane series; the inability of the enzyme to hydroxylate 2-phenylbutane or ortho substituted ethylbenzenes larger than 2-ethyltoluene; and the efficient hydroxylation of indan and tetralin but the absence of products from fluorene and acenaphthene.

The model proposed includes an aromatic binding pocket, approximately one carbon-carbon bond length away from the active oxygen species. A second region accommodating the aliphatic portion of the molecule also contains the oxygen-iron center, which must lie slightly above the plane of the aromatic ring (as depicted in the model diagram) in order to abstract the pro R hydrogen and account for the observed, predominant stereochemistry of products obtained.

The models presented here have been developed by the accumulation of data related to the particular organism, and put forth to account for these data. Extension of these models to other systems must be viewed very carefully, although the application of the *Calonectria decora* model for steroid hydroxylation to other fungal systems has been promising (76). The general similarities observed in the models for hydroxylation are beginning to form a more unified view of this class of enzymes as a whole.



A: aromatic binding pocket

B: aliphatic binding region

X: oxidation centre

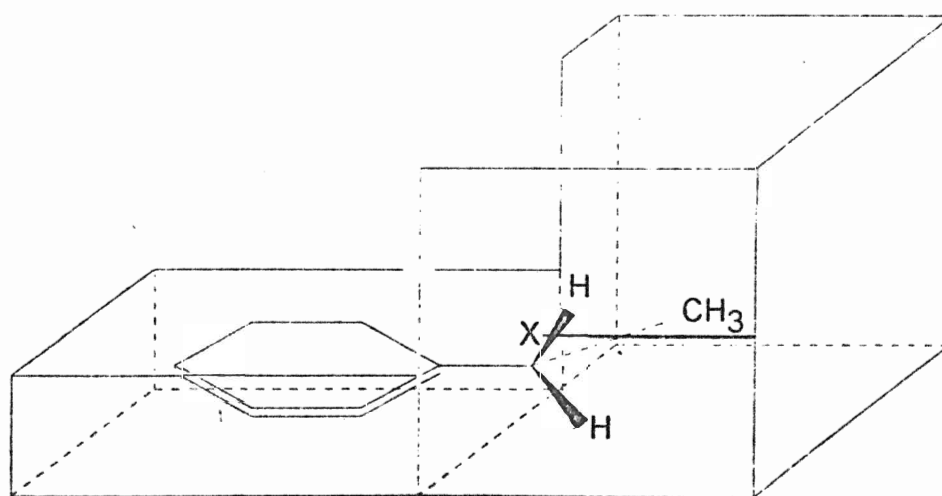


Figure 21. Active site model developed for the oxidative reactions performed by *Mortierella isabellina*.

Several key features, such as a three point interaction between the enzyme and the substrate, the fact that efficient binding requires both polar and non-polar interactions, and the proposition of multiple binding modes for a substrate are all recurring themes.

The information available for microbial hydroxylase enzymes does not begin to approach the wealth of information accumulated for mammalian systems or the camphor hydroxylase of *P. putida*, but many of the important features in the control of product formation seem to be common factors, and one may carefully extrapolate information from this data base.

Although the predictive value of these models has met with some success, one must be aware that in the absence of definitive information, it can only be assumed that the reactions performed on a particular group of substrates are the work of a single enzyme. The models have been developed to account for observed experimental data, and may not reflect the actual details of the active site. They are nevertheless useful in predicting the outcome of the microbial oxidative process. In the absence of more detailed information, such as is available for isolated enzymes, these models are currently the best method available to rationalize our observations with regards to microbial hydroxylation.

IV Current Research

The work presented in this thesis is a continuation of the development of the active site model for *M. isabellina* and has attempted to generate a more complete picture with regards to the oxidative function of the benzylic hydroxylase of this particular fungus. Substrates have

been chosen to test the dimensional limits of the active site, and to generate new data to quantify the three dimensional structure of our model.

The dimensions of the aromatic binding region of the active site have been examined using o-, m-, and p- substituted ethylbenzenes. Varying the size of the substituent in these positions has allowed the determination of the largest aromatic group acceptable into the active site and hence a dimensional limit of the aromatic binding pocket for acceptable substrates.

The width of the aromatic binding region has been examined using 2- and 3- substituted fluoroethylbenzenes and ethyltoluenes, 1,2,3- and 1,3,5- trimethylbenzenes, as well as information previously obtained.(18,21) The length has been examined using 4-ethylbiphenyl and 4-*tert*-butylethylbenzene.

The front end probes used for examining the second aliphatic binding region of the active site are divided into two groups, non-rigid which consist of alkyl and cycloalkylphenylmethanes and the rigid front end probes consisting of substituted indan and 1,2,3,4- tetrahydronaphthalene analogs as well as some fused ring systems and spirocycloalkanes. The various directional requirements of these substrates have provided much information on the architecture of this region.

RESULTS AND DISCUSSION

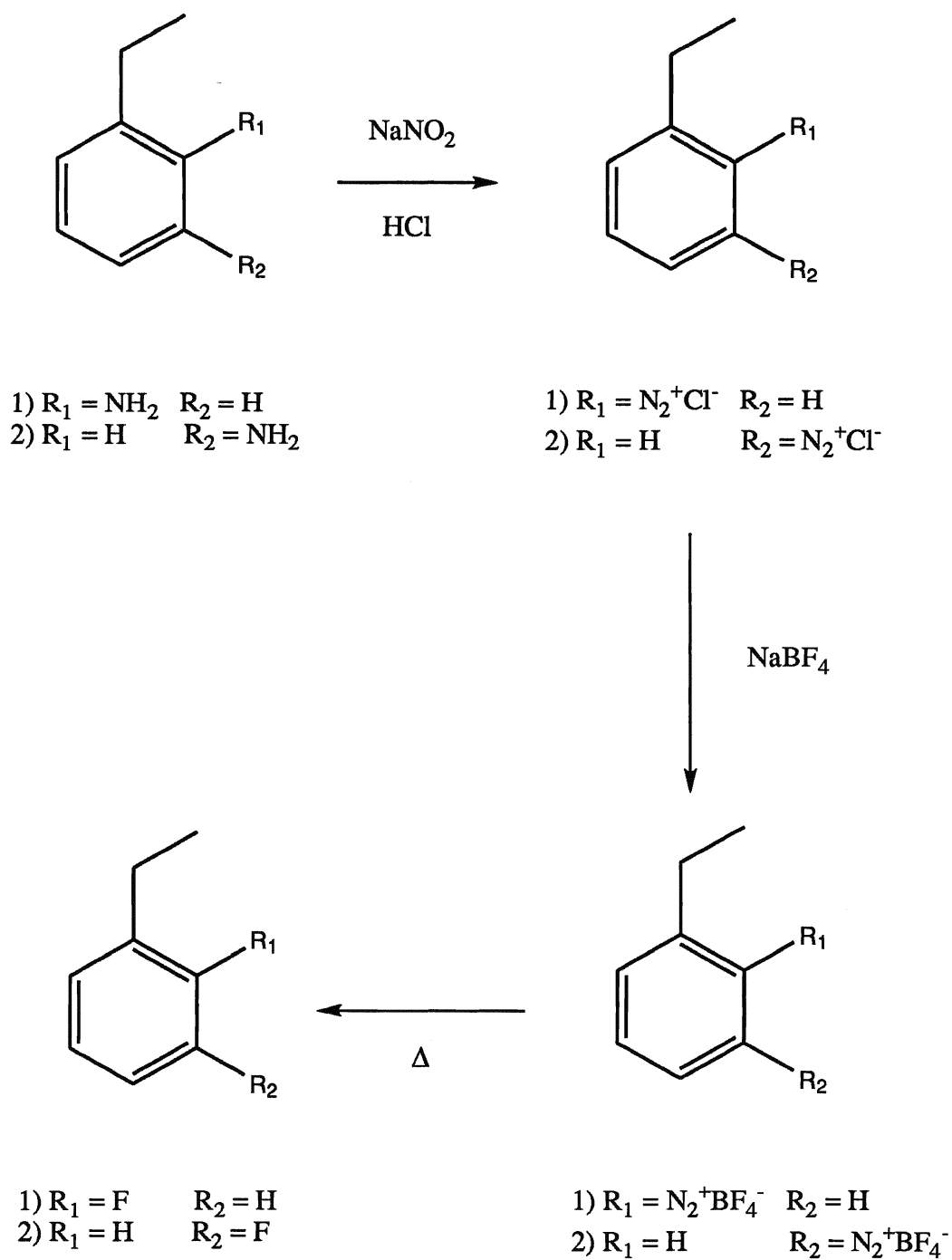
I Preparation of Substrates

I-1 Ortho and Meta Fluoroethylbenzene

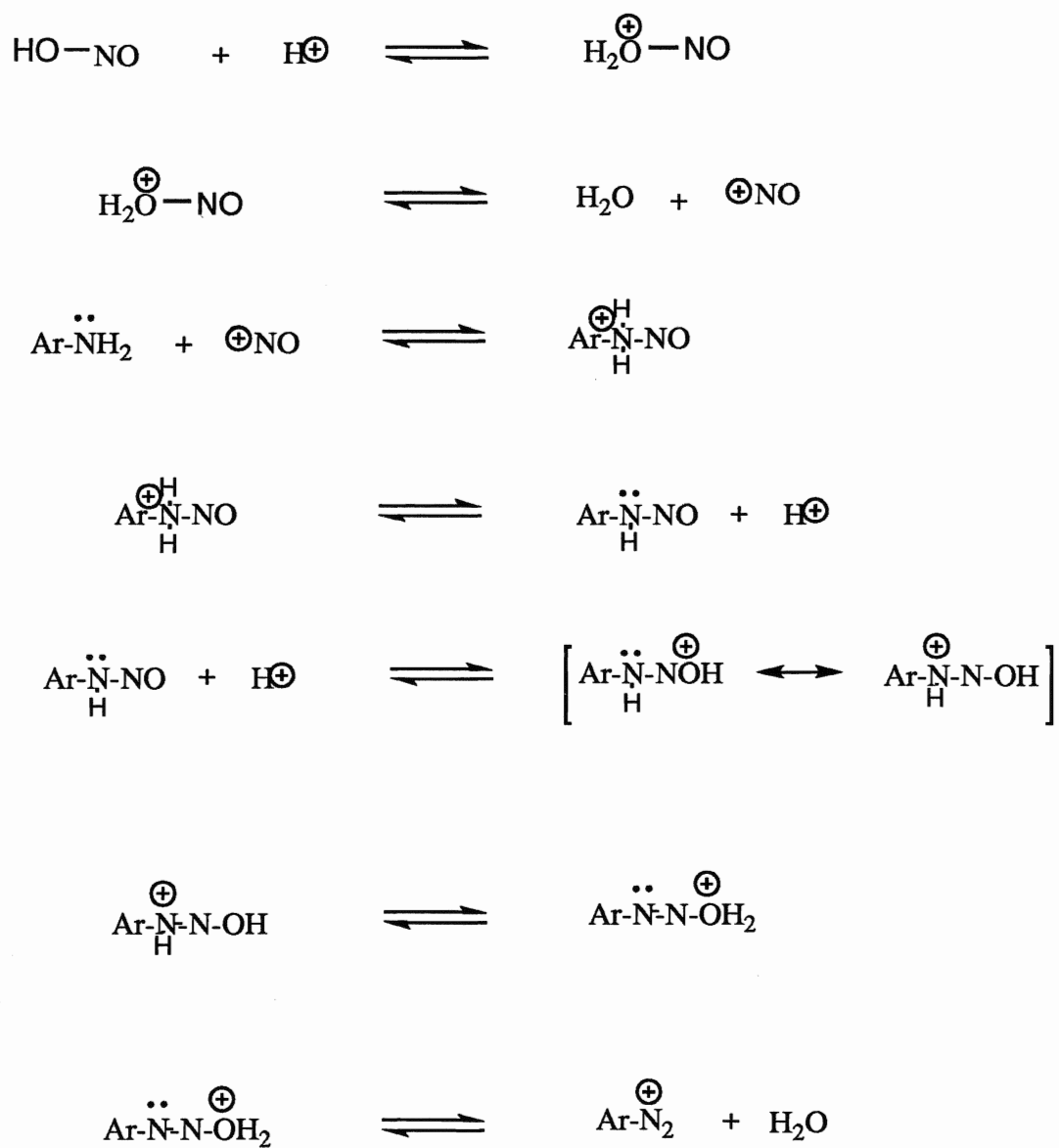
Among the methods available for introducing a fluorine atom into the aromatic ring, the Balz - Schiemann reaction (77) is one of the most widely used. The merits of this reaction stem from the remarkable properties of the aryl diazonium fluoroborate salts. Unlike other diazonium salts, they are not soluble in water, are easily dried on exposure to warm air, and are stable to shock and friction which allows for safe handling and large scale production. In general, most aromatic amine that can be diazotized, will form a BF_4^- salt, in high yields in most cases.

The target compounds 2-fluoroethylbenzene 2 and 3-fluoroethylbenzene 3 were prepared in a 3-step, 2-pot reaction starting from the substituted anilines (scheme 1). The amine is first converted to the hydrochloride salt with HCl, but despite the fact that the reaction is carried out under acidic conditions, it is the small amount of free amine that is the actual species attacked during the diazotization. (78,79,80) At high acidities, the attacking species can be thought of as NO^+ (scheme 2). (81,82)

The aryl diazonium chloride formed in this reaction is soluble under the reaction conditions. Addition of sodium fluoroborate precipitates the diazonium fluoroborate which is then isolated. The two fluoroborate salts prepared in these reactions were isolated in unusually low yields (35 - 38%) as compared to the yields reported in the literature (77), but the



Scheme 1: Synthetic route to ortho- and meta-fluoroethylbenzene.



Scheme 2: The formation of the aryl diazonium cation.

decomposition to form the fluorobenzenes was moderate to good (61 - 77%). The low yields in the preparation of the fluoroborate salts may be partially due to the solubility of the salts formed, or incomplete reaction in the diazotization step of the reaction.

The thermal decomposition of the salts to form the target compounds was self sustaining once the decomposition temperature was reached. Balz and Schiemann (83) made the suggestion that the energy required to dissociate the BF_4^- anion, into BF_3 and F^- , is approximately equal to the energy released in the decomposition of the diazonium cation. Decomposition yields are generally lowest for the ortho substituted compounds in any isomeric series of compounds (77), this trend was also observed in the preparation of the isomeric fluoroethylbenzenes 2 and 3.

The mechanism for the decomposition of the fluoroborate salt was shown to be ionic in character based on studies of the decomposition of these salts in a suitable solvent.(84) The aryl moiety produced during the decomposition of the diazonium salt underwent a substitution reaction with the solvent. The byproducts (other than the desired fluoro compound) were analyzed, and the identity of the intermediate deduced based on the results. Decomposition of the salt in hot nitrobenzene, produced meta-nitrobiphenyl as the only significant product (84). This result demonstrates that the intermediate aryl moiety is electrophilic in nature, whereas a radical intermediate would lead predominantly to the ortho and para substituted products. Additions to olefins also support a heterolytic cleavage by giving products that follow Markovnikov's rules for addition. Although dry decompositions are less understood, studies have

indicated that the fluorination process seems to be intramolecular in nature, as no intermolecular transfer of fluorine appears to occur.(85)

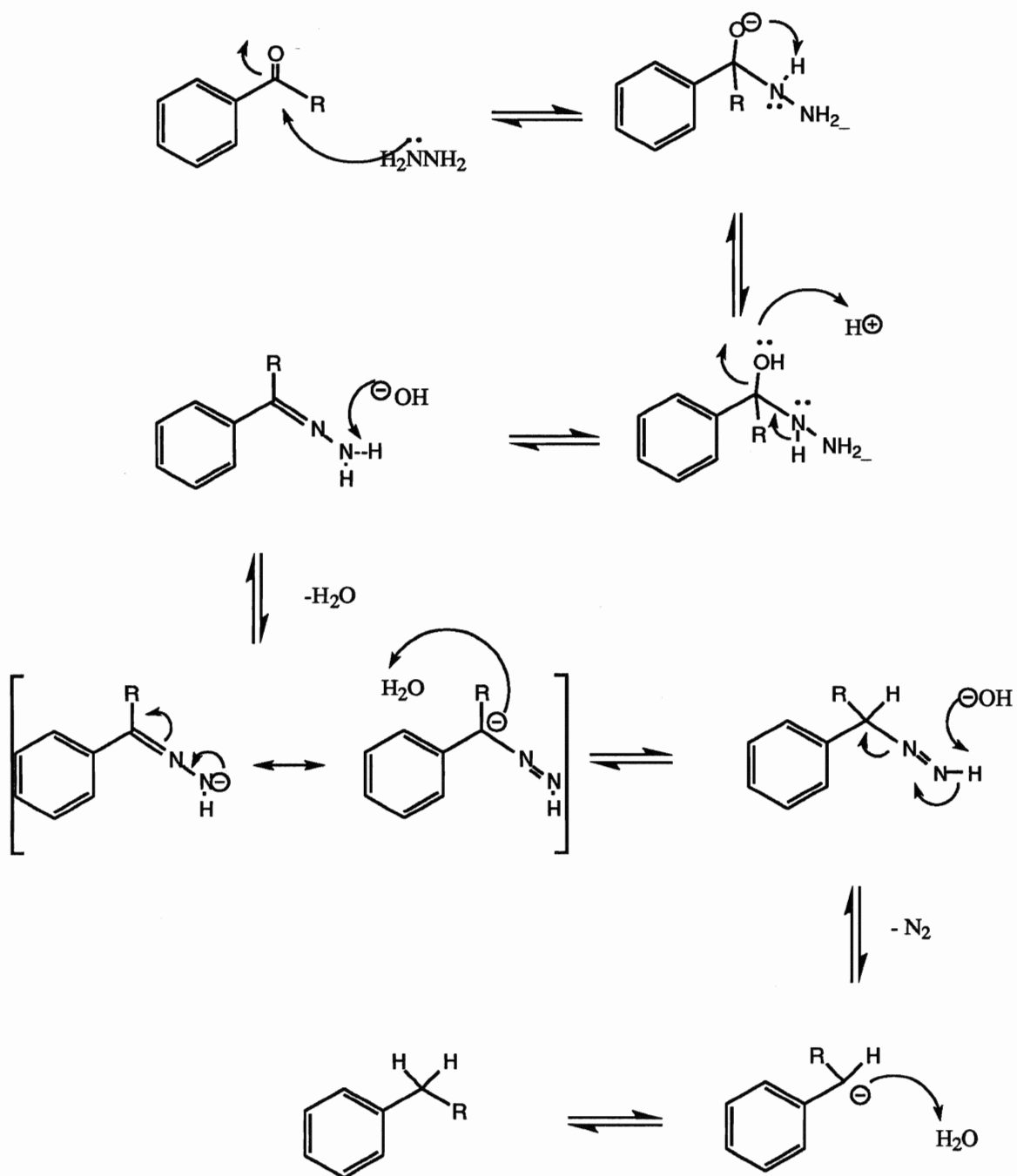
The first attempts at decomposition of the fluoroborate salts were plagued by low yields of the desired fluoro compounds due to the apparent high volatility of these compounds. This problem was overcome by cooling the receiving flask in liquid nitrogen, greatly reducing losses during the decomposition.

I-2 Reduction of Ketone Starting Materials

The readily available keto analogs of substrates 5, 10, 12, and 19 (appendix 1) were reduced to the saturated compounds using the Huang-Minlon modification of the Wolff-Kishner reduction.(86) In the original procedure, the aldehyde or ketone was converted to the hydrazone, and heated in a sealed tube containing sodium methoxide in absolute ethanol. Huang-Minlon improved on the techniques put forth by Soffer et. al. (87) and Herr et. al..(88) The use of diethylene or triethylene glycol as the solvent allows the reaction to be conducted at atmospheric pressure, with hydrazone formation and decomposition performed in a one pot procedure

Condensation of the carbonyl function with hydrazine to form the intermediate hydrazone is the first step in the sequence. The two stage base catalyzed elimination of nitrogen, followed by hydrogen abstraction from water or solvent produces the reduced product (scheme 3).

The yields of the reduced products were moderate to good, with the exception of 10. Several factors could account for this case, including incomplete hydrazone formation, and losses due to the volatility of the formed hydrocarbon at the elevated reaction temperatures.



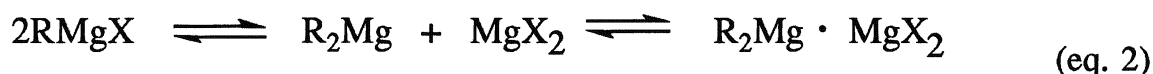
Scheme 3: General route for the production of saturated compounds from the corresponding ketones.

I-3 Rigid Front End Probes

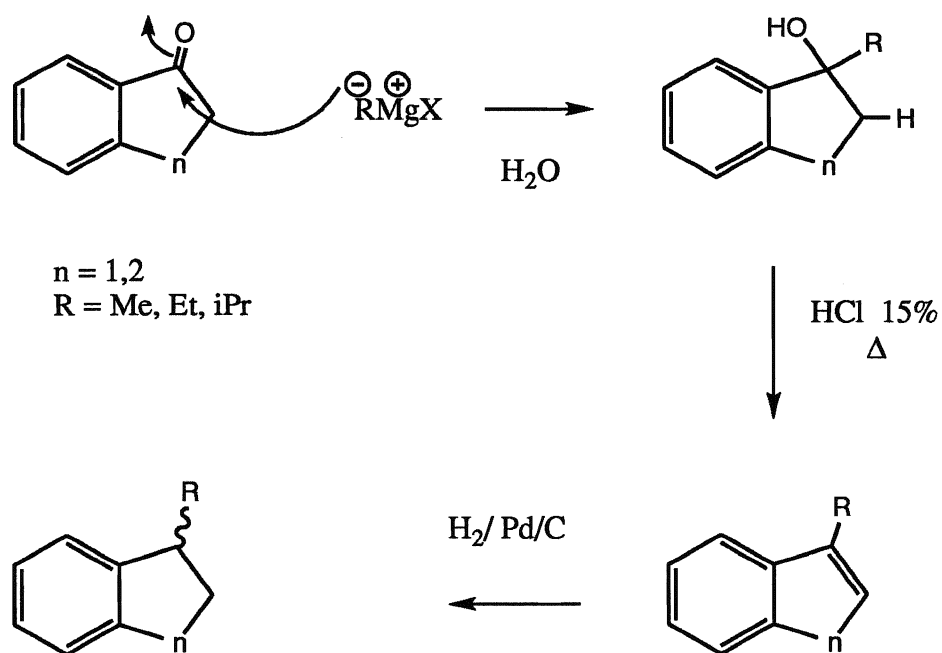
The rigid front end probes (front end refers to the region of the active site other than the aromatic binding pocket, see figure 21 p 36) consisted of the 1-alkylindan and 1-alkyl-1,2,3,4-tetrahydronaphthalene series of compounds, which were prepared in three steps from 1-indanone and 1-tetralone respectively (scheme 4). The initial reaction was a Grignard addition of the required alkyl group (methyl, ethyl, isopropyl) to the ketone, producing the 1-alkyl-1-hydroxy compounds.

The organometallic Grignard reagent is formed using metallic magnesium and the required alkyl halide, the iodide being used in these cases. The Grignard reaction is one of the most widely used methods for the preparation of carbanion nucleophiles in synthetic chemistry. The formation of the reagent is an example of a heterogeneous reaction, occurring at the interface between the two different phases. The reaction of RX at the magnesium surface produces an alkyl radical, and a halomagnesium radical which is associated with the solid surface. The radicals then combine to form the reagent.

The nature of the reagent can be described by the Schlenk equilibrium (89) shown in eq. 2.



The position of the equilibrium varies depending on the identity of R, X, solvent, concentration and temperature. The structure of the reagent



Scheme 4: Synthesis of 1-alkylindans and 1-alkyl-1,2,3,4-tetrahydronaphthalenes.

in solution (ether) at low concentrations is largely monomeric, the coordination sphere of magnesium also being occupied by two molecules of ether. At higher concentrations the molecule can also exist as a dimer or higher polymer.

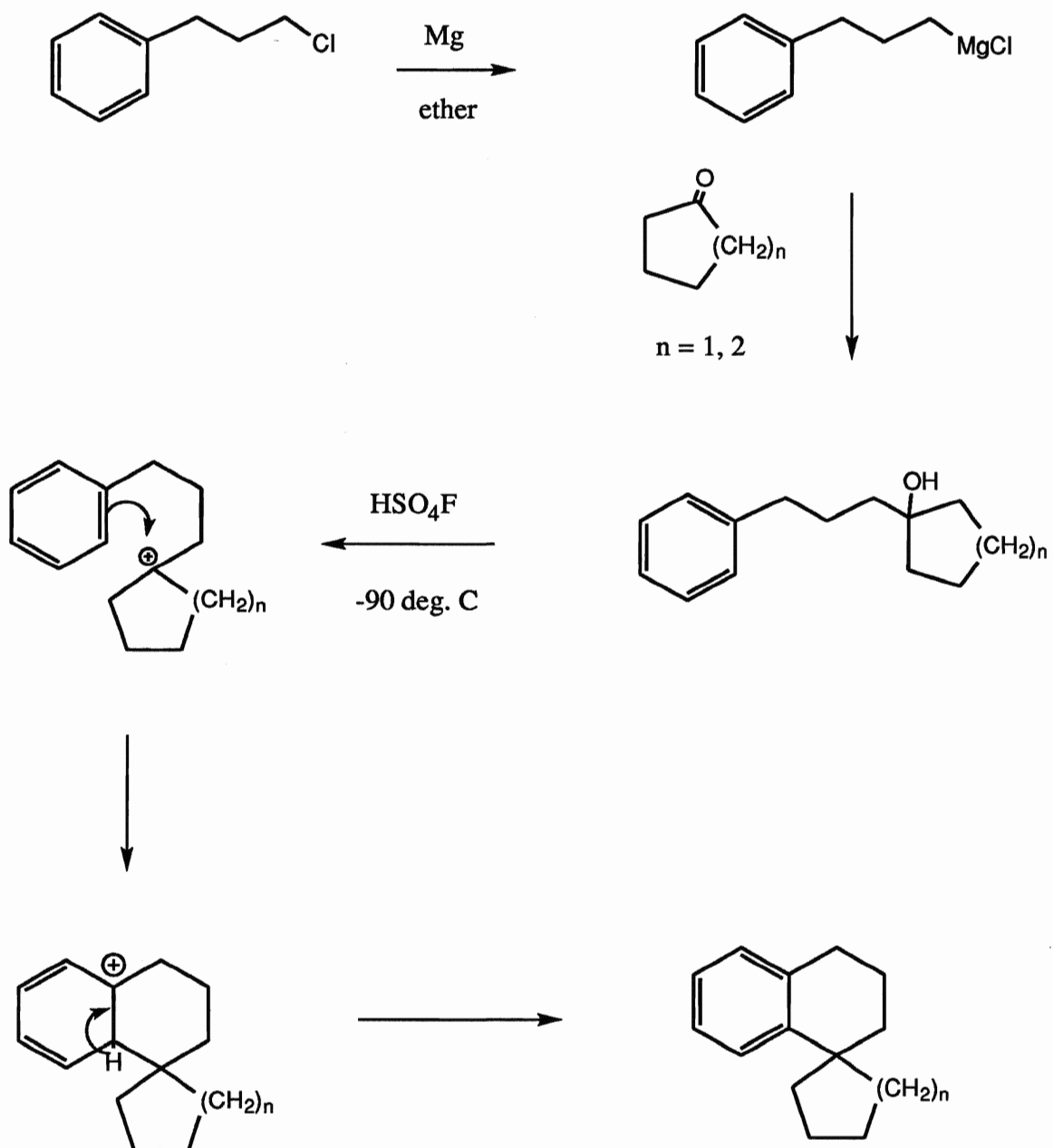
Dehydration with acid catalysis prior to work-up was quite facile, as the elimination of a water molecule produced a stable tertiary cation center. Regeneration of the catalyst by loss of an α -hydrogen produced the conjugated alkenes in a convenient one-pot reaction. Purification by chromatography was done at this point to remove any impurities which might foul the catalyst in the subsequent stage.

Catalytic hydrogenation was performed in ethyl acetate, at 30 psi hydrogen pressure, using palladium on charcoal as the catalyst. The reductions were complete in under two hours, with excellent conversions.

I-4 Preparation of Spiro Compounds

The spiro compounds **20** and **21** were prepared in two stages from 3-phenylpropylchloride using the method of Bright et. al..(90) The Grignard reagent of the chloride was first prepared, and reacted with the desired cyclic ketone to give the respective alcohols in excellent yields (greater than 97%). The alcohols were then treated with fluorosulfuric acid to form the intermediate carbocation which underwent intramolecular cyclization to form the desired spiro compounds **20** and **21** in 72% and 64% yields respectively (scheme 5).

Superacids, the term used for fluorosulfuric acid among others, have been used extensively in the generation of long lived carbocations since the pioneering work of Olah et. al..(91) Under these conditions, the



Scheme 5: Synthetic route for the preparation of spiro compounds.

carbocation can undergo reactions not normally accessible under less strongly acidic conditions. Although carbocations undergo rearrangement readily to form the most stable cation, this was not a problem in these cases as the charge was formed at a tertiary center. The cation then acts as an electrophile towards the aromatic ring to form a stable six-membered ring and hence the desired product.

II Incubation of Substrates

The purpose of this particular study is to test the limits of the various regions of the active site of the benzylic hydroxylase enzyme of the fungus *Mortierella isabellina*. The information extracted from these and all previous incubations with this system allow us to formulate a picture of the active site. The information gathered from the incubations are the yield and stereochemistry of the isolated products.

The yields of the catalytic hydroxylase reactions give us information on the accessibility of the substrate into the active site. High yields allow us to postulate that the substrate has free access to the active site, and low yields are interpreted as a sign of restricted access.

Yields are also affected in general by the ability of a particular substrate to find its way from the aqueous medium, across the cellular membrane, migrate to the organelle where the hydroxylase resides, before its trip down the access channel into the active site can even begin to take place.

Once inside the active site, the question of a particular substrate's orientation and fit inside the pocket can be addressed by observing the stereochemical distribution of the isolated products.

II-1 Aromatic Binding Site Probes

The results of the incubation of compounds 1 through 7 (see appendix I for structures) are listed in table I. The isolated products in these cases were identified by routine spectral analysis, and the assignments were straightforward. The substrates used were chosen to examine the width (1,2,3,6) and (7) and the depth (4,5) of the aromatic binding region of the active site as shown in the model.

The limit of the depth of this region had been determined by Holland et. al. (21), utilizing 2-ethylanthracene as a probe. Only a trace of hydroxylated product (approx. 0.1% yield) was isolated whereas 2-ethylnaphthalene proved to be a good substrate.(18) Figure 22 shows a dimensional analysis of compounds 4 and 5, as well as 2-ethylnaphthalene and 2-ethylanthracene.

The molecular dimensions were defined using Cambridge Scientific Computing Inc. Chem 3D Plus modeling program. All measurements were made from outer shell to outer shell (i.e. Van der Waals radii included) when measuring hydrogen to hydrogen, or center to outer shell when measuring carbon to hydrogen and unless otherwise stated are maximized distances and not planar projections.

In the case of 2-ethylanthracene, only a trace of product was isolated.(21) The aromatic portion of the molecule at 9.5 Angstroms was, for all intents and purposes, crowded out of this binding region, forcing the benzylic carbon out of the reactive sphere of the active iron-oxo species and / or restricting access to the bulk of the substrate into the pocket altogether.

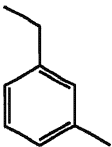
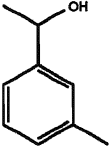
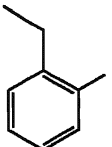
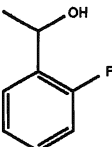
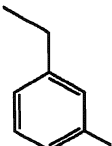
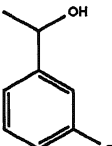
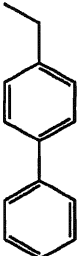
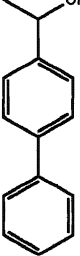
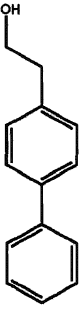
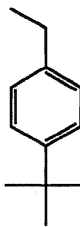

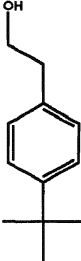
SUBSTRATE	PRODUCTS (YIELD, STEREOCHEMISTRY, EE)	
 1	 1a (1.5, R, 0.0)	
 2	 2a (4.3, R, 52)	
 3	 3a (2.3, R, 18)	
 4	 4a (0.6, R, 52)	 4b (1.0)
 5	 5a (1.7, R, 36)	 5b (0.2)

Table 1: Products of biotransformation of compounds 1 through 7 by *M. isabellina*.

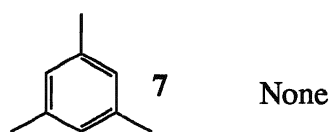
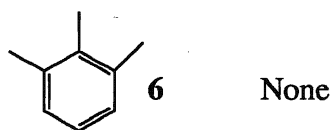
SUBSTRATE PRODUCTS (YIELD, STEREOCHEMISTRY, EE)

Table 1: continued.

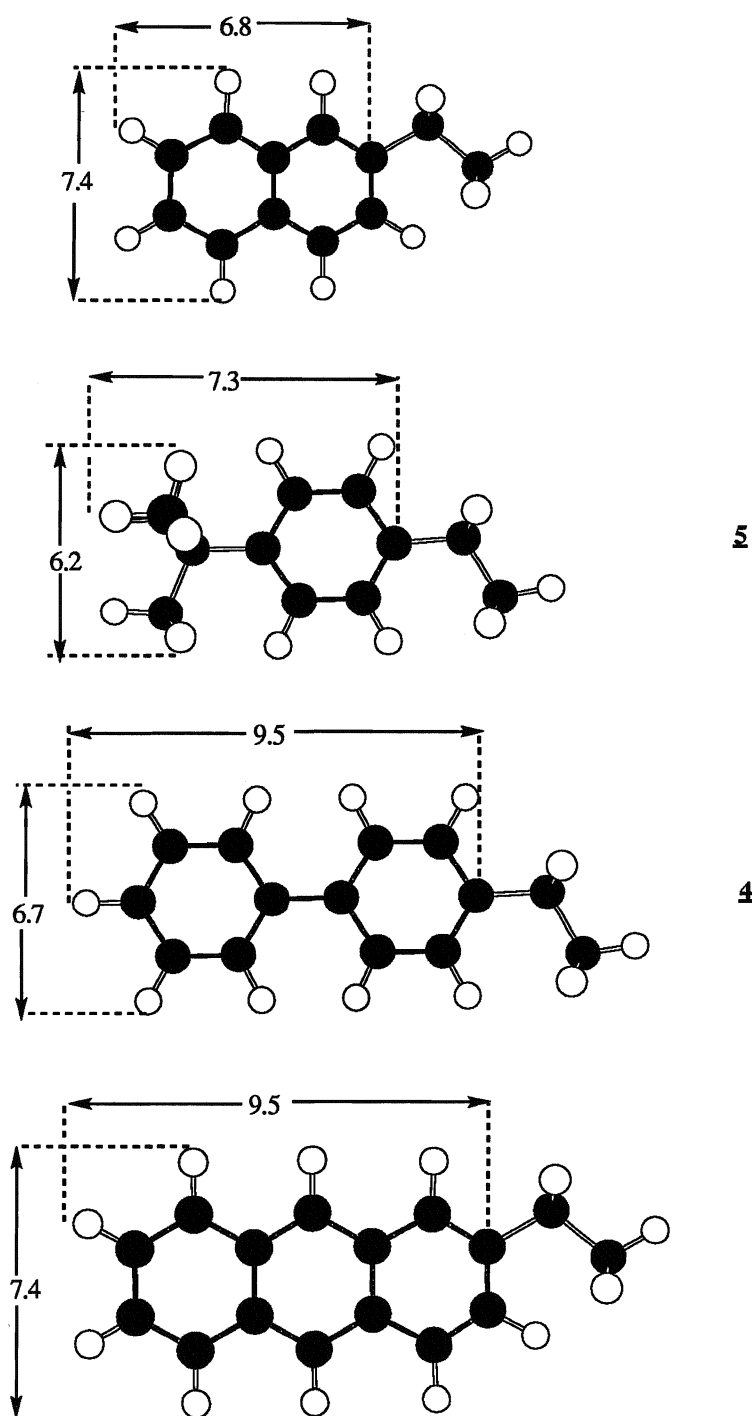


Figure 22: Dimensional analysis of compounds 4 and 5, 2-ethylnaphthalene and 2-ethylanthracene.

The compound 2-ethylnaphthalene however, was processed by the enzyme in an 8% yield, demonstrating that this is an acceptable substrate, with the aromatic portion of an appropriate size as to allow proper positioning of the benzylic carbon in the proper vicinity for hydroxylation to occur. These two compounds effectively bracket the dimension of this region. The analysis of 4-ethylbiphenyl **4** shows an identical depth requirement as for 2-ethylanthracene, and like the latter compound, **4** was processed in less than 1% yield. The compound, 4-*tert*-butyl ethyl benzene **5** was chosen as a substrate, as its dimensions lie between the previously examined aromatic hydrocarbons. Compound **5** was accepted as a substrate but processed in a much lower yield. This may be attributable to the volume requirements of the bulky *tert*-butyl group, providing some information on the height of this particular zone.

The width of the aromatic binding pocket was tested with several compounds; **1**, **2**, **3**, **6**, **7**, (see appendix 1 for structures) 2-ethyltoluene (**21**), 1,2-diethylbenzene and 1,3-diethylbenzene. (**18**) Figures 23a and 23b present the dimensions of interest for these compounds.

Incubation of the isomeric diethylbenzenes produced no products, demonstrating that these compounds were precluded from entering the active site. The trimethylbenzenes **6** and **7** were also recovered in bulk as would be expected, having the same spatial requirements as the diethylbenzenes. The isomeric 2-ethyltoluene (**21**), and 3-ethyltoluene were in contrast, accepted as substrates by the enzyme, the *ortho* compound giving a product alcohol of *S* configuration, and the *meta* compound giving a racemic alcohol. The yields would indicate that access into the active site is not a problem, but the stereochemical results

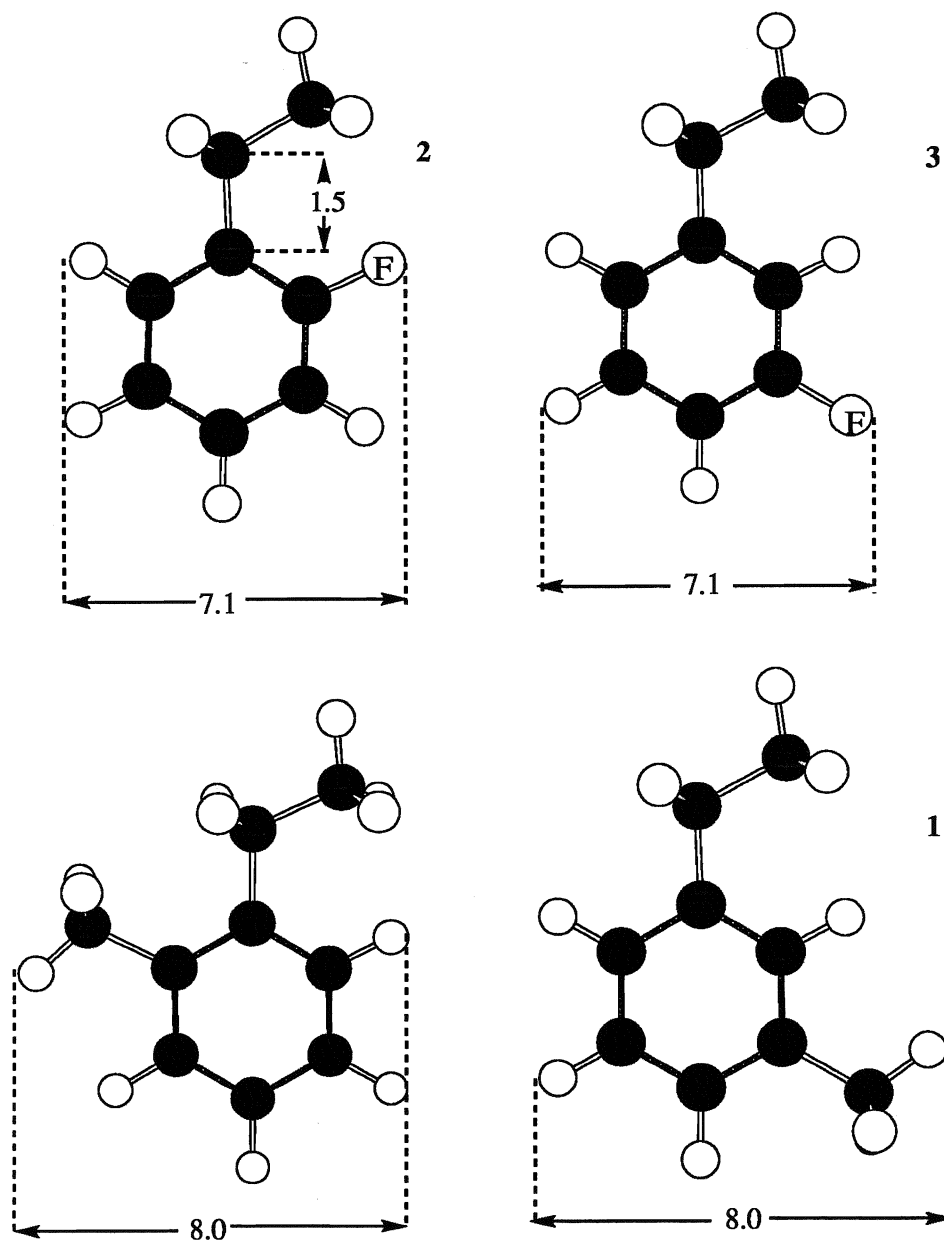


Figure 23a: Dimensional analysis of compounds 1, 2, 3 and 2-ethyltoluene.

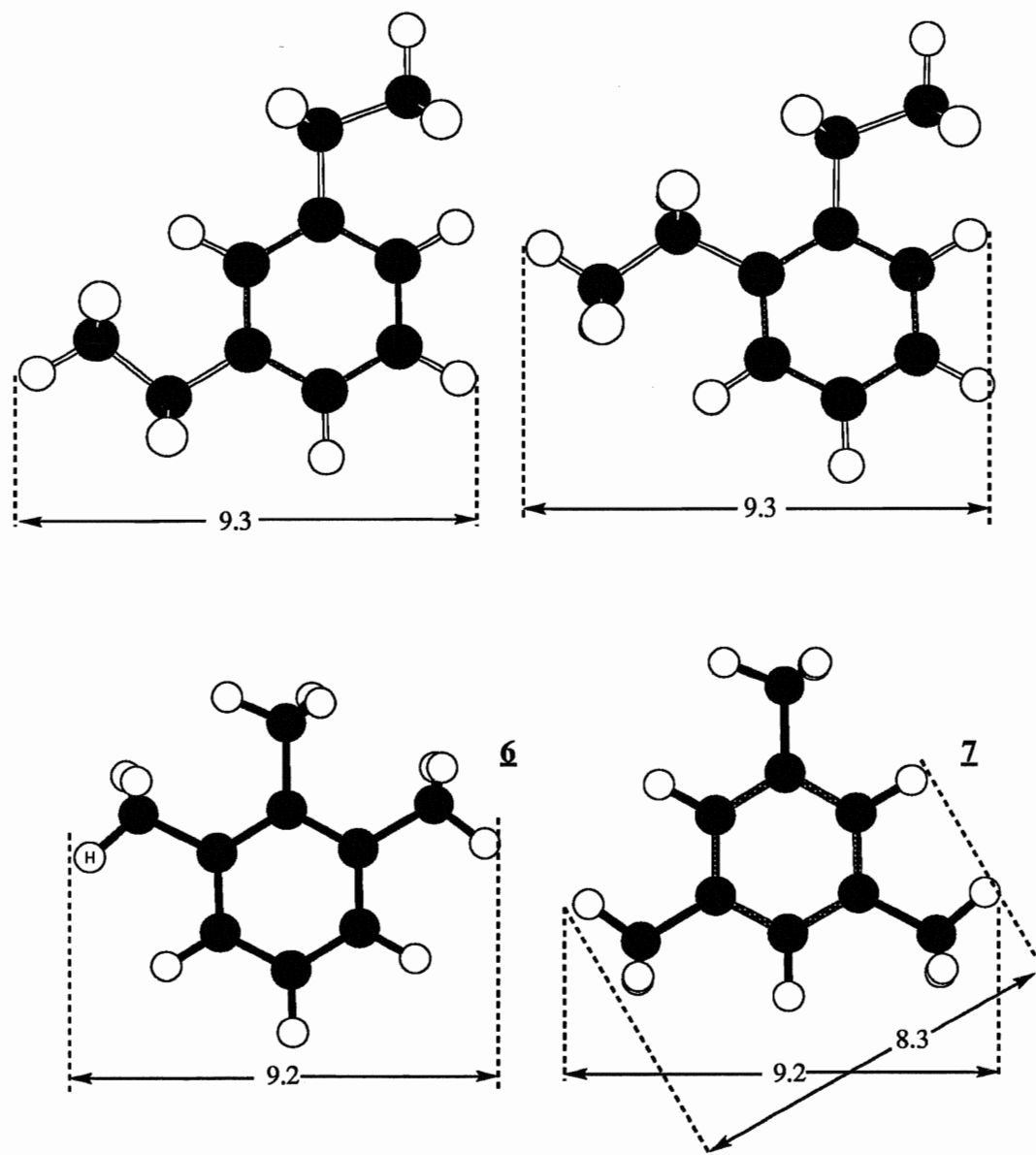


Figure 23b: Dimensional analysis of compounds **6**, **7**, 1,2-diethylbenzene and 1,3-diethylbenzene.

indicate a perturbation in the orientation of the substrate in the active site. The bulk of the substrates examined to date generally produce the R alcohols in a 2:1 ratio (enantiomeric excesses of 33%). A possible explanation of these results is that the methyl group causes the substrate to tilt in the active site, presenting the Pro S hydrogen to the active species (and hence the bottom face of the substrate for oxygen delivery) or positioning the molecule so as to place both hydrogens equidistant from the active center, allowing abstraction and delivery from either face of the substrate (figure 24). The use of 2-fluoro- and 3-fluoroethylbenzenes **2** and **3** as substrates produced alcohols in both cases demonstrating acceptability as substrates. The enantiomeric excesses however differ greatly **2** having an ee value of 52% and **3** an ee value of 18% (16). Since the dimensional requirements are identical for the two compounds, and these requirements are less than the dimensions of the ethyltoluene series, we can assume that dimensional limitations are not a factor. The existence of an electrophilic site in the aromatic binding region has been demonstrated by Holland et. al. (21) using 5,6,7,8-tetrahydroquinoline as a substrate. Hydroxylation occurs specifically at C-5, although two spatially equivalent benzylic sites exist in the molecule, suggesting a preferred orientation for the heteroatom (figure 25). A fluorine atom may also be interacting with this electrophilic site causing perturbations in the orientation of the molecule, and hence perturbations in stereochemistry.

II-2 Front End Probes

The results from the incubations of **8,9,10,11,12** and **13** (see appendix 1 for structures) are presented in table 2. This second series of

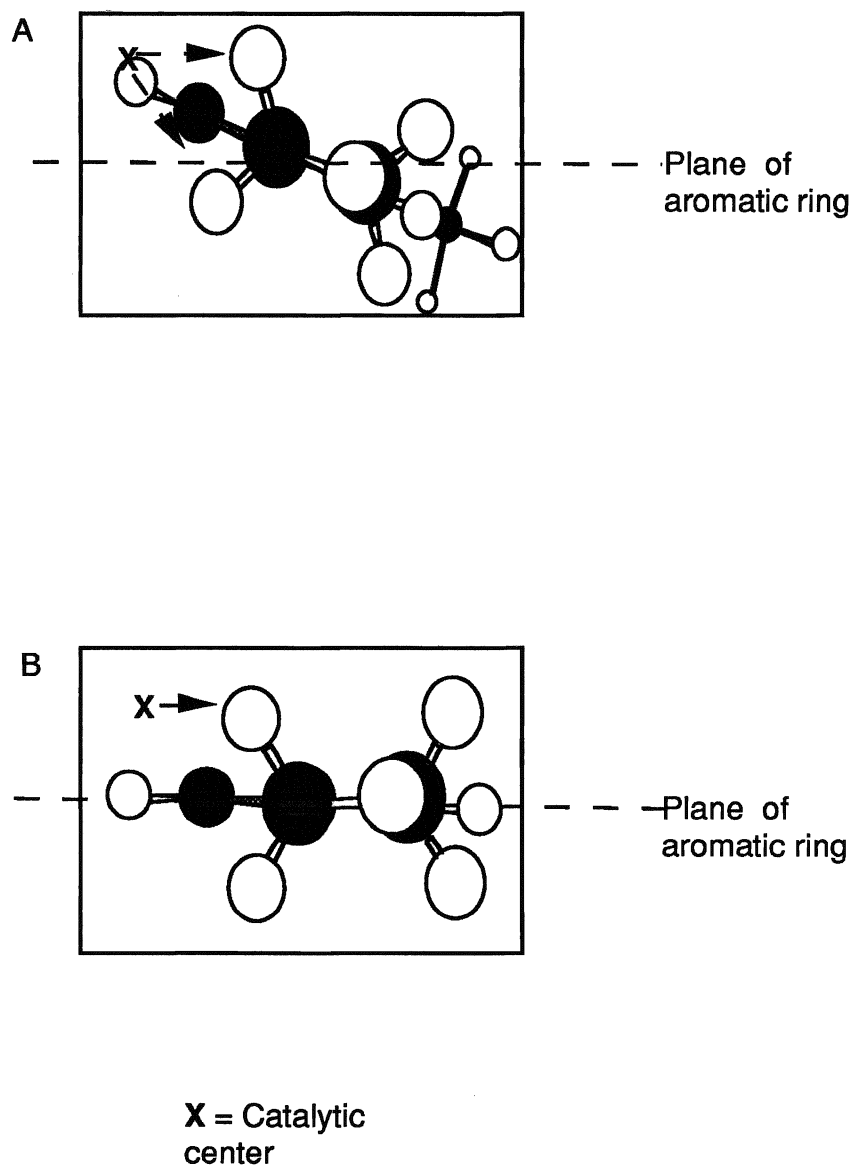


Figure 24: Perturbed orientation of 3-ethyltoluene 1, and normal orientation of ethylbenzene.

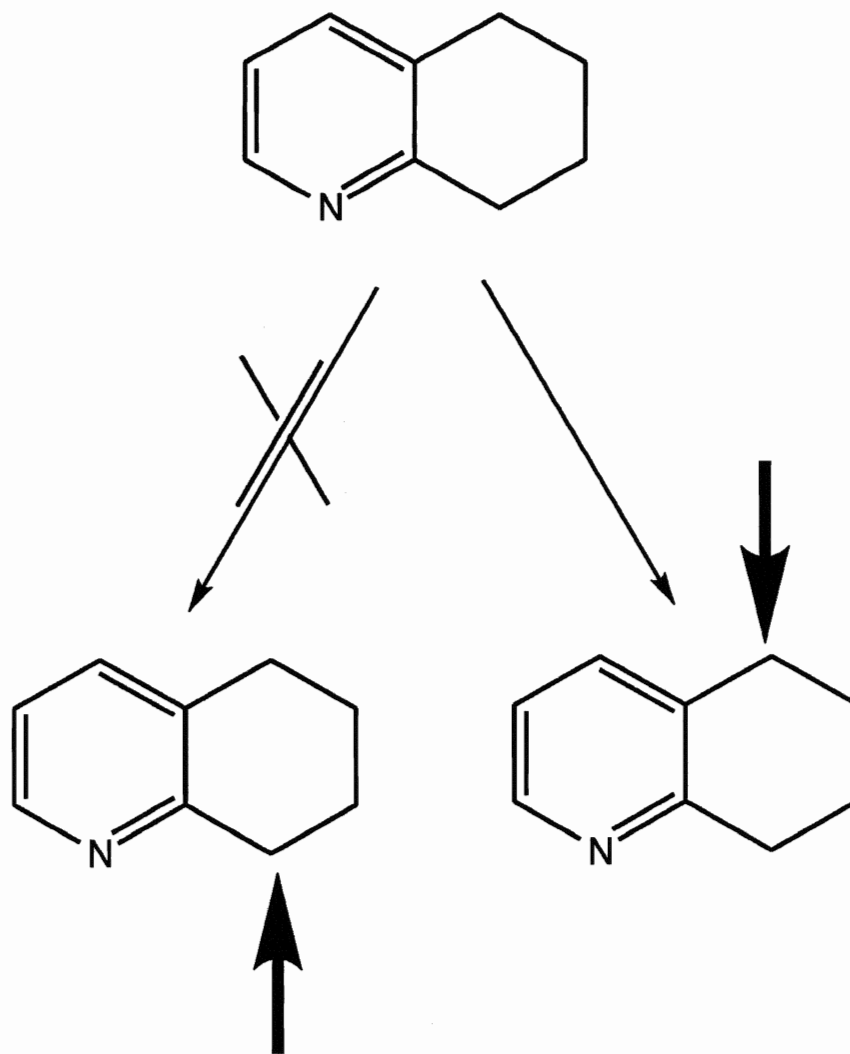


Figure 25: Specific hydroxylation of 5,6,7,8-tetrahydroquinoline.

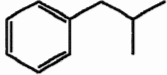
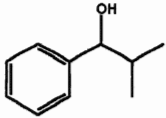
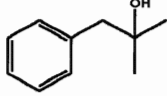
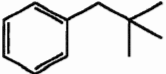
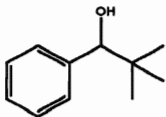
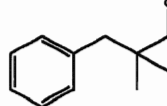
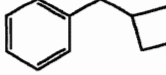
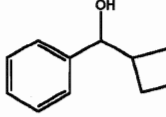
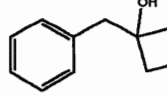
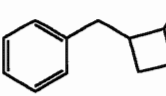
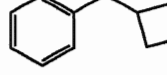
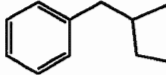
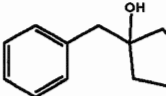
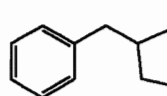
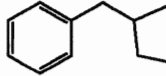
SUBSTRATE	PRODUCTS (YIELD, STEREOCHEMISTRY, EE)	
 8	 8a (0.7, R, 36)	 8b (8.0)
 9	 9a (1.6, R, 55)	 9b (2.3)
 10	 10a (5.3, R, 100)	 10b (2.4)
	 10c (7.7)	 10d (3.8)
 11	 11a (1.6)	 11b (0.7)
	 11c (5.3, cis/trans)	

Table 2: Products of biotransformation of compounds **8** through **13** by *M. isabellina*.

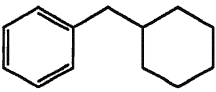
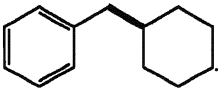
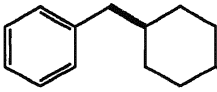
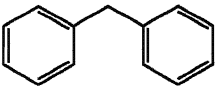
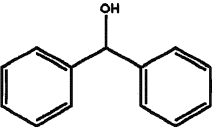
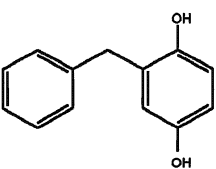
SUBSTRATE	PRODUCTS (YIELD, STEREOCHEMISTRY, EE)	
 12	 12a (1.9, trans)	 12b (0.7, cis)
 13	 13a (0.9)	 13b (0.5)

Table 2: continued.

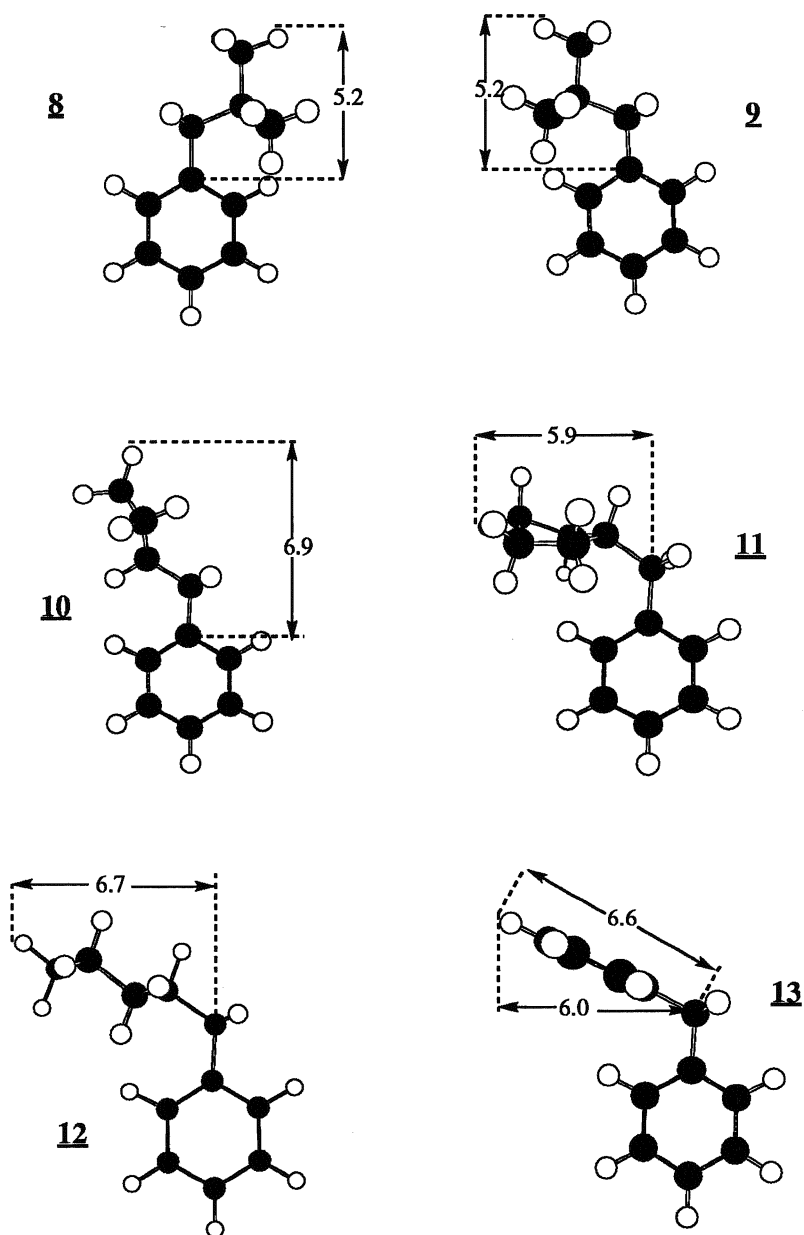


Figure 26: Dimensional analysis of compounds 8 through 13.

compounds was utilized to extract information on the spatial requirements of the region where the catalytic center exists. A dimensional analysis of these compounds is presented in figure 26. The distance between points was maximized by rotating the substituent before recording dimensions to take into account the rotation of the group attached to the benzylic carbon, in which case it would rotate through this maximum, making this the minimum distance required for the substrate to fit in the site.

The phenylpropane series (1-phenylpropane, 2-methyl-1-phenylpropane **8**, and 2,2-dimethylphenylpropane **9**) shows a drastic reduction in yield as methyl groups are added in sequence to the 2 position in the propane chain. The ee values on the other hand show an increase from 25% for 1-phenylpropane to 55% for 2,2-dimethylphenylpropane. The reduction in yields is a sign that the bulkier substrates are restricted in access to the enzyme active site, but the higher ee values are a sign that the substrate is more restricted in the active site. Since all three of these groups would sweep out the same area if rotating about the 1,2 bond (effectively giving them all the same steric requirement), these results are an indication that rotation in the active site is not occurring, or is at least restricted in some manner.

When the carbons were "tied together", in the form of a cyclobutyl group, as in the compound cyclobutylphenylmethane **10**, the enantiomeric excess rose to 100%, reflecting a best fit scenario for this compound. The value was checked by chemically reducing the ketone to give an ee of 0 % by H nmr shift reagent studies. As the ring size increases, the production of benzylic alcohol ceases, in favor of hydroxylation elsewhere in the ring. This same trend is also noted in the phenylcycloalkane series with phenylcyclobutane being accepted as a

substrate, and the higher phenylcycloalkanes being hydroxylated elsewhere in the rings. (21) The production of non-benzylic alcohols is thought to be due to the existence of other P-450 isozymes, and similar results have been noted elsewhere. (92,93)

The five and six membered cycloalkylphenylmethanes **11** and **12** are hydroxylated exclusively at positions other than the benzylic carbon, **11** giving three products (all saturated ring positions being oxidized), and **12** giving a cis / trans mixture of the C-4 hydroxylated compound, these results again correlating well with the phenylcycloalkane series. (21)

At first glance compounds **10** and **11** seem to be very similar dimensionally, but a 3-dimensional analysis shows the folding of the cyclopentyl moiety, severely hindering access of the aromatic portion of the molecule into its binding pocket (figure 27); the sheer bulk of the cyclohexyl moiety may be the cause of compound **12** being denied access into the active site. Diphenylmethane was accepted as a marginal substrate and the free rotation of the phenyl ring establishes a minimum height in this region of 6.7 Angstroms. This information would indicate preclusion of the cyclopentyl and cyclohexyl analogs on the basis of the height swept by these rotating groups.

II-3 Front End Rigid Probes

The results of incubations of **14,15,16,17** and **18** (see appendix 1 for structures) are presented in Table 3. The products were identified by routine spectral analysis, and assignments for the most part were straight forward. Several of the products in the indan series coeluted, and consequently had to be identified based on spectral data for the mixture.

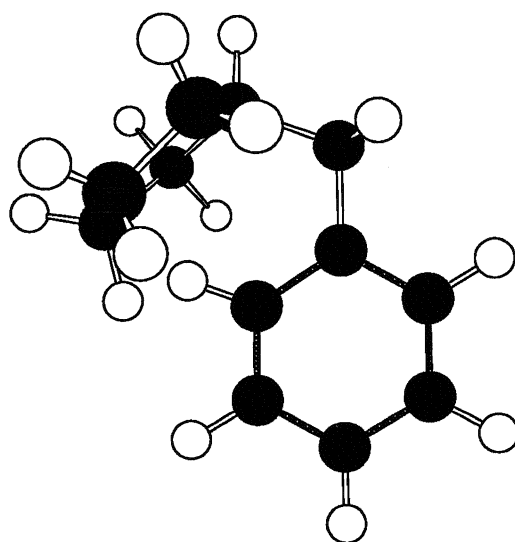


Figure 27: The folding of cyclopentylphenylmethane, restricting access of the phenyl ring into the binding pocket.

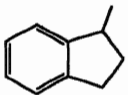
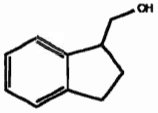
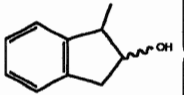
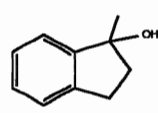
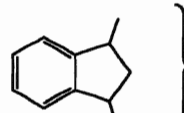
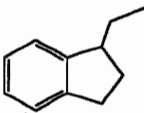
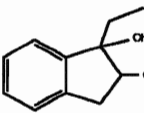
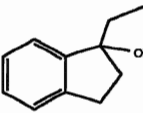
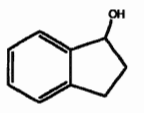
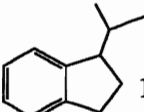
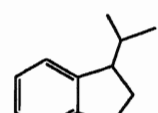
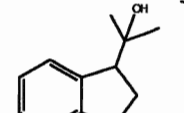
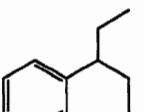
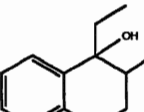
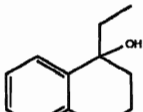
SUBSTRATE	PRODUCTS (YIELD, STEREOCHEMISTRY, EE)
 14	<div>   </div> 14a and 14b (2.9, combined) <div>   </div> 14c and 14d (4.4, combined)
 15	 15a (0.3)  15b (2.0)  15c (0.5)
 16	<div>   </div> 16a and 16b (2, combined)
 17	 17a (0.2)  17b (0.3)

Table 3: Products of biotransformation of compounds **14** through **18** by *M. isabellina*.

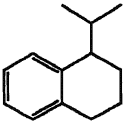
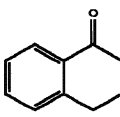
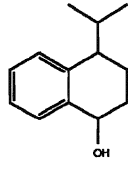
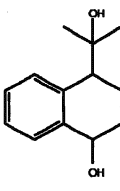
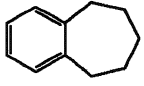
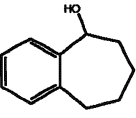
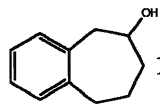
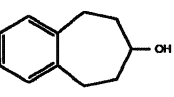
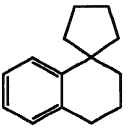
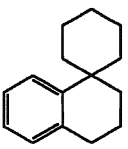
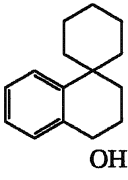
SUBSTRATE		PRODUCTS (YIELD, STEREOCHEMISTRY, EE)	
	18		18a (3.7)
			18b (2.0)
			18c (3.4)
	19		19a (2.4, R, 48)
			19b (2.5, ?, 56)
			19c (3.8)
	20	None	
	21		21a (3.6)

Table 3: Continued.

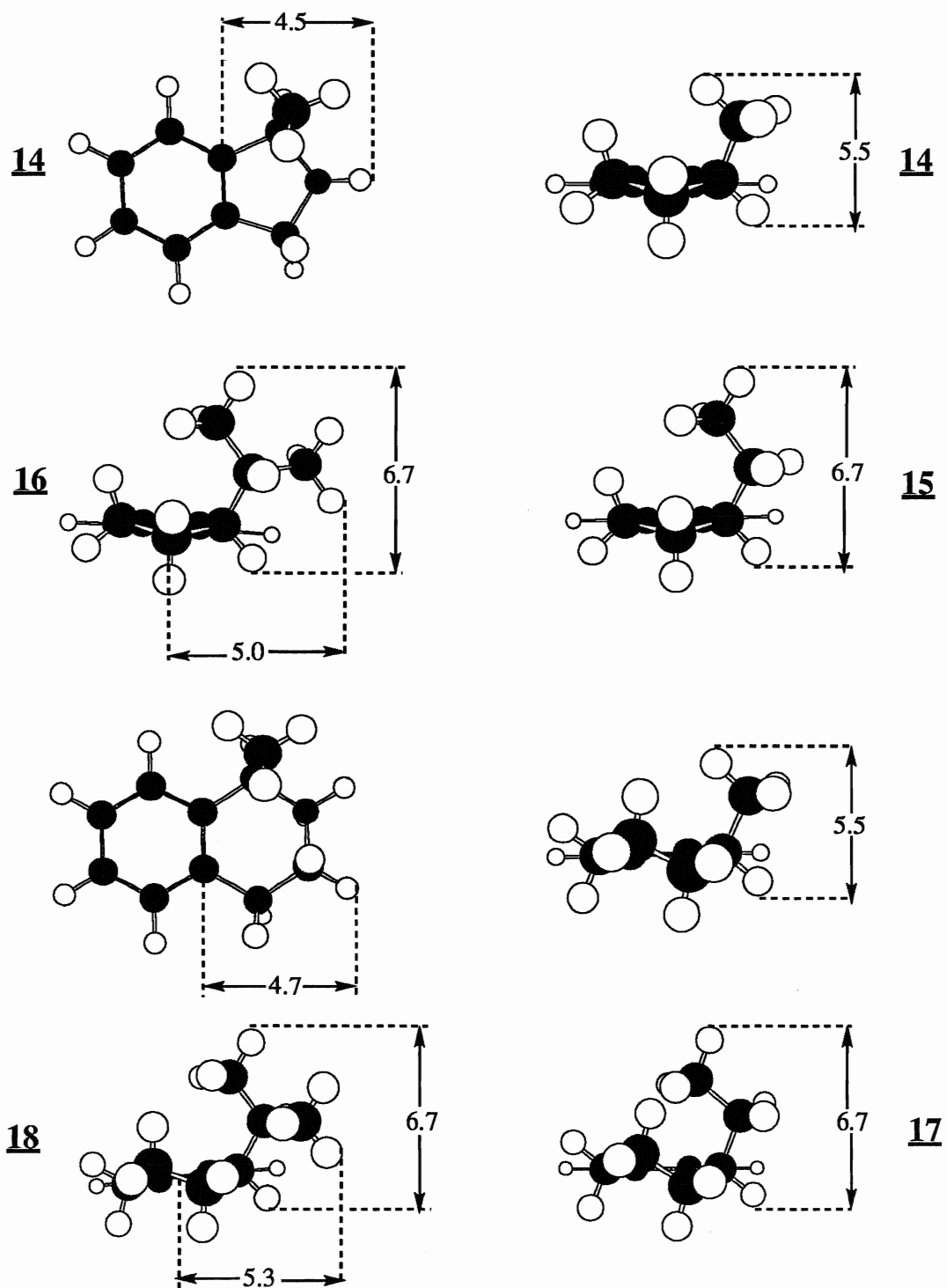


Figure 28: A dimensional analysis of compounds 14 through 18.

All of the substrates were mixtures of stereoisomers, further complicating the analysis of the product distribution. A dimensional analysis is presented in figure 28. The addition of alkyl groups to the indan and tetrahydronaphthalene skeleton, is more a test of the spatial limitations of the region above and / or below the plane of the aromatic ring, as they require little more space in the plane than the parent compounds. The parent compounds, indan and 1,2,3,4-tetrahydronaphthalene proved to be good substrates, producing alcohols in 12-17% yields, and ee values of 33%, which is a typical 2:1 ratio of enantiomers seen in many benzylic hydroxylations performed by *M. isabellina*. The addition of alkyl groups to C-1 in these molecules, although showing large reductions in yield of the corresponding alcohols, did not suppress hydroxylation at the benzylic position. The optical rotation measurements were omitted for this series of compounds as the information extracted from the diastereomeric products would reveal little information regarding the chiral center of interest.

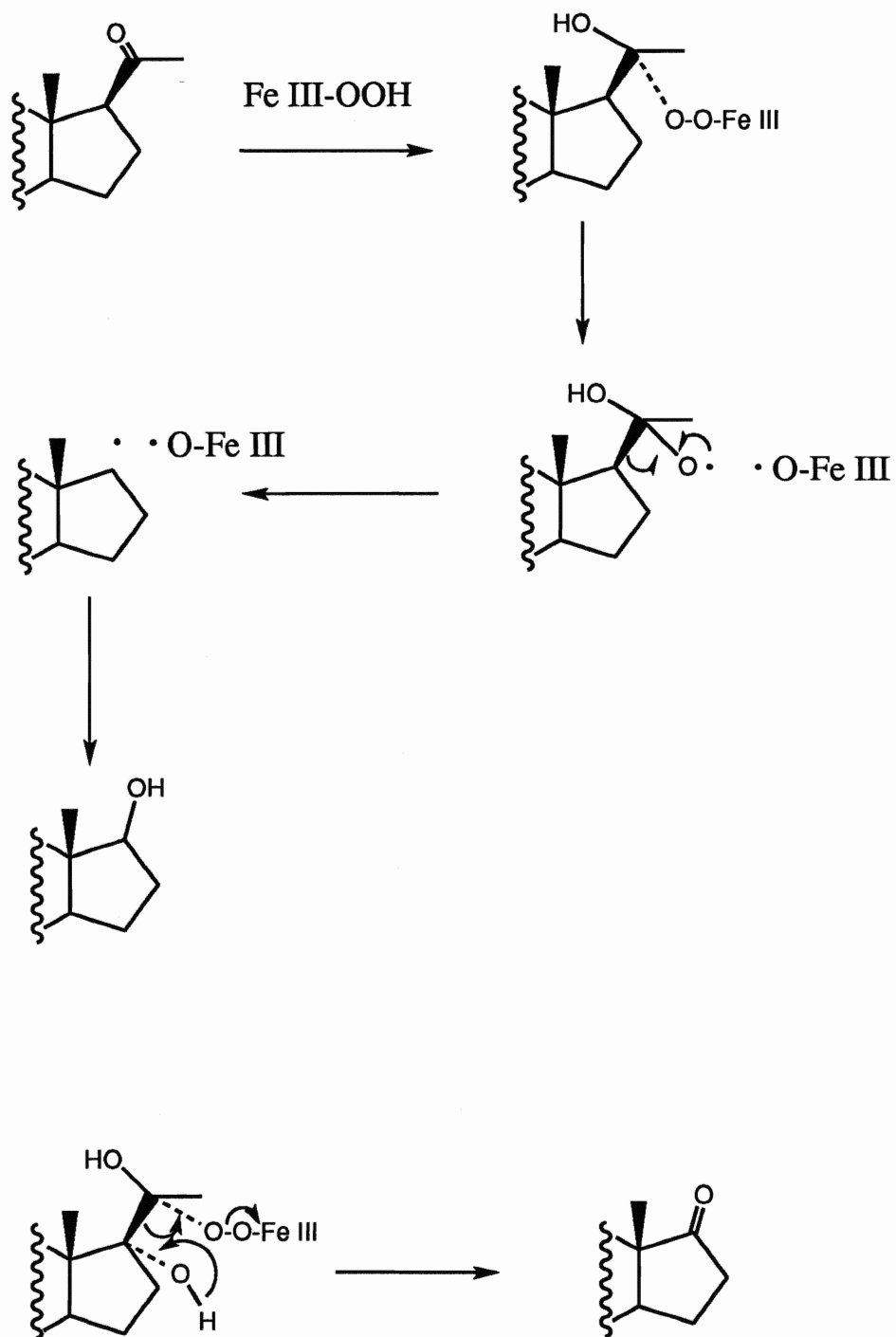
The question of access of one or both of the enantiomers of the substrate into the active site could only be answered by performing the experiments with the chiral compounds individually. In the absence of information on the absolute configuration of the isolated products in these experiments, assumptions have been made to explain at least some of the isolated compounds. The incubations of 1-ethylindan 15 and 1-ethyl-1,2,3,4-tetrahydronaphthalene 17 both produced trace amounts of 1,2-diols (94). Although these diols could arise from contamination of substrate with small amounts of the alkene that may have been present from synthesis of these compounds, their existence also confirms access into the active site.

Two curiosities arose during the incubations of **14** and **16** in which the alkyl side chains of these molecules had been cleaved, producing 1-indanol and α -tetralone respectively. The cleavage of alkyl groups is not unknown in the repertoire of reactions catalyzed by P-450, an example being the side chain cleavage in steroid biosynthesis (94) (Scheme 6), but the exact nature of the reactions involved in the present case is not known.

The compound benzocycloheptene **19** was utilized to probe region A (Figure 21, p36), in the same plane as the aromatic ring. Like the indan and tetrahydronaphthalene substrates, **19** was hydroxylated in the benzylic position in a 2.4% yield, but the ee value rose to 48%, implying a much better fit than the smaller cyclo compounds.

The spiro compounds were chosen specifically to examine the height limitations of the front region of the active site. A dimensional analysis is presented in Figure 29. Preliminary results for the six membered spiro compound shows a triplet in the ^1H nmr spectrum at 4.82 ppm a similar signal of between 4.6 and 4.7 ppm assigned to the hydrogen geminal to the hydroxyl in α tetralol supports a benzylic product although these shifts are at slightly higher field than most of the benzylic alcohols produced in this study. The fact that the signal is a triplet supports the assignment. The ^{13}C nmr spectrum shows a peak at 75.2 ppm which is further evidence that the alcohol produced is indeed benzylic. Incubation of the cyclopentyl spiro compound **20** produced no detectable products, which is unusual in light of the fact that the six membered analog produced the expected product.

The compounds 1,4-epoxy-1,2,3,4-tetrahydronaphthalene **22**, 9,10-dihydroanthracene **23** and 9,10-dihydrophenanthrene **24** were all utilized



Scheme 6: Mechanisms of side chain cleavage in steroids.

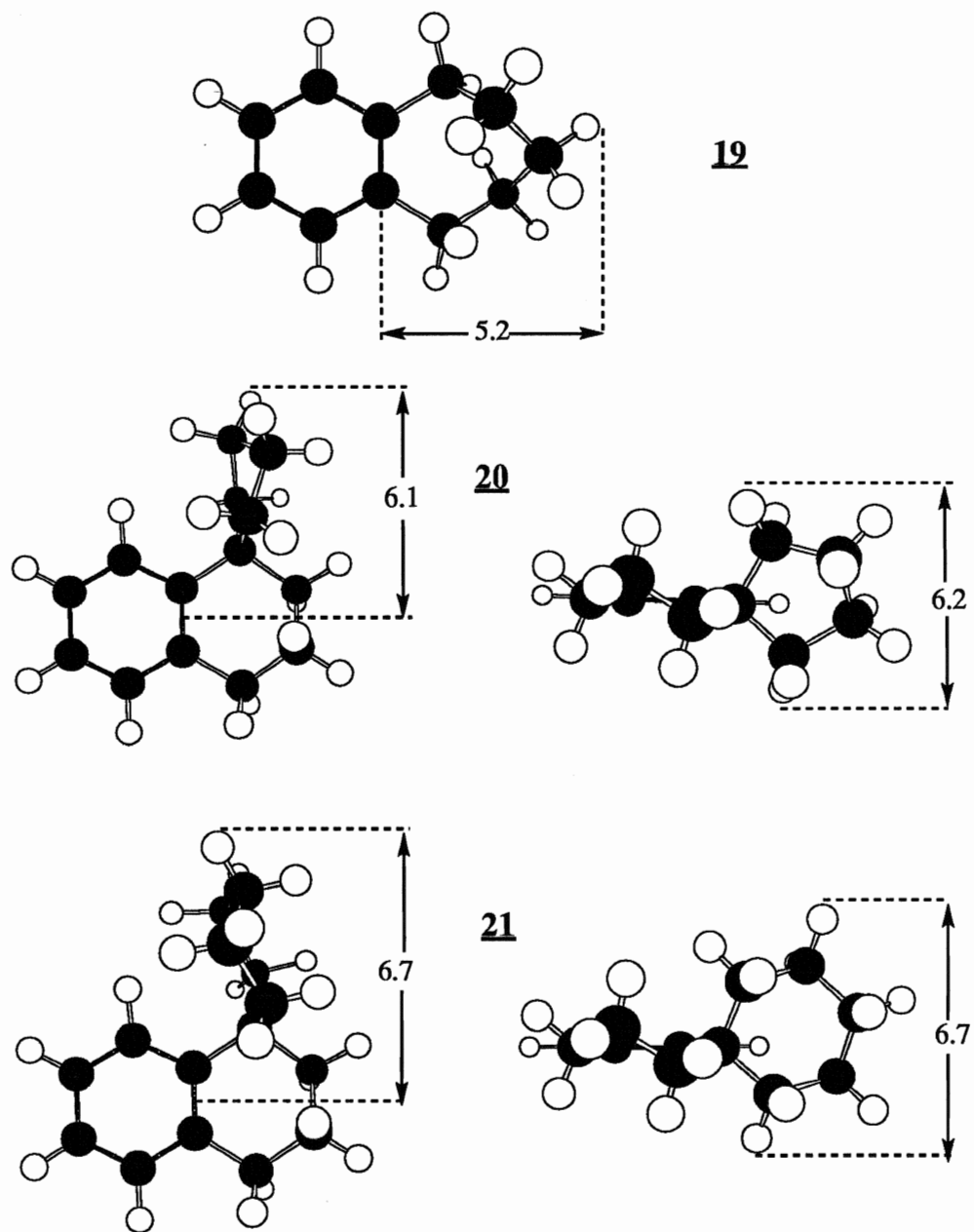


Figure 29: A dimensional analysis of compounds 19, 20 and 21.

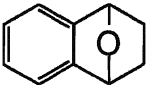
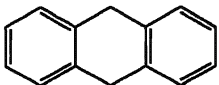
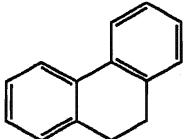
SUBSTRATE	PRODUCTS (YIELD, STEREOCHEMISTRY, EE)	
	22	None
	23	None
	24	None

Table 4: Products of biotransformation of compounds 22 through 24 by *M. isabellina*.

to investigate the front end dimensions, but were not accepted as substrates as evident by the bulk recovery of starting materials (table IV).

III Stereochemical Considerations

We have seen variation in the enantiomeric excesses as a function of the fit of a particular substrate in the active site. A common feature seen in many hydroxylations during the course of study of this particular enzyme is ee values in the range of 33% which seems to be a baseline value of a 2:1 ratio of **R** to **S** enantiomers. As perturbations occur in the orientation of a molecule in the active site, the ee values change as the ratios of **R** to **S** changes. During the development of this model, the catalytic center was postulated to be above the plane of, but in close proximity to, the aromatic ring and the benzylic carbon (Figure 30). At this location, the benzylic hydrogen that lies above the plane of the phenyl ring lies in the reactive sphere of the catalytic center, and the other benzylic hydrogen (below the plane) does not. Likewise, during the oxygen delivery step in the catalytic cycle, the radical centered at the benzylic carbon lies in a p-orbital which again is perpendicular to the plane of the ring. Thus the upper lobe of this orbital lies in the reactive sphere, and the other does not.

In support of results obtained in these studies (i.e. ee's of 33%), the bottom face of the molecule must move so as to allow access of the reactive species to both faces of the molecule; the reactive center must "see" the bottom face at least 33% of the time (figure 31).

This freedom of movement is only observed for the less restricted molecules. The fact that the oxidizing center lies above the plane of the

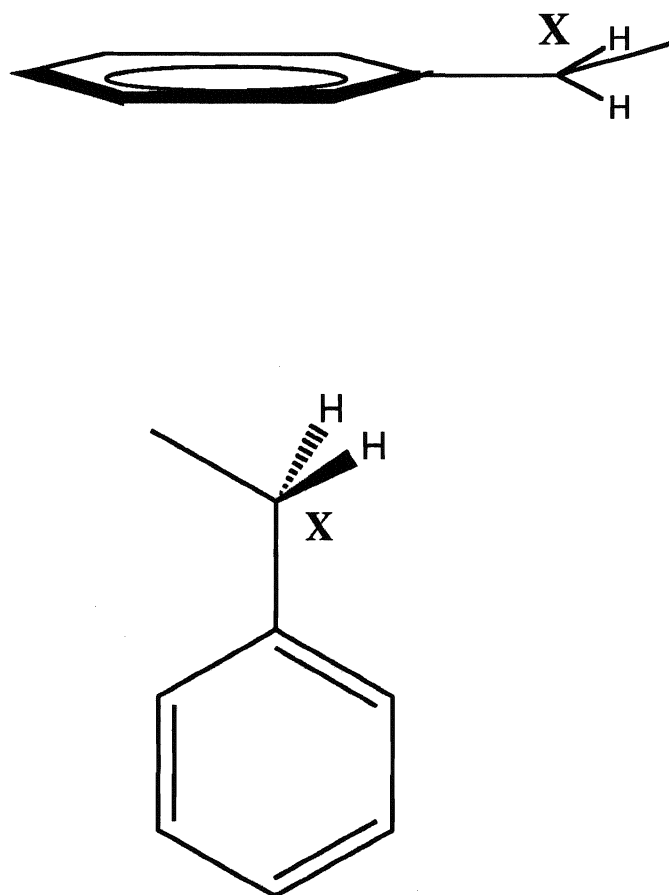


Figure 30: Two views showing the relative location of the oxidation center in the benzylic hydroxylase of *M. isabellina*.

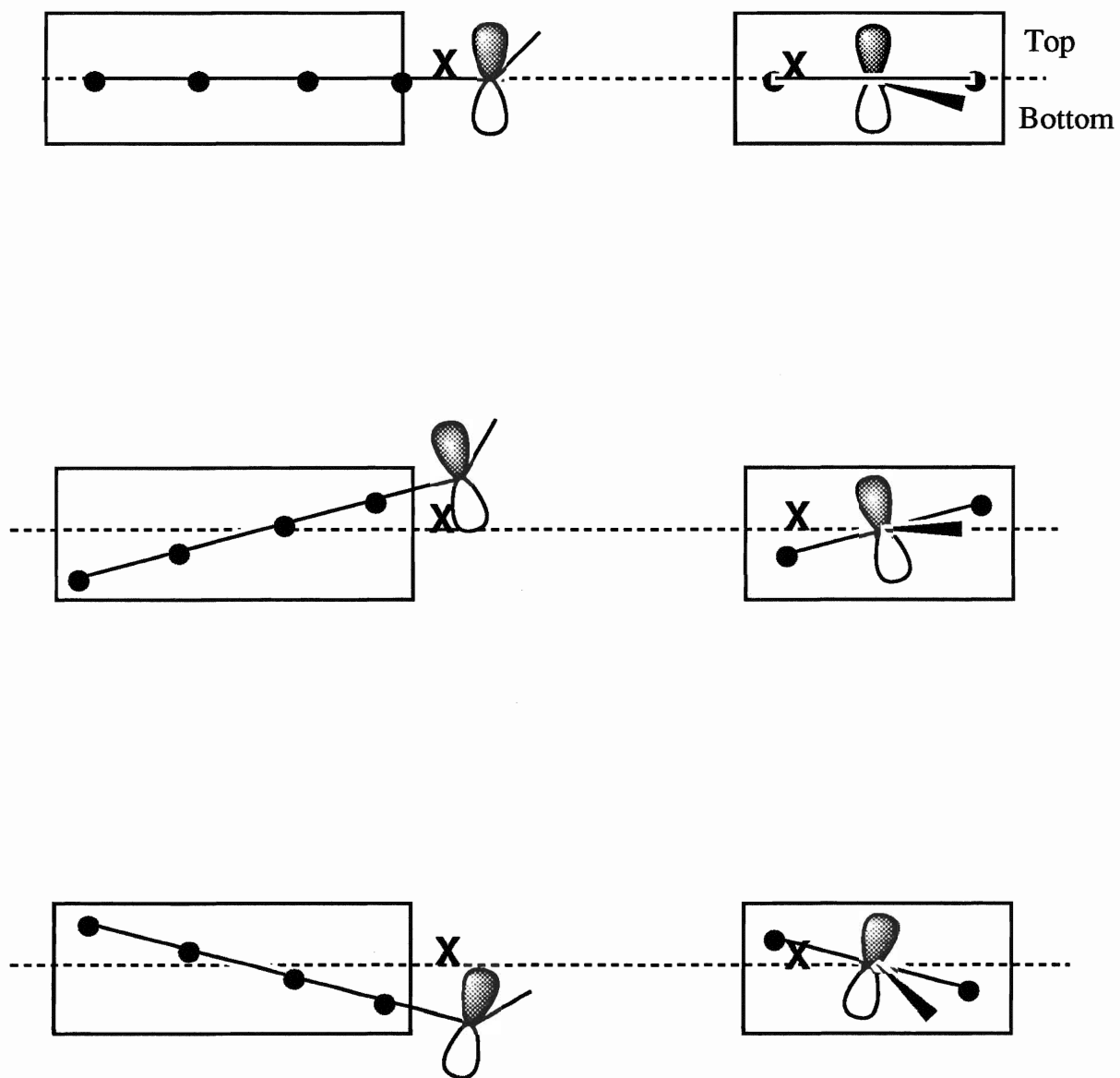


Figure 31: Two possible ways in which the oxidation center could have access to the bottom face, accounting for the observed enantiomeric ratios.

aromatic ring explains the predominance of one enantiomer over another. Deviations from the 33% value are reflected by a "better fit" in the active site which would tend to restrict these motions, and the time the active species "sees" the bottom face of the substrate. In the case of the ethyl toluenes, the molecules are approaching the dimensional limits of the pocket. This situation results in a perturbed orientation, deviating from the norm resulting in the active center "seeing" the bottom face predominantly or both faces equally.

IV Model for the Benzylic Hydroxylase

The results of these experiments will be examined using the schematic representation of the first generation model put forth by Holland et. al. (21) as a template (figure 31). All measurements were made from center to outer shell when carbon to hydrogen measurements were made, and outer shell to outer shell when measurements from hydrogen to hydrogen or fluorine were made (i.e. Van der Waals radii).

The depth limitation of the aromatic binding pocket was exceeded both by 2-ethylanthracene and 4-ethylbiphenyl which were identical in length at 9.5 Angstroms for the aromatic portion of the molecules. The largest acceptable substrate in this study was 4-*tert*-butylethylbenzene 5 which brackets dimension **b** between 7.3 and 9.5 Angstroms. This compound also has a height requirement; assuming that the *tert*-butyl group is freely rotating, the maximum height of 6.2 Angstroms would be required to accommodate this rotation, setting dimension **c** at a minimum of 6.2 Angstroms.

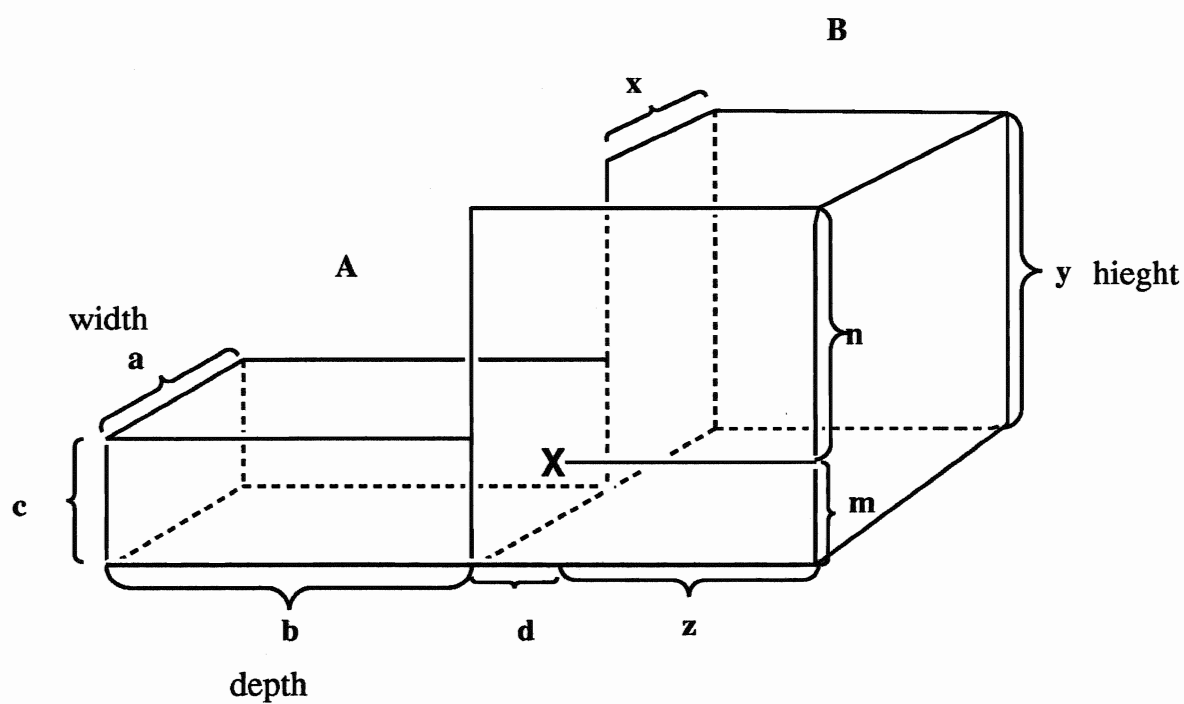


Figure 32: A schematic representation of the active site of the benzylic hydroxylase of *M. isabellina*. X denotes oxidation center.

The width of region A was examined using several compounds of varying widths; 2-ethyl and 3-ethyltoluenes were accepted into the active site but with greatly perturbed orientations, accounting for the products obtained. These compounds set the limits below the 8.0 Angstrom measurement. The fluoroethylbenzenes **2** and **3** were processed in good yields. The data from these experiments bracket dimension a between 7.1 and 8.0 Angstroms.

The distance between the front of the aromatic binding pocket and the active center is evident in all the substrates accepted by this enzyme; dimension d has been set at one carbon - carbon bond length 1.5 Angstroms.

Region B of the active site has been examined with various free rotating and rigid structures, and they will be discussed in turn. It has been shown in these experiments that as methyl groups are added to phenyl propane (at the 2 position of propane), the ee values increase, demonstrating a tighter fit of the R group in region B. The distance from the phenyl carbon to the most distant hydrogen in **9** is 5.2 Angstroms, this distance also applying to the other two analogs. Based on the idea of a restricted rotation, **9** is the only compound in this series that would always have a methyl group directed at the front barrier of the region, whereas the other two members of this series can have a hydrogen directed at the front barrier thereby reducing the effective "reach" of the molecule, resulting in a looser fit in the pocket.

Cyclobutylphenylmethane produced an alcohol with 100% ee, representing a best fit in this region. The distance from the aromatic carbon center to the most distant hydrogen is 6.9 Angstroms. Subtracting

the 1.5 Angstroms of dimension **d**, places a value for the **z** dimension of 5.4 Angstroms.

The rigid front end probes used produced information that was cloudy at best. The use of racemic starting materials is a problem as it is unknown if one or both isomers is accepted into the active site. Although based on some of the products obtained, and the knowledge that the parent compounds are acceptable substrates, some information can be extracted from these experiments.

The 1-methyl and 1-ethylindans **14** and **15** both produced tertiary benzylic alcohols during their respective incubations. In light of the fact that no other major structural differences exist between the alkyl indans and the parent compounds, the assumption is made that carbon 1 faces the active center, with the substituent extending downwards below the plane of the structure, thereby presenting the hydrogen to the active center as in the parent compounds. This would establish a minimum distance below the plane of the molecule of 4.7 Angstroms.

The other compounds in this group of substrates produced more qualitative data, in the absence of information on absolute stereochemistry, it is unclear as to which direction the measurements apply.

The incubation of benzocycloheptene produced a benzylic alcohol with an ee value of 48%. The distance from the aromatic carbon to the most distant hydrogen is 5.2 Angstroms, which lies within the limit set by cyclobutylphenylmethane. It is interesting to note that this measurement is the same as that for 2,2-dimethylphenylpropane **9** (i.e. beginning to approach the barrier) and very similar ee values (48 and 52%) were obtained from both products.

The use of spiro compounds allowed a look at the total height of region B and the x dimension. Only one product was isolated from these incubations, that of spiro [1,1'-cyclohexyl-4-hydroxy-1,2,3,4-tetrahydronaphthalene]. The distance was measured from half way between the aromatic carbon - carbon bond and the furthest hydrogen. A distance of 6.8 Angstroms was obtained thereby setting a minimum for x at 6.8 Angstroms. The height requirement of this molecule also setting a minimum height for region B is 6.7 Angstroms.

Figure 33 shows the model with the experimentally determined dimensions in place.

V Conclusions

A dimensional analysis of the spatial requirements of the benzylic hydroxylase in *M. isabellina*, has been performed to prepare a model capable of aiding one in predicting the nature of the products formed for any particular substrate.

The distance to the front barrier of region B seems to have been found with relative accuracy, as has the depth of the aromatic binding pocket, but further refinement of the other dimensions will be needed in order to determine the maxima. All the substrates examined to date seem to fit well within the established dimensions and no anomalies exist in these experiments.

Future work with chiral substrates, larger fused ring systems, and spiro compounds seems to be in order to refine the data put forth in this study.

The postulate presented to account for the enantiomeric ratios, covers both fused and free rotating systems and seems to explain the anomalies in stereochemistry obtained with some of the compounds examined.

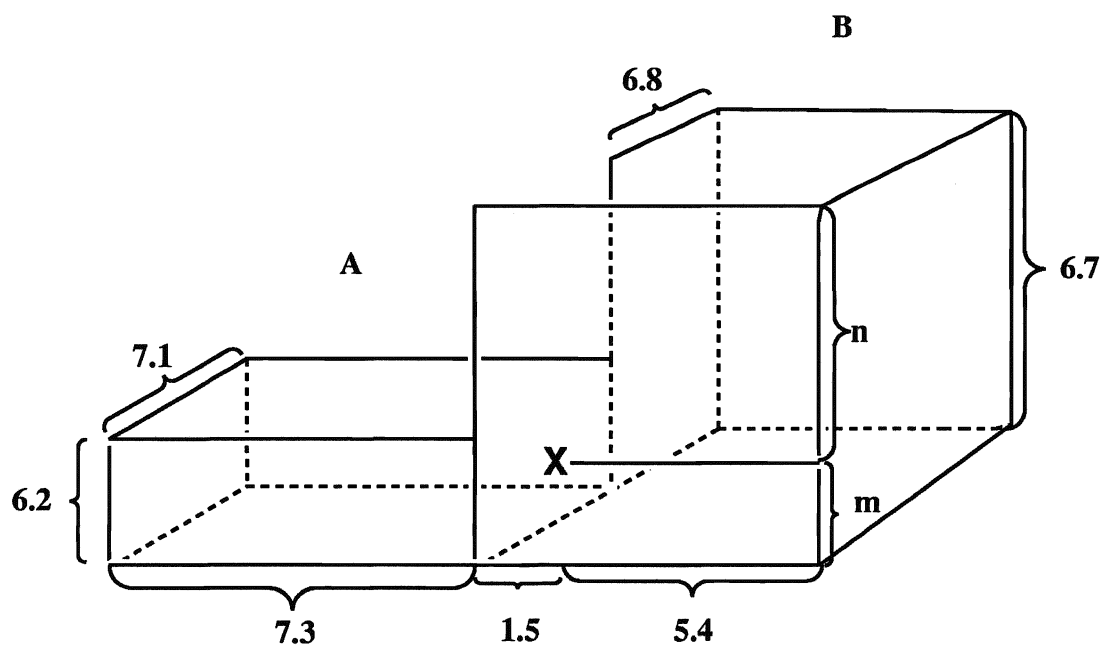


Figure 33: The experimentally determined dimensions of the benzylic hydroxylase of *M. isabellina*.

EXPERIMENTAL

I EXPERIMENTAL

I-1 Apparatus, Materials, and methods

Melting points (uncorrected) were determined on a Kofler heating stage. Proton nuclear magnetic resonance spectra were recorded at 200 MHz and carbon nmr at 50.3 MHz with a Bruker AC200 spectrometer, using CDCl₃ as the solvent (unless otherwise specified) with TMS as the internal standard. Enantiomeric ratios were determined by nmr in CDCl₃ in the presence of tris[3-(heptafluoropropylhydroxymethylene)-*d*-camphorato] europium (III). Electron impact mass spectra were obtained using a Kratos Concept 1S mass spectrometer. Infrared spectra were recorded on an Analect 6260FX spectrometer. Optical rotations were obtained on a Rudolph Autopol III instrument at 20 deg. C in 95% ethanol. Thin layer chromatography (TLC) was performed on Merck silica gel 60F-254 and column chromatography using silica gel (230 - 400 mesh). Commercial substrates were purchased from Aldrich with the exception of cyclopentylphenylmethane which was obtained from MIT. *Mortierella isabellina* NRRL 1757 was grown at 27 deg. C, and maintained at 4 deg. C on slopes composed of 4% malt agar.

I-2 Incubations with *Mortierella isabellina* NRRL 1757

Growth medium for the fungus was composed of glucose (120 g), soybean flour (15 g), yeast extract (15 g), sodium chloride (15 g), and dibasic potassium phosphate (15 g) in 3 Litres of distilled water

(for 15 flasks). One Litre flasks (15) each containing 200 mL of the medium were sterilized in an autoclave and allowed to cool. The medium was then inoculated from a growing slope of *M. isabellina*. The flasks were then placed on a rotary shaker at 27 deg. C without shaking for 24 h then stirred at 150 rpm for 72 h. After the initial growth period, the fungal solids were filtered and resuspended in distilled water (200 mL). The substrate (1.0 g in 15 mL of ethanol) was then added to the flasks (1 mL per flask) and the incubation continued for an additional 72 h. Subsequently, the fungus was removed by filtration and the filtrate extracted using continuous extraction with CH₂Cl₂ for 72 h. The solvent was then evaporated using a rotary evaporator under reduced pressure. The extract was then examined by TLC to determine the best solvent system for column chromatography. Metabolites were then purified by column chromatography and the products subjected to spectral analysis.

II Preparation of Substrates

2-Fluoro ethylbenzene (2) (Ref. 77)

To a 125 mL Erlenmeyer flask was added 20 mL of distilled water and 15 mL of conc. HCl. To this solution at room temperature was added dropwise, 2-ethyl aniline 5.0 g (.0413 mole). The slurry was then cooled to 0 deg. C in an ice bath and 9.5 mL of a 30 % solution (1 eq.) of NaNO₂ was added, the slurry dissolved and becoming a clear deep orange solution at the beginning of the addition and lighter orange at the end of the addition. The solution was then treated slowly with 16 mL of a 40 % solution of NaBF₄ (1.4 eq.). The thick paste was then suction filtered, washed with a small amount of cold NaBF₄ solution, minimal cold ethanol, and then ether, and allowed to dry in air. The solid was then put into a 50 mL round bottomed flask with an equal volume of sand, which was set up for distillation at reduced pressure (water aspirator, 15 mm Hg), and the receiving flask cooled in liquid nitrogen. The flask was then heated slowly to 100 deg. C, until the solid began to decompose at which point the temperature was maintained until the reaction was complete. The product 2-fluoroethylbenzene (2) was collected as an oil, with a yield of 1.51 g (22 % from ethyl aniline).

¹Hnmr δ 1.22 (3H, t, CH₃, J=7.5 Hz), 4.82 (2H, q, CH₂, J=7.5 Hz), 6.96 (4H, m, aromatic H's) ppm; ¹³Cnmr δ 14.3 (C-7), 22.2 (C-8), 114.3 (C-3), 123.9 (C-5), 127.4 (C-4), 129.8 (C-6), 158.7 (C-1), 163.6 (C-2) ppm; MS m/z(%) 124 (M⁺, 30), 109 (100).

3-Fluoro ethylbenzene (3) (Ref. 77)

To a 125 mL Erlenmeyer flask was added 20 mL of distilled water and 15 mL of conc. HCl. To this solution at room temperature was added dropwise, 3-ethyl aniline 5.0 g (0.0413 mole). The slurry was then cooled to 0 deg. C in an ice bath and 9.5 mL of a 30 % solution (1 eq.) of NaNO₂ was added, the slurry dissolving and becoming a clear deep orange at the beginning of the addition and lighter orange at the end of the addition. The solution was then treated slowly with 16 mL of a 40 % solution of NaBF₄ (1.4 eq.). The thick paste was then suction filtered, washed with a small amount of cold NaBF₄ solution, minimal cold ethanol, and then ether, and allowed to dry in air. The solid was then put into a 50 mL round bottom flask with an equal volume of sand, which was set up for distillation at reduced pressure (water aspirator, 15 mm Hg), and the receiving flask cooled in liquid nitrogen. The flask was then heated slowly until the solid began to decompose at which point the temperature was maintained at 100 deg. C until the reaction was complete. The product 3-fluoroethylbenzene (3) was collected as an oil, with a yield of 1.10 g (21 % from ethyl aniline).

¹Hnmr δ 1.22 (3H, t, CH₃, J= 7.6 Hz), 2.63 (2H, q, CH₂, J=7.6 Hz), 6.81-7.26 (4H, m, aromatic H's) ppm; ¹³Cnmr δ 15.2 (C-8), 28.6 (C-7), 112.4 (C-4), 114.7 (C-2), 123.5 (C-6), 129.7 (C-5), 147.0 (C-1), 163 (C-3) ppm; MS m/z(%) 124 (M⁺, 34), 109 (100).

4-tert-Butyl ethylbenzene (5) (Ref. 86)

A 100 mL two necked flask fitted with a reflux condenser and thermometer contacting the solvent was charged with a solution of 4-tert-butylacetophenone (2.0 g, 0.0114 mole), potassium hydroxide (1.92 g, 3 eq.) and 85% hydrazine hydrate (2.15 g, 5 eq.) in 50 mL of diethylene glycol and the mixture was brought to reflux. After 1 h, the condenser was exchanged for a distillation set up and distillation began until the temperature of the solution reached 195 deg. C. At this time the reflux condenser was replaced and reflux continued for 1 h, after which time the solution was allowed to cool. A 5% solution of HCl was then added to the reaction mixture which was then extracted with ether. The ether extract was washed with saturated sodium bicarbonate and distilled water before drying with anhydrous magnesium sulfate. Evaporation of the solvent under reduced pressure and purification by chromatography using hexane as the eluting solvent, afforded 1.34 g (73%) of 4-t.butyl ethylbenzene (5) as an oil.

$^1\text{Hnmr}$ δ 2.86 (3H, t, CH₃, J= 7.6 Hz), 1.31 (9H, s, t-butyl), 2.62 (2H, q, CH₂, J=7.6 Hz) ppm; $^{13}\text{Cnmr}$ δ 15.4 (C-8), 28.3 (C-7), 31.4 (C-10), 34.3 (C-9), 125.4 (C-3,-5), 127.5 (C-2,-6), 141.1 (C-4), 148.4 (C-1) ppm; MS m/z(%) 162 (M⁺, 15), 147 (100).

Cyclobutylphenylmethane (10) (Ref. 86)

A solution of 3 g (0.0188 mole) of cyclobutyl phenyl ketone, 3.15 g of potassium hydroxide (3 eq.), and 3 ml of 95% hydrazine hydrate was prepared and treated in the usual way (as above). Workup and purification by chromatography using hexane as the eluting solvent afforded 1.21 g (44%) cyclobutylphenylmethane as a clear oil.

$^1\text{Hnmr}$ δ 1.70-2.05 (6H, m, CH_2 's), 2.59 (1H, m, CH), 2.69 (2H, d, benzylic CH_2 , $J=7.4$ Hz) ppm; $^{13}\text{Cnmr}$ δ 18.3 (C-3), 28.3 (C-2,-4), 37.3 (C-1), 43.0 (C-5), 125.8 (C-4'), 128.2 (C-2',-6), 128.5 (C-3',-5'), 141.4 (C-1') ppm; MS $m/z(\%)$ 146 (M^+ , 38), 118 (100), 104 (47), 91 (67).

Cyclohexylphenylmethane (12) (Ref. 86)

A solution of 4 g cyclohexylphenylketone (0.0213 mole), 3.58 g potassium hydroxide (3 eq.), and 2 mL 95% hydrazine hydrate (2 eq.) was prepared and treated in the usual way. Workup and purification by chromatography using hexane as the eluting solvent afforded 2.52 g (68%) cyclohexylphenylmethane (12) as a clear oil.

$^1\text{Hnmr}$ δ 0.80-1.75 (11H, m, cyclic CH_2 's), 2.45 (2H, d, benzylic CH_2), 7.05-7.27 (5H, m, aromatic H's) ppm; $^{13}\text{Cnmr}$ δ 26.5 (C-3,-5), 26.6 (C-4), 33.2 (C-2,-6), 40.0 (C-1), 44.2 (C-7), 125.6 (C-4'), 128.0 (C-3',-5'), 129.2 (C-2',-6'), 141.3 (C-1') ppm; MS $m/z(\%)$ 174 (M^+ , 28), 92 (100), 83 (38).

Benzocycloheptene (19) (Ref. 86)

A solution of 3 g (0.0188 mole) benzosuberone, 3.15 g (3 eq) potassium hydroxide, and 3.16 g (5 eq) 95% hydrazine hydrate was treated in the usual way. Workup and purification by chromatography gave a yield of 1.86 g (68%) benzocycloheptene (19) as a clear oil.

$^1\text{Hnmr}$ δ 1.64 (4H, m, CH₂'s), 1.81 (2H, m, CH₂), 2.77 (4H, dd, benzylic H's) ppm; $^{13}\text{Cnmr}$ δ 28.3 (C-2,-4), 32.8 (C-3), 36.7 (C-1,-5), 125.9 (C-7,-8), 128.9 (C-6,-9), 123.4 (C-10,-11) ppm; MS $m/z(\%)$ 146 (M⁺, 100), 131 (41), 117 (64), 104 (76), 91 (40).

1-Methylindan (14)

To a 250 mL two necked flask (flamed under argon) containing 1.36 g (1.5 eq.) magnesium turnings (oven dried) was added 40 mL of ether (distilled from sodium) and the reaction vessel was then cooled in an ice bath. Methyl iodide (3.54 mL, 1.5 eq) was introduced in a dropwise fashion, the reaction mixture was then stirred for two hours and the temperature allowed to equilibrate. After 2 h, 5.0 g (0.0379 mole) of 1-indanone was added dropwise and the resulting solution stirred for 16 h. The reaction was then cooled in an ice bath and quenched with 50 mL of 15% HCl, and the solution allowed to reach room temperature over about 1 h. The product was then extracted into ether, washed with saturated sodium bicarbonate, distilled water, saturated sodium chloride, and the ether layer dried

over anhydrous magnesium sulfate prior to removal of solvent under reduced pressure. The crude product was then chromatographed using hexane : ethyl acetate 3 : 1 as the eluting solvent to yield 4.89 g (99 %) of 1-methyl-1-indene as a yellow oil. To 100 mL of ethyl acetate containing 0.5 g of palladium on charcoal in a hydrogenation vessel was added 4.0 g (0.0308 mole) of 1-methyl-1-indene. The vessel was then connected to a Parr hydrogenation apparatus, and the solvent degassed under water aspirator before flushing with hydrogen (3X). The pressure of hydrogen was then brought to 35 psi. and the shaker started. The pressure drop subsided at 32 psi (2 h) at which time the catalyst was removed by filtration, the solvent removed under reduced pressure, with a yield of 2.82 g (69%) of 1-methyl indan (14) as a clear oil, and recovered starting material.

$^1\text{Hnmr}$ δ 1.27 (3H, d, CH_3 , $J=6.8$ Hz), 1.57 (2H, m, CH_2), 2.85 (2H, m, benzylic H's), 3.16 (1H, m, benzylic H), 7.15 (4H, m, aromatic H's) ppm; $^{13}\text{Cnmr}$ δ 19.9 (C-10), 31.4 (C-2), 34.7 (C-3), 39.4 (C-1), 123.2 (C-5), 124.3 (C-6), 126.1 (C-4,-7), 143.8 (C-8), 148.7 (C-9) ppm; MS $m/z(\%)$ 132 (M^+ , 36), 117 (100).

1-Ethylindan (15)

To a flame dried (under argon) 250 mL two necked flask was added a solution of 5.0 g (0.0431 mole) of indene in 20 mL of dried ether. The flask was cooled to -78 deg. C in methanol / liquid nitrogen and 3.8 mL (1.5 eq.) of 1.45 M t-butyl lithium was added dropwise. The solution was stirred until temperature reached ambient, at which time 3.8 mL (1.1 eq) of ethyl iodide was introduced in a dropwise

manner. The reaction was continued for an additional 16 h at which time the solution was heated at reflux for 1 h. The reaction was then quenched carefully with 15% HCl and extracted into ether.

Work-up in the usual way followed by chromatography using hexane as the eluting solvent, afforded 1-ethyl-1-indene (3.74 g, 66%).

Hydrogenation was carried out in 100 mL ethyl acetate containing 0.5 g of palladium on charcoal by the usual procedure (as above); 1-ethyl-1-indene (3.74 g) afforded 3.38 g (90 %) of 1-ethylindan (**15**) as a clear oil.

$^1\text{Hnmr}$ δ 0.99 (3H, t, CH_3 , $J=7.3$ Hz), 1.35-1.70 (1H, m, CH_2), 2.25 (1H, m, CH_2), 2.88 (2H, dq, ethyl CH_2). 2.70-3.10 (3H, m benzylic H's) 7.12 (4H, m, aromatic H's) ppm; $^{13}\text{Cnmr}$ δ 12.0 (C-10), 27.7 (C-11), 31.4 (C-2), 32.9 (C-3), 46.5 (C-1), 123.6 (C-5), 124.4 (C-6), 125.9 (C-7), 126.2 (C-4), 144.1 (C-8), 147.6 (C-9) ppm; MS $m/z(\%)$ 145 (M^+ , 30), 131 (12), 117 (99), 103 (35), 91 (100).

1-(1-Methylethyl)indan (**16**)

To a flame dried two necked 250 mL flask containing 1.36 g Mg in 50 mL dried ether was added 5.7 mL (1.5 eq.) of isopropyl iodide in a dropwise manner at a rate as to allow a gentle reflux to be maintained. To the reaction was then added 5.0 g (0.0379 mole) of 1-indanone in 50 mL of dry ether over a 1 h period. The solution was heated at reflux for 12 h, after which time it was cooled in an ice bath and 50 mL of 15 % HCl was added. The solution was allowed to warm, before being extracted into ether and worked up in the usual

way. The crude product was chromatographed using hexane : ethyl acetate 3 : 1 to yield 3.69 g (62 %) 1-isopropyl-1-indene.

Hydrogenation was carried out in 100 mL ethyl acetate containing 0.5 g of palladium on charcoal by the usual procedure; 1-isopropyl-1-indene 2 g (0.0127 mole) gave a yield of 1.91 g (94 %) 1-isopropylindane as a clear oil.

$^1\text{Hnmr}$ δ .76 (3H, d, CH_3 , $J=6.9$ Hz), .98 (3H, d, CH_3 , $J=6.9$ Hz), 1.86 (1H, m, isopropyl CH), 2.01 (2H, m, CH_2), 2.79 (2H, m, benzylic CH_2), 3.06 (1H, m, benzylic CH) ppm; $^{13}\text{Cnmr}$ δ 21.0 (C-11), 26.6 (C-10), 30.8 (C-2), 31.6 (C-3), 51.2 (C-1), 124.2 (C-5,-6), 125.7 (C-4), 126.0 (C-7), 144.4 (C-9), 146.2 (C-8) ppm; MS $m/z(\%)$ 160 (M^+ , 20), 117 (100), 91 (9).

1-Ethyl-1,2,3,4-tetrahydronaphthalene (17)

To a 250 mL flame dried two neck flask was added 1.23 g (1.5 eq.) Mg turnings and 40 mL dry ether. The solution was cooled in an ice bath and 4.1 mL (1.5 eq.) of ethyl iodide was added slowly. After the reaction reached room temperature, α -tetralone 5.0 g (0.0342 mole) in 20 mL of dry ether was introduced in a dropwise manner and the solution stirred for a further 4 h. The reaction vessel was again cooled in an ice bath, and 50 mL of 15 % HCl was added slowly and the reaction stirred an additional 12 h. Ether extraction and work-up in the usual way, followed by purification of the crude product by chromatography with hexane gave a yield of 4.23 g (78 %) of 1-ethyl-3,4-dihydronaphthalene as a clear oil.

Hydrogenation was carried out in 100 mL ethyl acetate containing 0.5 g of palladium on charcoal by the usual procedure; 3.0 g (0.0188 mole) of 1-ethyl-3,4-dihydronaphthalene afforded 2.45 g (81 %) 1-ethyl-1,2,3,4-tetrahydronaphthalene as a clear oil.

$^1\text{Hnmr}$ δ 0.96 (3H, t, CH_3 , $J=7.4$ Hz), 1.50-1.95 (6H, m, ring CH_2 's, ethyl CH_2), 2.64-2.76 (3H, m, benzylic H's), 7.04-7.23 (4H, m, aromatic H's) ppm; $^{13}\text{Cnmr}$ δ 11.9 (C-11), 19.9 (C-3), 26.9 (C-2), 29.4 (C-4), 29.8 (C-12), 39.2 (C-1), 125.3 (C-7), 125.4 (C-6), 128.6 (C-8), 129.0 (C-5), 137.1 (C-10), 141.3 (C-9) ppm; MS $m/z(\%)$ 160 (M^+ , 18), 131 (100), 115 (9), 91 (15).

1-(1-Methylethyl)-1,2,3,4-tetrahydronaphthalene(18)

To a 250 mL flask containing 1.15 g (1.5 eq.) of Mg that had been flame dried, was added 40 mL of dried ether, followed by the dropwise addition of 4.8 mL (1.5 eq) of isopropyl iodide at such a rate as to maintain a gentle reflux. The reaction was then allowed to stir for 1 h. α -Tetralone (5.0 g, 0.0321 mole) in 45 mL of dry ether was introduced at a slow rate, after which the reaction was heated at reflux for 5 h. After cooling in an ice bath, 50 mL of 15 % HCl was added and the reaction continued for an additional 12 h. Extraction into ether followed by the usual work-up procedure and chromatography of the crude product with hexane gave a yield of 1-isopropyl-3,4-dihydronaphthalene, 2.16 g (37 %).

Hydrogenation was carried out in 100 mL ethyl acetate containing 0.5 g of palladium on charcoal by the usual procedure; 2.5 g (0.0145

mole) of 1-isopropyl-3,4-dihydronaphthalene gave a yield of 2.37 g (94 %) of 1-isopropyl-1,2,3,4-tetrahydronaphthalene (**18**).

$^1\text{Hnmr}$ δ 0.72 (3H, d, CH_3 , $J=6.9$ Hz), 0.98 (3H, d, CH_3 , $J=6.9$ Hz), 1.50- 2.10 (4H, m, CH_2 's), 2.22 (1H, dq, isopropyl CH), 2.70 (3H, m, benzylic H's), 7.02-7.21 (4H, m, aromatic H's) ppm; $^{13}\text{Cnmr}$ δ 17.4 (C-13), 21.2 (C-12), 21.3 (C-11), 23.3 (C-3), 29.8 (C-2), 31.4 (C-4), 43.5 (C-1), 125.0 (C-7), 125.2 (C-6), 128.1 (C-5), 128.8 (C-8), 137.9 (C-10), 140.2 (C-9) ppm; MS $m/z(\%)$ 174 (M^+ , 12), 146 (20), 131 (100), 118 (28), 91 (25).

(9,10-Benzo)spiro[4,5]decane (**20**) (Ref. 90)

A 250 mL two necked flask containing 1.6 g (1 eq.) of Mg turnings was flame dried under a flow of argon. To this flask was added 40 mL of dry ether, followed by the dropwise addition of 10 g (0.0649 mole) of 1-chloro-3-phenylpropane over 0.5 h. The solution was then heated at reflux for 2 h. Freshly distilled cyclopentanone 5.5 g (1 eq.) in 30 mL of dry ether was then introduced dropwise over 0.5 h, and the solution refluxed for 16 h. A solution of 5% HCl was then added slowly until effervescence was no longer visible and the product extracted into ether. The ether was washed with saturated NaHCO_3 solution, distilled water, and dried over anhydrous MgSO_4 . The ether was then removed under reduced pressure to yield 12.84 g (97%) 1-(3-phenylpropyl)cyclopentanol as a clear oil.

$^1\text{Hnmr}$ δ 1.48-1.79 (12H, m, CH_2 's), 2.62 (2H, t, benzylic CH_2), 7.14-7.30 (5H, m, aromatic H's) ppm; $^{13}\text{Cnmr}$ δ 23.7 (C-6,-7), 26.5 (C-2), 36.3 (C-1), 39.6 (C-5,-8), 41.0 (C-3), 83.3 (C-4), 125.6 (C-4'),

128.2/128.3 (C-2',-6',-3',-5'), 142.4 (C-1') ppm; MS m/z(%) 189 (13), 104 (100), 91 (58).

The above alcohol (5 g, .0245 mole) was dissolved in 20 mL of dry dichloromethane, in a polypropylene container, and cooled to -90 deg. C in a liquid nitrogen/ methanol bath. To this solution was added dropwise, with good stirring, 15 mL (10 eq.) of fluorosulfuric acid. The solution was stirred for .5 h, at which time it was added dropwise (reaction extremely violent) to 350 mL of ice cold water. The aqueous solution was then neutralized with solid NaHCO₃, extracted into ether, and the ether layer washed with distilled water, and dried over anhydrous MgSO₄. The ether was then removed under reduced pressure, and the crude product chromatographed using hexane as the eluting solvent, to yield 3.26 g (72%) of (9,10-benzo)spiro[4,5]decane (20) as a clear oil.

¹Hnmr δ 1.67 (14H, m, CH₂'s), 2.75 (2H, t, benzylic CH₂), 6.99 (4H, m, aromatic H's) ppm; ¹³Cnmr δ 20.8 (C-6), 25.9 (C-3,-4), 30.5 (C-7), 37.4 (C-8), 43.5 (C-1,-4), 45.8 (C-5), 124.9 (C13), 125.9 (C12), 126.9 (C11), 128.9 (C14), 136.7 (C9), 146.3 (C10) ppm; MS m/z(%) 186 (M⁺, 57), 157 (36), 144 (100), 129 (58), 115 (17).

10,11-Benzospiro[5,5]undecane(21) (Ref. 90)

1-(3-phenylpropyl)cyclohexanol was prepared as above using 10 g (0.0649 mole) 1-chloro-3-phenylpropane, 1.6 g (1 eq.) Mg turnings and 6.4 g (1 eq.) freshly distilled cyclohexanone. After extraction and work-up, 14.0 g (99%) 1-(3-phenylpropyl)cyclopentanol was obtained as a clear oil.

$^1\text{Hnmr}$ δ 1.15-1.68 (14H, m, CH_2 's), 2.60 (2H, t, benzylic CH_2), 7.15-7.26 (5H, m, aromatic CH_2 's) ppm; $^{13}\text{Cnmr}$ δ 22.2 (C6,8), 24.7 (C7), 25.8 (C2), 36.4 (C1), 37.4 (C5,9), 41.9 (C3), 71.2 (C4), 125.6 (C4'), 128.2/128.3 (C2',3',5',6'), 142.5 (C1') ppm; MS $m/z(\%)$ 200 (12), 104 (100).

The alcohol 5 g (.0229 mole) was treated as above, after extraction and work-up, the crude mixture was chromatographed using hexane as the eluting solvent to yield 2.95 g (64%) (10,11-

benzo)spiro[5,5]undecane(21) as a clear oil.

$^1\text{Hnmr}$ δ 1.59-1.85 (16H, m, CH_2 's), 2.74 (2H, t, benzylic CH_2), 7.01-7.67 (4H, m, aromatic H's) ppm; $^{13}\text{Cnmr}$ δ 19.3 (C-3), 22.1 (C-4,-2), 22.3 (C-7), 26.4 (C-8), 31.1 (C-9), 35.3 (C6), 38.8 (C-1,-5), 125.1 (C-14), 125.7 (C-13), 126.7 (C-12), 128.8 (C-15), 137.1 (C-10), 146.6 (C-11) ppm.

III Incubation of Substrates

3-Ethyltoluene (1)

1-(3-Methylphenyl)-ethanol (**1a**) was isolated as an oil from the crude extract (0.03 g) using hexane:ethyl acetate 3:2 as the eluting solvent, in a 1.5 % overall yield. $R_f = 0.48$

$^1\text{Hnmr } \delta$ 1.48 (3H, d, ethyl CH_3 , $J=6.5\text{Hz}$), 2.35 (3H, s, methyl CH_3), 4.85 (1H, q, CHOH , $J=6.5\text{ Hz}$), 7.06-7.27 (4H, m, aromatic H's) ppm;
 $^{13}\text{Cnmr } \delta$ 21.4 (C-7), 25.1 (C-9), 70.4 (C-8), 122.4 (C-4), 126.1 (C-6), 128.2 (C-5), 128.4 (C-2), 138.1 (C-1), 145.8 (C-3) ppm; MS $m/z(\%)$ 136 (M^+ , 47), 121 (58), 119 (95), 103 (15), 91 (100); I.R. 3396 cm^{-1} , broad OH stretch; $[\alpha]_D = 0.0$ ($c = .56$, ethanol); ee = 0%.

2-Fluoroethylbenzene (2)

1-(2-Fluorophenyl)ethanol (**2a**) was isolated as an oil from the extract (0.29 g), using hexane : ethyl acetate 3:2 as the eluting solvent, in a 5.5% overall yield. $R_f = 0.58$

$^1\text{Hnmr } \delta$ 1.47 (3H, d, CH_3 , $J=6.5\text{ Hz}$), 5.15 (1H, q, CHOH , $J=6.5\text{ Hz}$), 6.94-7.25 (3H, m, aromatic H's), 7.41-7.49 (1H, m, aromatic H) ppm;
 $^{13}\text{Cnmr } \delta$ 23.9 (C-8), 84.5 (d, C-7), 115.2 (d, C-3), 124.2 (d, C-5), 126.6 (d, C-4), 128.7 (d, C-6), 132.7 (d, C-1), 159.8 (d, C-2) ppm;
 MS $m/z(\%)$ 140 (M^+ , 35), 125 (100), 123 (24), 105 (25), 97 (99), 77 (89); I.R. 3349 cm^{-1} , broad OH stretch.; $[\alpha]_D = +24.3$ ($c = 2.9$, ethanol); ee = 52%.

3-Fluoroethylbenzene (3)

1-(3-Fluorophenyl)ethanol (**3a**) was isolated as an oil from the extract (0.29 g), using hexane : ethyl acetate 3:2 as the eluting solvent, in a 2.5% overall yield. $R_f = 0.47$

$^1\text{Hnmr } \delta$ 1.47 (3H, d, CH_3 , $J=6.5$ Hz), 4.88 (1H, q, CH, $J=6.5$ Hz), 6.89-7.35 (4H, m, aromatic H's) ppm; $^{13}\text{Cnmr } \delta$ 25.2 (C-8), 69.8 (C-7), 112.3 (d, C-4), 114.2 (d, C-2), 120.9 (C-6), 130.0 (d, C-5), 148.6 (d, C-1), 163.0 (d, C-3) ppm; MS $m/z(\%)$ 140 (M^+ , 43), 125 (100), 123 (25), 97 (88); $[\alpha]_D = +2.2$; ee = 18%.

4-Ethylbiphenyl (4)

Two products were isolated from the crude extract (0.1 g) using hexane : ethyl acetate 3:2 as the eluting solvent. The products in order of elution were.

1-(4-Biphenyl)ethanol (**4a**) was isolated as a solid, mp 73 - 76 deg C in an overall yield of 0.6 %. $R_f = 0.32$

$^1\text{Hnmr } \delta$ 1.54 (3H, d, CH_3 , $J=6.4$ Hz), 4.96 (1H, q, CH, $J=6.4$ Hz), 7.25-7.61 (9H, m, aromatic H's) ppm; $^{13}\text{Cnmr } \delta$ 25.1 (C-8), 70.2 (C-7), 125.9 (C-3, -5), 127.1 (C-2, -6), 127.3 (C-2', -4', -6'), 128.8 (C-3', -5'), 140.6 (C-4), 140.9 (C-1'), 144.9 (C-1) ppm; MS $m/z(\%)$ 198 (M^+ , 73), 183 (100); IR 3335 cm^{-1} , broad OH stretch; $[\alpha]_D = +14.9$ ($c=0.31$, ethanol); ee = 48%.

2-(4-Biphenyl)ethanol (**4b**) was isolated as a solid, mp 86 - 89 deg C in a 1.0 % overall yield. $R_f = 0.21$

$^1\text{Hnmr}$ δ 2.92 (2H, t, benzylic CH_2 , $J=6.5$ Hz), 3.91 (2H, t, terminal CH_2 , $J=6.5$ Hz), 7.25-7.60 (9H, m, aromatic H's) ppm; $^{13}\text{Cnmr}$ δ 38.5 (C-7), 63.6 (C-8), 127.0 (C-2', -6'), 127.1 (C-4'), 127.3 (C-3, -5), 128.7 (C-2, -6), 129.4 (C-3', -5'), 137.6 (C-4), 139.5 (C-1'), 141.0 (C-1) ppm; MS $m/z(\%)$ 198 (M^+ , 37), 167 (100); IR 3387 cm^{-1} , broad OH stretch.

4-*tert*-Butylethylbenzene (5)

Two products were isolated from the crude extract (0.11 g) using hexane : ethyl acetate 3:2 as the eluting solvent. The products in order of elution were.

1-(4-*tert* -Butylphenyl)ethanol (**5a**) was isolated as an oil in an overall yield of 1.7 %.

$^1\text{Hnmr}$ δ 1.32 (9H, s, t-butyl H's), 1.49 (3H, d, CH_3 , $J= 6.5$ Hz), 4.87 (1H, q, CH, $J= 6.5$ Hz), 7.20-7.41 (4H, m, aromatic H's) ppm; $^{13}\text{Cnmr}$ δ 24.9 (C-8), 31.4 (C1-0, 3C), 34.5 (C-9), 70.2 (C-7), 125.2 (C-3, -5), 125.4 (C-2, -6), 142.8 (C-1), 150.5 (C-4) ppm; MS $m/z(\%)$ 178 (M^+ , 28), 163 (72), 161 (31), 160 (33), 145 (100); I.R. 3361 cm^{-1} , broad OH stretch; $[\alpha]_{\text{D}} = + 12.6$ ($c = .77$, ethanol); ee = 36%.

2-(4-*tert* -Butylphenyl)ethanol (**5b**) was isolated as an oil in a 0.2 % yield.

$^1\text{Hnmr}$ δ 1.31 (9H, s, t-butyl H's), 2.85 (2H, t, benzylic CH_2 , $J= 6.5$ Hz), 3.86 (2H, t, terminal CH_2 , $J= 6.5$ Hz), 7.17 and 7.35 (4H, ABq) ppm; $^{13}\text{Cnmr}$ δ 31.4 (C-10), 34.4 (C-9), 38.7 (C-7), 63.7 (C-8), 125.5 (C-3, -5), 128.7 (C-2, -6), 135.3 (C-1), 149.0 (C-4) ppm; MS

m/z(%) 178 (M^+ , 29), 163 (100), 147 (23), 132 (17), 117, (32);
I.R. 3341 cm^{-1} , broad OH stretch.

1,2,3-Trimethylbenzene (6)

Only starting material was recovered from the extract; no alcohol products were obtained.

1,3,5-Trimethylbenzene (7)

Only starting material was recovered from the extract; no alcohol products were obtained.

2-Methyl-1-phenylpropane (8)

Two products were isolated from the crude extract (0.36 g) using hexane : ethyl acetate 3:2 as the eluting solvent. The products in order of elution.

1-Hydroxy-2-methyl-1-phenylpropane (**8a**) was isolated as an oil in a 0.7% yield. $R_f = 0.8$

$^1\text{Hnmr}$ δ 0.80 (3H, d, CH_3 , $J = 6.8$ Hz), 1.01 (3H, d, CH_3 , $J = 6.8$ Hz), 1.96 (1H, q, CH, $J = 6.8$ Hz), 7.32 (5H, m, aromatic H's) ppm; $^{13}\text{Cnmr}$ δ 18.2 (C-3 or C-4), 19.1 (C-3 or C-4), 35.3 (C-2), 80.1 (C-1), 126.6 (C-3', -5'), 127.4 (C-4), 128.2 (C-2', -6'), 143.7 (C-1) ppm; MS m/z(%) 150 (M^+ , 18), 133 (28), 105 (25), 91 (100); I.R. 3409 cm^{-1} , broad OH stretch; $[\alpha]_D = +6.8$ ($c = 0.22$, ethanol); ee = 36%.

2-Hydroxy-2-methylphenylpropane (**8b**) was isolated in an 8.0% yield. $R_f = 0.62$

$^1\text{Hnmr } \delta$ 1.21 (6H, s, CH_3 's), 2.75 (2H, s, benzylic CH_2) 7.18 (5H, m, aromatic H's) ppm; $^{13}\text{Cnmr } \delta$ 29.1 (C-3, -4), 49.7 (C-1), 70.6 (C-2), 126.4 (C-4'), 128.1 (C-3', -5'), 130.4 (C-2', -6'), 137.8 (C-1') ppm; MS $m/z(\%)$ 150 (M^+ , 7), 135 (15), 117 (15), 92 (100), 91 (47), 59 (57); I.R. 3390 cm^{-1} , broad OH stretch.

2,2-Dimethylphenylpropane (9)

Two products were isolated from the crude extract (0.14 g) using hexane : ethyl acetate 3:2 as the eluting solvent. The products in order of elution.

2,2-Dimethyl-3-hydroxyphenylpropane (**9a**) was isolated in a 1.6% yield. $R_f = 0.34$

$^1\text{Hnmr } \delta$ 0.87 (6H, s, 2 methyls), 2.58 (2H, s, benzylic H's), 3.32 (2H, s, CH_2OH), 7.14-7.28 (5H, m, aromatic H's) ppm; $^{13}\text{Cnmr } \delta$ 23.9 (2 X methyl), 36.4 (C-2), 71.2 (C-3), 125.9 (C-4'), 127.6 (C-3', -5'), 130.5 (C-2', -6'), 138.7 (C-1') ppm; MS $m/z(\%)$ 164 (M^+ , 18), 146 (3), 133 (10), 131 (8), 92 (100), 91 (81), 73 (22); I.R. 3373 cm^{-1} , broad OH stretch.

2,2-Dimethyl-1-hydroxyphenylpropane (**9b**) was isolated in a 2.3% yield. $R_f = 0.24$

$^1\text{Hnmr } \delta$ 0.92 (9H, s, CH_3 's), 4.39 (1H, s, CHOH), 7.28-7.32 (5H, m, aromatic H's) ppm; $^{13}\text{Cnmr } \delta$ 25.9 (3 X methyl), 35.7 (C-2), 82.5 (C-1), 127.3 (C-4'), 127.5 (C-3', -5'), 127.6 (C-2', -6'), 142.3 (C-1') ppm; MS $m/z(\%)$ 149 (100), 131 (19), 117 (36), 91 (22), 57 (54);

I.R. 3445 cm^{-1} , broad OH stretch; $[\alpha]_D = +19.2$ ($c = .38$, ethanol); ee = 55%.

Cyclobutylphenylmethane (10)

Four products were isolated from the crude extract (.03 g) using hexane : ethyl acetate 3:2 as the eluting solvent. The products in order of elution.

Cyclobutylphenylmethanol (**10a**) was obtained as an oil in a 5.3% overall yield.

$^1\text{Hnmr } \delta$ 1.78-2.06 (6H, m, cyclobutyl CH_2 's), 2.62 (1H, m, cyclobutyl CH), 4.57 (CHOH), 7.25-7.34 (5H, m, aromatic H's) ppm; $^{13}\text{Cnmr } \delta$ 17.8 (C-3), 24.8 (C-2, -4), 42.5 (C-1), 78.4 (C-5), 126.2 (C-3',-5'), 127.5 (C-4'), 129.3 (C-2, -6), 143.2 (C-1') ppm; MS $m/z(\%)$ 162 (M^+ , 13), 144 (10), 129 (12), 107 (100), 91 (33), 79 (62), 77 (47); $[\alpha]_D = +8.6$ ($c = 0.8$, ethanol); ee = 100%.

(1-Hydroxycyclobutyl)phenylmethane (**10b**) was obtained as an oil in a 2.4% overall yield.

$^1\text{Hnmr } \delta$ 1.77-2.21 (6H, m, cyclobutyl CH_2 's), 2.90 (2H, s, benzylic CH_2), 7.24-7.33 (5H, m, aromatic H's) ppm; $^{13}\text{Cnmr } \delta$ 12.2 (C-3), 35.5 (C-2, -4), 45.6 (C-5), 75.1 (C-1), 126.6 (C-4'), 128.3 (C-3', -5'), 130.0 (C-2', -6'), 137.5 (C-1') ppm; MS $m/z(\%)$ 162 (M^+ , 15), 147 (5), 134 (27), 129 (7), 116 (36), 105 (22), 92 (69), 91 (100); I.R. 3375 cm^{-1} , broad OH stretch.

(2-Hydroxycyclobutyl)phenylmethane (**10c**) and (3-hydroxycyclobutyl)phenylmethane (**10d**) coeluted and were

obtained in a 11.5% combined yield. Products determined by Carbon nmr in a ratio of 2:1 (**10d**):(**10c**).

(2-Hydroxycyclobutyl)phenylmethane (**10c**)

$^{13}\text{Cnmr } \delta$ 28.7 (C-3), 37.4 (C-5), 41.2 (C-1), 66.2 (C-2), C-4 buried, 141 (C-1') ppm.

(3-Hydroxycyclobutyl)phenylmethane (**10d**)

$^{13}\text{Cnmr } \delta$ 26.7 (C-1), 39.6 (C-2, -4), 43.0 (C-5), 64.0 (C-3), 140.8 (C-1') ppm.

Cyclopentylphenylmethane (**11**)

Three products were isolated from the crude extract (0.14 g) using hexane : ethyl acetate 3:2 as the eluting solvent. The products in order of elution.

(1-Hydroxycyclopentyl)phenylmethane (**11a**) was isolated as an oil in a 1.6% yield. $R_f = 0.58$

$^1\text{Hnmr } \delta$ 1.49-1.77 (6H, m, cyclopentyl CH_2 's), 2.81 (2H, s, benzylic CH_2), 7.12-7.26 (5H, m, aromatic H's) ppm; $^{13}\text{Cnmr } \delta$ 23.5 (C-3, -4), 39.5 (C-2, -5), 74.1 (C-1), 47.5 (C-6), 126.5 (C-4'), 128.3 (C-3', -5'), 130.2 (C-2', -6'), 138.3 (C-1') ppm; (MS $m/z(\%)$) 176 (M^+ , 9), 158 (36), 92 (91), 92 (100).

(2-Hydroxycyclopentyl)phenylmethane (**11b**) was isolated as an oil in a 0.7% yield. The cis/trans ratio determined by H nmr was approximately 2:1. $R_f = 0.30$

$^1\text{Hnmr } \delta$ 1.17-1.92 (6H, m, cyclopentyl CH_2 's), 2.60 (2H, d, benzylic H's, major isomer), 2.67 (2H, d, benzylic H's, minor isomer), 3.78 (1H, t, CHOH), 7.06-7.16 (5H, m, aromatic H's) ppm; $^{13}\text{Cnmr } \delta$ 21.8

(C-4), 30.2 (C-5), 34.3 (C-3), 40.1 (C-6), 50.0 (C-1), 126.5 (C-4'), 128.3 (C-3',-5'), 128.7 (C-2', -6'), 141.9 (C-1') ppm; MS m/z(%) 176 (M⁺, 16), 158 (11), 143 (4), 129 (8), 117 (22), 92 (100), 91 (66). (3-Hydroxycyclopentyl)phenylmethane (**11c**) was isolated as an oil in a 5.3% yield. The *cis/trans* ratio determined by Hnmr was approximately 1:1. R_f = 0.27

¹Hnmr δ 1.17-2.12 (7H, m, cyclopentyl CH₂'s), 2.60 (2H, d, benzylic isomer 1), 2.68 (2H, d, benzylic isomer 2), 7.13-7.30 (5H, m, aromatic H's) ppm; ¹³Cnmr δ (ring carbons all two peaks), 30.1 (C-5), 35.1 (C-4), 39.1 (C-6 isomer 1), 40.2 (C-6 isomer 2), 42.0 (C-1), 42.4 (C-1), 125.6 (C-4'), 128.1 (C-3',- 5'), 128.7 (C-2', -6'), 141.7 (C-1') ppm; MS m/z(%) 176 (M⁺, 22), 158 (25), 143 (3), 129. (8), 117 (100), 92 (59), 91 (66).

Cyclohexylphenylmethane (12)

Two products were isolated from the crude extract (0.06 g) using hexane : ethyl acetate 3:2 as the eluting solvent. The products in order of elution.

trans-(4-Hydroxycyclohexyl)phenylmethane (**12a**) was isolated as an oil in a 1.9% yield. R_f = 0.52

¹Hnmr δ 1.41-1.76 (9H, cyclohexyl CH₂'s), 2.54 (2H, d, benzylic H's), 3.96 (1H, m, CHOH), 7.13-7.31 (5H, m, aromatic H's) ppm; ¹³Cnmr δ 26.8 (C-2, -6), 32.3 (C-3, -5), 38.4 (C-1), 42.8 (C-7), 67.0 (C-4), 125.7 (C-4'), 128.1 (C-3', -5'), 129.1 (C-2', -6'), 141.1 (C-1') ppm; MS m/z(%) 190 (M⁺, 23), 172 (14), 92 (75), 91 (48), 81 (100); I.R. 3267 cm⁻¹, broad OH stretch.

cis-(4-Hydroxycyclohexyl)phenylmethane (**12b**) was isolated as an oil in a 0.7% yield. $R_f = 0.40$

$^1\text{Hnmr } \delta$ 0.91-1.98 (9H, m, cyclohexyl CH₂'s), 2.84 (2H, d, benzylic CH₂), 3.55 (1H, m, CHOH), 7.12-7.32 (5H, m, aromatic H's) ppm;

$^{13}\text{Cnmr } \delta$ 31.1 (C-2, -6), 35.6 (C-3, -5), 38.8 (C-1), 43.3 (C-7), 71.1 (C-4), 125.8 (C-4'), 128.2 (C-3', -5'), 129.1 (C-2', -6'), 141.0 (C-1') ppm; MS $m/z(\%)$ 190 (M^+ , 23), 172 (21), 144 (3), 130 (11), 92 (76), 91 (57), 81 (100); I.R. 3363 cm^{-1} , broad OH stretch.

Diphenylmethane (13)

Two products were isolated from the crude extract (0.05 g) using hexane : ethyl acetate 3:2 as the eluting solvent. The products in order of elution.

Diphenylmethanol (**13a**) was isolated as an oil in a 0.9% yield. $R_f=0.56$

$^1\text{Hnmr } \delta$ 5.84 (1H, s, CHOH), 7.25-7.36 (10H, m, aromatic H's) ppm;

$^{13}\text{Cnmr } \delta$ (D₆ DMSO) 74.2 (C-7), 126.1 (C-2, -2', -6, -6')), 126.8 (C-4, -4'), 127.9 (C-3, -3', -5, -5'), 143.9 (C-1, -1') ppm; MS $m/z(\%)$ 184 (M^+ , 40), 183 (18), 165 (14), 105 (100); I.R. 3360 cm^{-1} , broad OH stretch.

(2,5-dihydroxyphenyl)phenylmethane (**13b**) was isolated as an oil in a 0.5% overall yield. $R_f = 0.31$

$^1\text{Hnmr } \delta$ 3.93 (2H, s, benzylic H's), 6.57-6.64 (3H, m, aromatic H's), 7.20-7.32 (5H, m, aromatic H's) ppm; $^{13}\text{Cnmr } \delta$ 36.3 (C-7), 114.1

(C-4), 116.7 (C-6), 117.6 (C-3), 126.4 (C-4'), 128.6 (C-2', -6'), 128.7 (C-3', -5'), 130.4 (C-1), 139.7 (C-1'), 147.7 (C-2), 149.6 (C-5) ppm;

MS $m/z(\%)$ 200 (M^+ , 74), 183 (19), 181 (34), 165 (16), 152 (23), 122 (100), 105 (62), 91 (53), 77 (42).

1-Methylindan (14)

Four products were isolated from the crude extract (0.56 g) using hexane : ethyl acetate 3:2 as the eluting solvent. The products in order of elution.

1-(Hydroxymethyl)indan (14a) and *cis* and *trans* 2-hydroxy-1-methylindan (14b) coeluted with fungal material, in a 2.9% combined yield, in a ratio of 70 : 30 respectively.

1-Hydroxymethylindan (14a)

$^1\text{Hnmr}$ included peaks are δ 3.73 (2H, d, CH_2OH), 7.38 (4H, m, combined aromatic H's) ppm; $^{13}\text{Cnmr}$ included peaks are δ 72.0 (C-10) ppm.

cis/trans 2-Hydroxy-1-methylindan (14b)

$^1\text{Hnmr}$ included peaks are δ 5.09 (1H, m, CHOH), 7.38 (4H, m, combined aromatic H's) ppm; $^{13}\text{Cnmr}$ included peaks are δ 61.5 and 62.1 (C2, *cis* and *trans*).

1-Hydroxy-1-methylindan (14c) and 3-hydroxy-1-methylindan (14d) coeluted in a 4.4% combined yield.

1-Hydroxy-1-methylindan (14c)

$^1\text{Hnmr}$ included peaks are δ 1.55 (3H, s, CH_3), 7.18-7.40 (4H, m, aromatic) ppm; $^{13}\text{Cnmr}$ δ 27.3 (C10), 29.3 (C3), 44.7 (C2), 81.2 (C1), 122.2 (C5), 124.9 (C6), 126.8 (C7), 128.1 (C4), 142.6 (C9), 148.3 (C8) ppm.

3-Hydroxy-1-methylindan (14d)

$^1\text{Hnmr } \delta$ 1.27 (3H, d, CH_3), 5.21 (1H, dd, CHOH), 7.18-7.40 (4H, m, aromatic) ppm; $^{13}\text{Cnmr } \delta$ 20.3 (C-10), 36.7 (C-2), 44.7 (C-1), 75.1 (C-3), 123.7 (C-5), 124.4 (C-6), 128.7 (C-4), 143.5 (C-8), 148.6 (C-9) ppm;

Combined (14c) and (14d) MS m/z(%) 148 (M^+ , 46), 131 (100), 130 (67), 115 (57).

1-Ethylindan (15)

Three products were isolated from the crude extract (0.12 g) using hexane : ethyl acetate 3:2 as the eluting solvent. The products in order of elution.

1,2-Dihydroxy-1-ethylindan (15a) was isolated in a 0.2 % yield along with some fungal material, the structure was based on mass spectral data.

MS m/z(%) 161 (M^+ -17, 59), 143 (100), 128 (70)

1-Hydroxy-1-ethylindan (15b) was isolated in a 2.0% yield.

$^1\text{Hnmr } \delta$ 0.95 (3H, t, CH_3), 1.73-2.36 (4H, m, CH_2 's), 2.65-3.00 (2H, m, benzylic H's) 7.23-7.37 (4H, m, aromatic H's) ppm; $^{13}\text{Cnmr } \delta$ 8.6 (C-11), 29.5 (C-3), 33.0 (C-10), 39.4 (C-2), 84.1 (C-1), 122.8 (C-5), 124.9 (C-6), 126.6 (C-7), 128.2 (C-4), 143.2 (C-9), 147.4 (C-8) ppm;

MS m/z(%) 162 (M^+ , 10), 144 (15), 133 (100), 115 (22).

1-Hydroxyindan (15c) was isolated in a 0.5% yield.

$^1\text{Hnmr } \delta$ 1.72 (2H, m, CH_2), 2.77-3.06 (2H, m, benzylic H's), 5.23 (1H, t, CHOH), 7.26-7.41 (4H, m, aromatic H's) ppm; $^{13}\text{Cnmr } \delta$ 29.8 (C-2), 36.0 (C-3), 76.4 (C-1), 124.2 (C-5), 124.9 (C-6), 126.8 (C-7),

128.4 (C-4), 143.3 (C-9), 145.1 (C-8) ppm; MS m/z(%) 134 (M⁺,48), 133 (100), 115 (23), 91 (16), 77 (16).

1-(1-Methylethyl)indan (16)

Two products were isolated from the crude extract (0.17 g) using hexane : ethyl acetate 3:2 as the eluting solvent. The products in order of elution.

3-Hydroxy-1(1-methylethyl)indan (**16a**) and 1-(1-hydroxy-1-methylethyl)indan (**16b**) coeluted and were obtained in a 2.0% combined yield.

3-Hydroxy-1-(1-methylethyl)indan (**16a**)

¹Hnmr included peaks are δ 0.73 (3H, d, isopropyl CH₃), 0.97 (3H, d, isopropyl CH₃), 5.24 (1H, t, benzylic CHOH), 7.14-7.50 (4H, m, aromatic H's) ppm; ¹³Cnmr included peaks are δ 17.9 (C-12), 21.0 (C-11), 31.3 (C-10), 31.9 (C-2), 48.9 (C-1), 75.6 (C-3) ppm.

1-(2-Hydroxy-1-methylethyl)indan (**16b**)

¹Hnmr included peaks are δ 1.14 (3H, s, isopropyl CH₃), 1.26 (3H, s, isopropyl CH₃), 7.14-7.50 (4H, m, aromatic H's) ppm; ¹³Cnmr included peaks are δ 25.9 (C-2), 28.6 (C-12), 29.7 (C-11), 38.2 (C-3), 56.5 (C-1), 74.5 (C-10) ppm.

Combined (**16a**) and (**16b**), MS m/z(%) 176 (M⁺,13), 158 (21), 143 (37), 133 (83), 118 (100).

1-Ethyl-1,2,3,4-tetrahydronaphthalene(17)

Two products were isolated from the crude extract (0.38 g) using hexane : ethyl acetate 3:2 as the eluting solvent. The products in order of elution.

1-Ethyl-1-hydroxy-1,2,3,4-tetrahydronaphthalene (17a) was obtained as an oil in a 0.2% overall yield.

$^1\text{Hnmr}$ δ 1.00 (3H, t, CH_3), 2.87 (2H, q, CH_2CH_3), 2.09-2.95 (6H, m, CH_2 's), 7.32-7.44 (1H, m, aromatic H), 7.53-7.69 (2H, m, aromatic H's), 7.94-8.03 (1H, d, aromatic H) ppm; $^{13}\text{Cnmr}$ δ 8.2 (C-12), 29.7 (C-3), 33.6 (C-2), 34.9 (C-4), 35.4 (C-11), 125.4 (C-6, -7), 127.2 (C-5), 127.7 (C-8) ppm; MS m/z(%) 161 (M^+ -15, 100), 147 (6), 129 (9), 115 (15).

1-Ethyl-1,2-dihydroxytetralin (17b) was obtained as an oil in a 0.25% overall yield.

$^1\text{Hnmr}$ δ .96 (3H, t, CH_3), 1.67-1.98 (4H, m, CH_2 's), 2.20-2.34 (2H, m, benzylic CH_2), 4.80 (1H, t, CHOH), 7.28-7.55 (4H, m, aromatic H's) ppm; $^{13}\text{Cnmr}$ δ 8.7 (C-12), 28.9 (C-11), 31.1 (C-3), 34.9 (C-4), 68.5 (C-2), 72.6 (C-1), 126.2 (C-6), 127.8 (C-7), 128.36 (C-5), 128.44 (C-8), 138.3 (C-10), 142.0 (C-9) ppm; MS m/z(%) 174 (M^+ - H_2O , 10), 163 (M^+ - CH_2CH_3 , 61), 156 (10), 145 (100), 127 (25).

1-(1-Methylethyl)-1,2,3,4-tetrahydronaphthalene(18)

Three products were isolated from the crude extract (0.48 g) using hexane : ethyl acetate 3:2 as the eluting solvent. The products in order of elution.

α -tetralone (**18a**) was obtained as an oil in a 3.7% yield.

$^1\text{Hnmr}$ δ 2.13 (2H, q, CH_2), 2.63 (2H, t, benzylic CH_2), 2.94 (2H, t, CH_2 α -carbonyl), 7.20-7.45 (3H, m, aromatic H's), 8.02 (1H, d, aromatic H β -carbonyl) ppm; $^{13}\text{Cnmr}$ δ 22.9 (C-3), 29.3 (C-3), 38.7 (C-2), 125.9 (C-6), 126.8 (C-7), 128.2 (C-5), 132.1 (C-10), 132.9 (C-8), 144.5 (C-9), 198.2 (C-1) ppm; MS $m/z(\%)$ 146 (M^+ , 94), 118 (100), 90 (40).

4-Hydroxy-1-(1-methylethyl)-1,2,3,4-tetrahydronaphthalene (**18b**) was obtained as an oil in a 2.0 % yield as a *cis* / *trans* mixture.

$^1\text{Hnmr}$ included peaks are δ 4.74 (1H, t, CHOH), 7.08-8.02 (4H, m, aromatic H's) ppm; $^{13}\text{Cnmr}$ included peaks are δ 73.2 (C-4 *cis* or *trans*), 74.8 (C-4 *cis* or *trans*) ppm; MS $m/z(\%)$ 146 (M^+ - 43, 100), 129 (40).

4-Hydroxy-1-(1-hydroxy-1-methylethyl)-1,2,3,4-tetrahydronaphthalene (**18c**) coeluted with some (**18b**) as an oil in a 3.4 % overall yield.

$^1\text{Hnmr}$ included peaks are δ 0.70 (3H, d, CH_3), 1.13 (3H, d, CH_3), 1.30 (6H, d, CH_3 's), 4.77 (1H, t, CHOH) ppm; $^{13}\text{Cnmr}$ included peaks are δ 74.2 (C-4) benzylic compound, 68.0 (C-11) non-benzylic compound; MS $m/z(\%)$ 130 (M^+ - 59, 100).

Benzocycloheptene (19)

Three products were isolated from the crude extract using hexane : ethyl acetate 3:2 as the eluting solvent. The products in order of elution.

1-Hydroxybenzocycloheptene (**19a**) was obtained in a 2.4% overall yield. $R_f = 0.48$

$^1\text{Hnmr } \delta$ 1.44-2.08 (6H, m, CH_2 's), 2.65-2.98 (2H, m, benzylic CH_2), 4.94 (1H, d, CHOH), 7.07-7.27 (3H, m, aromatic H's), 7.42-7.46 (1H, d, aromatic H) ppm; $^{13}\text{Cnmr } \delta$ 27.6 (C-3), 27.7 (C-4), 35.8 (C-2), 36.6 (C-5), 124.7 (C-7), 126.1 (C-8), 127.0 (C-6), 129.5 (C-9), 140.8 (C-11), 144.3 (C-10) ppm; MS $m/z(\%)$ 162 (M^+ , 9), 144 (95), 129 (100), 115 (45), 91 (98); I.R. 3249 cm^{-1} , broad OH stretch; $[\alpha]_D = +7.7$ ($c = 0.84$, ethanol); ee = 48%.

2-Hydroxybenzocycloheptene (**19b**) was obtained in a 2.5% overall yield. $R_f = 0.28$

$^1\text{Hnmr } \delta$ 1.62 (2H, m, CH_2), 1.87 (2H, m, CH_2), 2.73 (2H, t, benzylic CH_2), 3.02 (2H, d, benzylic CH_2), 3.81 (1H, m, CHOH), 7.07-7.26 (4H, m, aromatic H's) ppm; $^{13}\text{Cnmr } \delta$ 24.3 (C-4), 35.7 (C-5), 40.7 (C-3), 44.7 (C-1), 69.3 (C-2), 126.3 (C-7), 126.6 (C-8), 129.0 (C-6), 130.7 (C-9), 136.5 (C-11), 143.5 (C-10) ppm; MS $m/z(\%)$ 162 (M^+ , 31), 144 (35), 129 (81), 118 (100), 105 (66), 91 (68), 77 (30); I.R. 3341 cm^{-1} , broad OH stretch; $[\alpha]_D = -10.7$ ($c = 0.71$, ethanol); ee = 56%.

3-Hydroxybenzocycloheptene (**19c**) was obtained in a 3.8% overall yield. $R_f = 0.22$

$^1\text{Hnmr } \delta$ 1.57 (4H, m, CH_2 's), 2.65 (2H, t, benzylic CH_a), 2.88 (2H, t, benzylic CH_b), 3.94 (1H, m, CHOH), 7.11 (4H, broad s, aromatic H's) ppm; $^{13}\text{Cnmr } \delta$ 30.3 (C2, 4), 36.5 (C1, 5), 73.5 (C3), 126.3 (C7, 8), 129.0 (C6, 9), 142.2 (C10, 11) ppm; MS $m/z(\%)$ 162 (M^+ , 13), 144 (28), 129 (100); I.R. 3340 cm^{-1} , broad OH stretch.

(9,10-Benzo)spiro[4,5]decane (20)

No products were obtained from this incubation.

10,11-Benzospiro[5,5]undecane(21)

One product was isolated from the crude extract (0.20 g) using hexane : ethyl acetate 3:2 as the eluting solvent. Preliminary results show the product that was obtained, was 9-hydroxy-10,11-Benzospiro[5,5]undecane as an oil in a 3.0 % overall yield.

$^1\text{Hnmr}$ included peaks are δ 2.2 (1H, t, benzylic), 6.8-7.5 (4H, m, aromatic) ppm; $^{13}\text{Cnmr}$ included peaks are δ 75.2 (C-9).

1,4-epoxy-1,2,3,4-tetrahydronaphthalene (22)

No products were obtained from this incubation. Bulk recovery of starting material was observed.

9,10-dihydroanthracene (23)

No products were obtained from this incubation. Bulk recovery of starting material was observed.

9,10-dihydrophenanthrene (24)

No products were obtained from this incubation. Bulk recovery of starting material was observed.

REFERENCES

1. Orville, A.M., Lipscomb, J.D., *J. Biol. Chem.* **264**,1989, 8791.
2. Guengerich, F.P., *Mammalian Cytochromes Vol. 1&2*, CRC Press 1987.
3. Peterson, J.A., *Arch. Biochem. Biophys.* **144**, 1971, 678.
4. Omura, T. and Sato, R., *Cytochrome P-450*. Academic Press, New York, 1978.
5. Smith, R.V., Rosazza, J.P., *Arch. Biochem. Biophys.* **161**,1974, 551.
6. Tang, S.C., Kock, S., Papaefthymiou, G.C., Foner, S., Frankel, R.B., Ibers, J.A., Holm, R.H., *J. Am. Chem. Soc.* **98**, 1976, 2414.
7. Poulos, T.L, Finzel, B.C., Howard, A.J., *J. Mol. Biol.*, **195**, 1987, 687.
8. Griffin, B.W., Petrson, J.A., *Biochemistry* **11**, 1972, 4740.
9. Petrson, J.A. *Arch. Biochem. Biophys.* **144**, 1971, 678.
10. Iyanagi, T., Mason, H.S., *Biochemistry* **12**,1973, 2297.
11. Vermillion, J.L., Coon, M.J., *J. Biol. Chem.* **253**,1978, 8812.
12. Ulrich, V., Cohen, B., Cooper, D.Y., Eastbrook, R.W., " *Structure and Functions of Cytochromes*" , University Park Press, Baltimore MD. 1968, p 649.
13. Dawson, J.H., Cramer, S.P., *FEBS Lett.* **88**, 1978, 127.
14. Groves, J.T., Krishnan, S., Avaria, G.E., Nemo, T.E. " *Biomimetic Chemistry*", (ed. D. Dolphin, C. McKenna, V. Murakami, and I. Tabushi.) *Am. Chem. Soc. Washington D.C.* 1980, p 277
15. Reuttinger, R.T., Fulco, A.J., *J. Biol. Chem.* **256**, 1981, 5728.
16. Holland, H.L., Munoz, B., Jones, T.R.B. *Bio-org. Chem.* **16**, 1988, 388.

17. Holland, H.L., Brown, F.M., Conn, M. *J. Chem. Soc. Perkin Trans. 2* 1990, 1651.
18. Holland, H.L., Bergen, E.J., Chenchiah, P.C., Kahn, S.H., Munoz, B., Ninniss, R.W., Richards, D., *Can. J. Chem.* **65**, 1987, 502.
19. Holland, H.L., Brown, F.M., Munoz, B., Ninniss, R.W., *J. Chem. Soc. Perkin Trans. 2* 1988, 1557.
20. Holland, H.L., Chernishenko, M.J., Conn, M., Munoz, A., Manoharan, T.S., Zawadski, M.A., *Can. J. Chem.* **68**, 1990, 696.
21. Holland, H.L., Kinderman, M., Kumaresan, S., Stefanac, T. *Tetrahedron: Asymmetry*. **4**, 1993, 1353.
22. Holland, H.L., Carter, I.M., Chenchiah, P.C., Khan, S.H., Munoz, B., Ninniss, R.W., Richards, D., *Tetrahedron Lett.* **26**, 1985, 6409.
23. Heinemann, F.S., Ozols, J., *J. Biol. Chem.* **257**, 1982, 14988.
24. Nelson, D.R., Strobel, H.W., *J. Biol. Chem.* **263**, 1988, 6038.
25. Black, S.D., *FASEB J.* **6**, 1992, 680.
26. Lu, A.Y.H., West, S.B., *Pharmacol. Rev.* **31**, 1980, 277.
27. Johnson, E.F., "Reviews in Biochemical Toxicology". (E. Hodgson, J.R. Bend, R.M. Philpot. eds.) Elsevier/North Holland, Amsterdam. p1-26.
28. Haugen, D.A., Coon, M.J., *J. Biol. Chem.* **251**, 1976, 7929.
29. Dus, K., Katagiri, M., Yu, C-A., Erbes, D.L., Gunsalus, I.C., *Biochem. Biophys. Res. Commun.* **401**, 1970, 1423.
30. Black, S.D., Coon, M.J., *Biochem. Biophys. Res. Commun.* **128**, 1985, 82.
31. Poulos, T.L., Finzal, B.C., Gunsalus, I.C., Wagner, G.C., Kraut, J., *J. Biol. Chem.* **260**, 1985, 16122.

32. White, R.E., Oprian, D.D., Coon, M.J., " Microsomes, Drug oxidations, and Chemical carcinogenesis", Vol 1. (M.J. Coon, A.H. Conney, R.W. Eastbrook, H.V. Gelboin, J.R. Gillette, and P.J. O'Brien eds.), Academic Press, New York. p 243-51.
33. Poulos, T.L., Finzel, B.C., "Peptide and Protein Reviews" Vol. 4 (M.T.W. Hearn ed.), Marcel Dekker Inc. New York. p115-71.
34. Waldmeyer, B, Bechfold, R., Bosshard, H.R., Poulos, T.L., *J. Biol. Chem.* **257**,1982, 6073.
35. Bisson, R., Capaldi, R.A., *J. Biol. Chem.* **256**,1981, 4362.
36. Bosshard, H.R., Banziger, J., Hasler, T., Poulos, T.L., *J. Biol. Chem.* **259**, 1984, 5683.
37. Poulos, T.L., Freer, S.T., Alden, R.A., Edwards, S.L., Skoglund, U, Takio, K, Xuong, N-L., Yonetani, T., Kraut, J., "Oxidases and Related Redox Mechanisms", (T.E. King, H.S. Mason, M. Morrison eds), Pergammon Press Inc. Elmsford New York. p639-52.
38. Lipscomb, J.D., *Biochemistry*. **19**, 1980, 3590.
39. Fuji-Kuriyama, Y., Mizukami, Y., Kawajiri, K., Sugawa, K., Muramatsu, M., *Proc. Natl. Acad. Sci. U.S.A.* **79**, 1982, 2793.
40. Haniu, M., Armes, L.G., Yasunoba, K.T., Shastry, B.A., Gunsalus, I.C., *J. Biol. Chem.* **257**, 1982, 12664.
41. Kawajiri, K., Gotoh, O., Sogawa, K., Tagashira, Y., Muramatsu, M., Fuji-Kuriyama, Y. *Proc. Natl. Acad. Sci. U.S.A.* **81**, 1984, 1649.
42. Sogawa, K., Gotoh, O., Kawajiri, K., Fuji-Kuriyama, Y. *Proc. Natl. Acad. Sci. U.S.A.* **81**, 1984, 5066.
43. Morohashi, Y., Fuji-Kuriyama, Y., Okoda, Y., Sogawa, K., Hirose, T., Inayama, S., Omura, T., *Proc. Natl. Acad. Sci. U.S.A.* **81**, 1984, 4647.
44. Coon, M.J., Black, S.D., "Cytochrome P-450, Structure, Mechanism and Biochemistry", (P. Ortiz de Montellano ed.) Plenum Press, New York.
45. Jones, E.R.H., *Pure Appl. Chem.* **33**, 1973, 39.

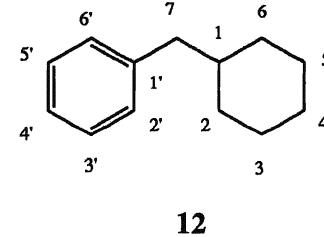
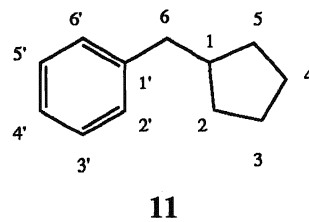
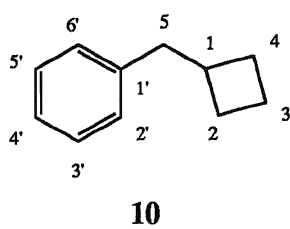
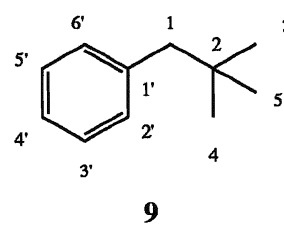
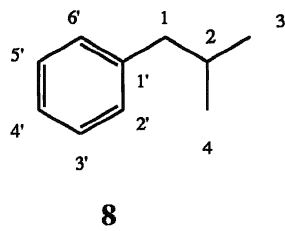
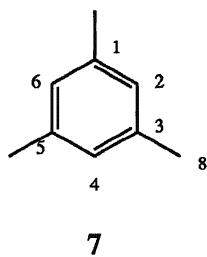
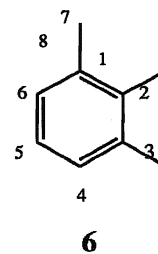
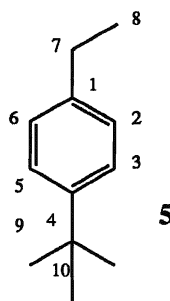
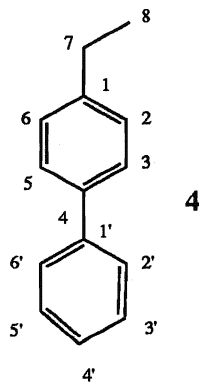
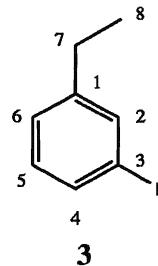
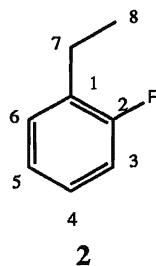
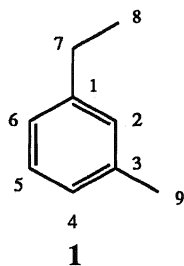
46. Bell, A.M., Cherry, P.C., Clark, I.M., Denny, W.A., Jones, E.R.H., Meakins, G.D., Woodgate, P.D., *J. Chem. Soc. Perkin Trans. 1* 1972, 2081.
47. Holland, H.L., *Chem. Soc. Rev.* 11, 1982, 371.
48. Browne, J.W., Denny, W.A., Jones, E.R.H., Meakins, G.D., Morisawa, Y., Pendlebury, A., Pragnell, J., *J. Chem. Soc. Perkin Trans. 1* 1973, 1493.
49. Chambers, V.E.M., Denny, W.A., Evens, J.M., Jones, E.R.H., Kasal, A., Meakins, G.D., Pragnell, J., *J. Chem. Soc. Perkin Trans. 1* 1973, 1500.
50. Bell, A.M., Clark, I.M., Denny, W.A., Jones, E.R.H., Meakins, G.D., Muller, W.E., Richards, E.E., *J. Chem. Soc. Perkin Trans. 1* 1973, 2131.
51. Chambers, V.E.M., Jones, E.R.H., Meakins, G.D., Miners, J.O., Wilkins, A.L., *J. Chem. Soc. Perkin Trans. 1* 1975, 55.
52. Bell, A.M., Jones, E.R.H., Meakins, G.D., Miners, J.O., Pendlebury, A., *J. Chem. Soc. Perkin Trans. 1* 1975, 357.
53. Denny, W.A., Fredricks, P.M., Ghilizan, I., Jones, E.R.H., Meakins, G.D., Miners, J.O., *J. Chem. Res. (M)*, 1980, 345.
54. Liu, W-G., Goswami, A., Steffek, R.P., Chapman, R.L., Sariaslani, F.S., Steffens, J.J., Rosazza, J.P.N., *J. Org. Chem.* **53**, 1988, 5700.
55. Hauson, J.R., Hitchcock, P.B., Jarvis, A.G., Ratcliffe, A.H., *J. Chem. Soc. Perkin Trans. 1*. 1992, 2079.
56. Funke, E., Tozyo, T., Ishii, H., Takeda, T., *J. Chem. Soc. (C)*, 1970, 2548.
57. Fonken, G.S., Herr, M.E., Murray, H.C., Reineke, L.M., *J. Org. Chem.* **33**, 1968, 3182.
58. Johnson, R.A., Herr, M.E., Murray, H.C., Fonken, G.S., *J. Org. Chem.* **33**, 1968, 3187.
59. Johnson, R.A., Herr, M.E., Murray, H.C., Reineke, L.M., Fonken, G.S., *J. Org. Chem.* **33**, 1968, 3195.
60. Herr, M.E., Johnson, R.A., Murray, H.C., Reineke, L.M. Fonken, G.S., *J. Org. Chem.* **33**, 1968, 3201.

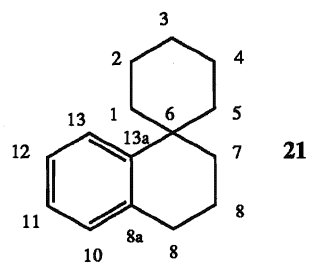
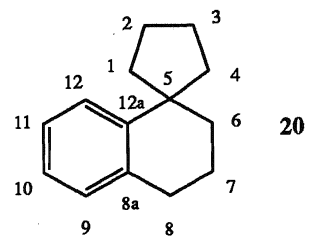
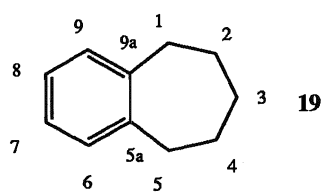
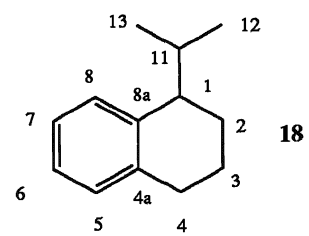
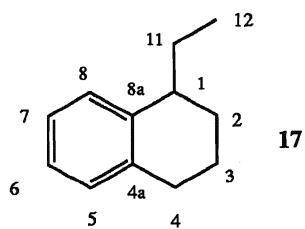
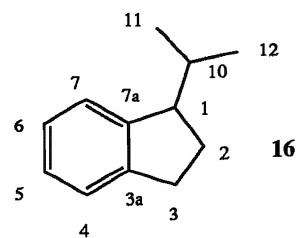
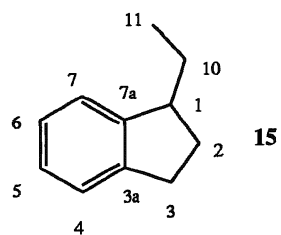
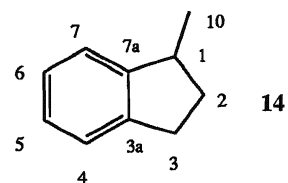
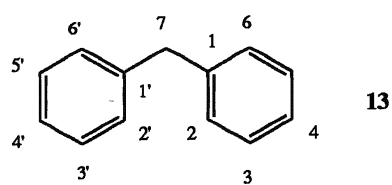
61. Johnson, R.A., Murray, H.C., Reineke, L.M., Fonken, G.S., *J. Org. Chem.* **33**, 1968, 3207.
62. Johnson, R.A., Herr, M.E., Murray, H.C., Fonken, G.S., *J. Org. Chem.* **33**, 1968, 3217.
63. Furstoss, R., Archelas, A., Waegell, J., Le Petit, J., Deveze, L., *Tetrahedron Lett.* **21**, 1980, 451.
64. Furstoss, R., Archelas, A., Waegell, J., Le Petit, J., Deveze, L., *Tetrahedron Lett.* **22**, 1981, 445.
65. Archelas, A., Furstoss, R., Waegell, J., Le Petit, J., Deveze, L., *Tetrahedron* **40**, 1984, 355.
66. Vigne, B., Archelas, A., Furstoss, R., *Tetrahedron* **47**, 1991, 1447.
67. Johnson, R.A., Herr, M.E., Murray, H.C., Chidester, C.G., Han, F., *J. Org. Chem.* **57**, 1992, 7209.
68. Carruthers, W., Prail, J.D., Roberts, S.M., Willets, A., *J. Chem. Soc. Perkin Trans. 1*. 1990, 2854.
69. Johnson, R.A., Herr, M.E., Murray, H.C., Kreuger, W.C., Pschigoda, L.M., Duchamp, D.J., *J. Org. Chem.* **57**, 1992, 7212.
70. Holland, H.L., Popperl, H., Ninniss, R.W., Chenchiah, P.C., *Can. J. Chem.* **63**, 1985, 1118.
71. Holland, H.L., Rand, C.G., Viski, P., Brown, F.M., *Can. J. Chem.* **69**, 1991, 1989.
72. Kutney, J.P., Singh, M., Hewitt, G.M., Salisbury, P.J., Worth, B.R., Servizi, J.A., Martens, D.W., Girdon, R.W., *Can. J. Chem.* **59**, 1981, 2334.
73. Kutney, J.P., Berset, J.D., Hewitt, G.M., Singh, M., *Appl. Environ. Microbiol.* **54**, 1988, 1015.
74. Holland, H.L., Conn, M., Chenchiah, P.C., Brown, F.M., *Tetrahedron Lett.* **29**, 1988, 6393.
75. Holland, H.L., Munoz, B., *Can. J. Chem.* **66**, 1988, 2299.

76. Holland, H.L., "Organic Synthesis with Oxidative Enzymes", VCH Publishers, New York, 1992. p 78.
77. Suschitzky, H., "Advances in Fluorine Chemistry" M. Stacey, J.C. Tattow and A.G. Sharp eds. Butterworth and Co. Ltd., London, 1965, p1.
78. Challis, B.C., Ridd, J.H., *J. Chem. Soc.* 1962, 5197.
79. Challis, B.C., Larkworthy, L.F., and Ridd, J.H., *J. Chem. Soc.* 1962, 5203.
80. Challis, B.C., and Ridd, J.H., *J. Chem. Soc.* 1962, 5208.
81. Hegarty, A.F. "The Chemistry of Diazonium Groups", Wiley, New York, 1978, Part 2, P551
82. Shank, R.C. "The Chemistry of Diazonium Groups", Wiley, New York, 1978, Part 2, P645.
83. Balz, G. and Schiemann, G., *Ber.* **60**, 1927, 1186.
84. Nesmeyanov, A.N., Makarova, L.G., Tolstaya, T.P., *Tetrahedron* **1**, 1957, 145.
85. Brunton, J.C., Suschitzky, H., *J. Chem. Soc.*, 1955, 1035.
86. Huang-Minlon, *J. Am. Chem. Soc.* **68**, 1946, 2487.
87. Soffer, M.D., Soffer, M.B., and Sherk, K.W. *J. Am. Chem. Soc.* **67**, 1945, 1435.
88. Herr, C.H., Whitmore, F.C., and Schiessler, R.W. *J. Am. Chem. Soc.* **67**, 1945, 2061.
89. Schlenk, T. and Schlenk, F. *Ber.* **62B**, 1929, 920.
90. Bright, S.T., Coxon, J.M., Steel, P.J., *J. Org. Chem.* **55**, 1990, 1338.
91. Olah, G.A., Prakash, G.K.S., Sommer, J., "Superacids", John Wiley and Sons, New York, 1985.
92. Fonken, G.S., Herr, M.E., Murray, H.C., U.S. Patent 3,281,330 (1964): Chem. Abstr. 66, 1967, 9974r.

93. Fonken, G.S., Herr, M.E., Murray, H.C., U.S. Patent 3,392,171 (1968):
Chem. Abstr. 69, 1968, 58586w.
94. Akhtar, M., Wright, J.N., *Nat. Prod. Rep.* **8**, 1991, 527.

APPENDICES

APPENDIX 1**Numbering schemes of compounds related to this work**



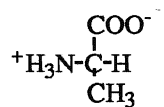
APPENDIX 2

Readily available substrates:

3-Ethyltoluene	1
4-Ethylbiphenyl	4
1,2,3-Trimethylbenzene	6
1,3,5-Trimethylbenzene	7
2-Methyl-1-phenylpropane	8
2,2-Dimethyl-1-phenylpropane	9
Cyclopentylphenylmethane	11
Diphenylmethane	13
1,4-Epoxy-1,2,3,4-tetrahydronaphthalene	22
9,10-Dihydroanthracene	23
9,10-Dihydrophenanthrene	24

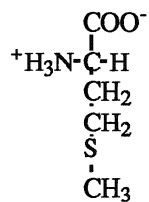
APPENDIX 3

The amino acids



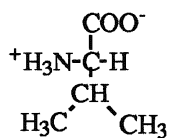
Ala

Alanine (A)



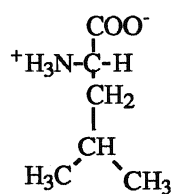
Met

Methionine (M)



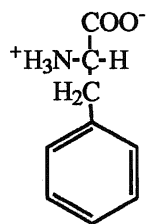
Val

Valine (V)



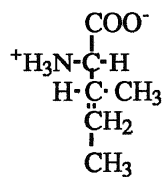
Leu

Leucine (L)



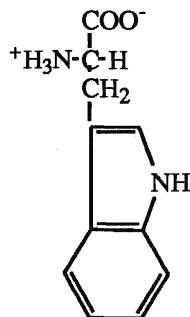
Phe

Phenylalanine (F)



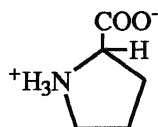
Ile

Isoleucine (I)



Trp

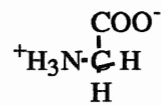
Tryptophan (W)



Pro

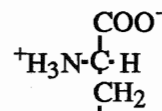
Proline (P)

Nonpolar (Hydrophobic) R Groups.

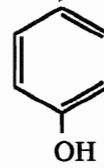


Glycine (G)

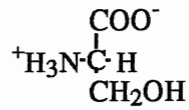
Gly



Tyrosine (Y)

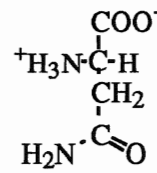


Tyr



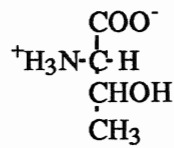
Serine (S)

Ser



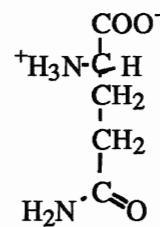
Asparagine (N)

Asn



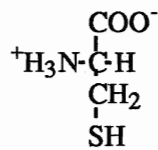
Threonine (T)

Thr



Glutamine (Q)

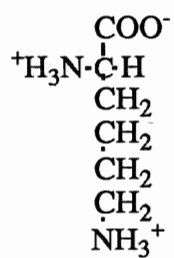
Gln



Cysteine (C)

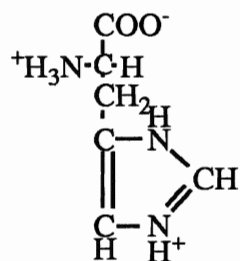
Cys

Polar R Groups (Uncharged)



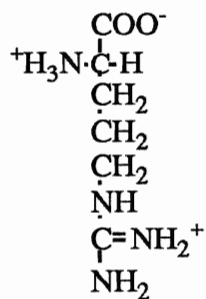
Lysine (K)

Lys



Histidine (H)

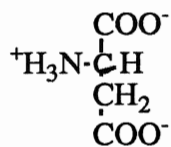
His



Arginine (R)

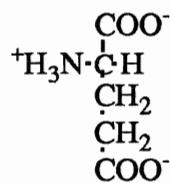
Arg

Positively Charged R Groups



Aspartic acid (D)

Asp



Glutamic acid (E)

Glu

Negatively Charged R Groups